FUSION OF LIPID BILAYERS INDUCED BY SYNTHETIC LIPIDS AND PEPTIDES

by

AUSTIN LOU BAILEY

B.Sc. (Hons.) Dalhousie University, 1986
M.Sc. University of British Columbia, 1989

A THESIS SUBMITTED IN PARTIAL FULFILLMENT OF

THE REQUIREMENTS FOR THE DEGREE OF

DOCTOR OF PHILOSOPHY

in

THE FACULTY OF GRADUATE STUDIES

(Department of Biochemistry and Molecular Biology)

We accept this thesis as conforming
to the required standard

THE UNIVERSITY OF BRITISH COLUMBIA

May 1996

Department of Biochemistry and Molecular Biology

The University of British Columbia
Vancouver, Canada

Date June 11, 1996

ABSTRACT

The fusion-inducing properties of three different synthetic lipid derivatives were investigated in model membranes. The results are discussed in terms of membrane destabilization caused by the formation of non-bilayer lipid structures following charge neutralization of the fusogenic components.

First, studies on the fusion of large unilamellar vesicles (LUVs) composed of equimolar 1,2-dioleoyl-*sn*-phosphatidylethanolamine (DOPE) and the synthetic cationic lipid *N,N*-dimethyl-*N,N*-di-9-octadecenylammonium chloride (DODAC) with target membranes of varying lipid composition are presented. Membrane fusion was promoted by increased negative surface charge and, for liquid-crystalline lipids, by increased acyl chain unsaturation in target liposomes. However, the presence of disaturated phospholipids promoted fusion below the gel-to-liquid-crystalline transition temperature, an effect which was eliminated by the addition of cholesterol. It was also shown that DOPE/DODAC (1:1) LUVs fused with erythrocyte membranes and that this fusion was blocked by the presence of serum.

Next, fusion of model lipid bilayers containing synthetic aminolipids and regulation of this fusion by inducing transbilayer asymmetry of these aminolipids via imposed pH gradients is discussed. Liposomes consisting of 5 mol% ±-1,2-dioleoyl-3-N,N-dimethylamino-propane (AL1) in egg phosphatidylcholine/DOPE/cholesterol (EPC/DOPE/Chol, 35:20:45) did not fuse at pH 4.0 or upon increasing the external pH of these vesicles to

7.5, which resulted in rapid transport of AL1 to the inner monolayer. However, dissipation of the imposed pH gradient led to redistribution of AL1 to the outer monolayer at pH 7.5 and caused liposomal fusion. The effect of varying the hydrocarbon structure of AL1 on the rate of fusion was demonstrated with five synthetic analogues.

Finally, fusion of lipid bilayers induced at low pH by a synthetic lipopeptide (Lipo-AcE4K) derived from the fusion peptide of influenza hemagglutinin is discussed. The secondary structure of Lipo-AcE4K was not affected by pH, but increased membrane penetration was indicated by tryptophan fluorescence. Lipo-AcE4K formed stable liposomes with 1-palmitoyl-2-oleoyl-*sn*-phosphatidylcholine (POPC) and EPC/Chol (55:45) at pH 7.5 but induced fusion of these vesicles at mildly acidic pH. Membrane destabilization increased with increasing lipopeptide concentrations, decreasing pH, inclusion of cholesterol, and incorporation of lipopeptide into the liposomal inner monolayer. Fusion of liposomes bearing Lipo-AcE4K with erythrocyte membranes was also demonstrated.

TABLE OF CONTENTS

ABSTRACT ..... **ii**

TABLE OF CONTENTS ..... **iv**

LIST OF FIGURES ..... **vii**

ABBREVIATIONS ..... **x**

ACKNOWLEDGEMENTS ..... **xii**

CHAPTER 1 - INTRODUCTION **1**

Lipid Components of Biological Membranes 2
Liposomes as Model Membranes 4

LIPID POLYMORPHISM 6
Pure Lipids 6
Lipid Mixtures 8
Factors Modulating Lipid Polymorphism 9

LIPID POLYMORPHISM AND FUSION 10
Detection of Non-Bilayer Structures 10
Non-Bilayer Structures as Intermediates in Fusion 12

QUANTITATIVE ASSAYS FOR FUSION IN LIPOSOMES 14
Lipid Mixing Assays 15
Contents Mixing Assays 16

STUDIES ON INDUCED MEMBRANE FUSION 17
Cationic Liposomes and Cellular Transfection 18
Transbilayer Lipid Asymmetry and Membrane Fusion 21
Liposomal Fusion Induced by Viral Fusion Peptides 23

CHAPTER 2 - MEMBRANE FUSION WITH CATIONIC LIPOSOMES: EFFECTS OF TARGET MEMBRANE LIPID COMPOSITION **27**

MATERIALS AND METHODS 27
Lipids and Chemicals. 27
Preparation of Liposomes. 28
Preparation of Erythrocyte Membranes. 28
Lipid Mixing Fusion Assays. 29

Freeze-Fracture Electron Microscopy and Size Analysis. 30
Fluorescence Microscopy. 30

RESULTS 31
DOPE/DODAC LUVs. 31
Effect of Negative Charge on Lipid Mixing. 31
Effects of Phospholipid Headgroup. 34
Effects of Acyl Chain Saturation. 36
Effect of Cholesterol on Disaturated Lipid Vesicles. 41
Lipid Mixing with Erythrocyte Ghosts. 41

DISCUSSION 45

CHAPTER 3 - MODULATION OF MEMBRANE FUSION BY ASYMMETRIC TRANSBILAYER DISTRIBUTIONS OF AMINOLIPIDS 49

MATERIALS AND METHODS 50
Lipids and Chemicals 50
Synthesis of ±-1,2-dioleoyl-3-N,N-dimethylaminopropane (AL1) 51
Synthesis of ±-1-oleoyl-2-hydroxy-3-N,N-dimethylamino-propane (AL2) and asymmetric ±-1,2-diacyl-3-N,N-dimethyl-aminopropanes (AL3-AL5) 51
Preparation of LUVs 53
Determination of pK_a for Aminolipids in Lipid Vesicles 53
Determination of Lipid Asymmetry by TNS Fluorescence 54
Lipid-Mixing Fusion Assay 54
Contents-Mixing Fusion and Leakage Assays 56
^{31}P-NMR and ^{2}H-NMR Spectroscopy: 56
Freeze-Fracture Electron Microscopy 57

RESULTS 58
Effects of pH on Aminolipid Charge 58
Asymmetry of Aminolipids in Liposomes 61
Fusion of Liposomes Containing AL1 63
^{31}P-NMR and ^{2}H-NMR Spectroscopy 70
Freeze-Fracture Electron Microscopy 72
Effects of Aminolipid Structure 74

DISCUSSION 74

CHAPTER 4 - pH-INDUCED DESTABILIZATION OF LIPID BILAYERS BY A LIPOPEPTIDE DERIVED FROM INFLUENZA HEMAGGLUTININ 80

MATERIALS AND METHODS 82
Lipids and Chemicals. 82
Preparation of AcE4K and Lipo-AcE4K. 82
Preparation of Liposomes. 85

Circular Dichroism. 85
Tryptophan Fluorescence. 86
Preparation of Erythrocyte Membranes. 87
Lipid Mixing Fusion Assays. 87
Exchange of Lipo-AcE4K Between Membranes. 88
Contents Mixing and Leakage. 89
Freeze-Fracture Electron Microscopy 90
Fluorescence Microscopy. 90
RESULTS 91
Solubilities of AcE4K and Lipo-AcE4K. 91
Circular Dichroism and Tryptophan Fluorescence. 91
Fusion of POPC LUVs Induced by Lipo-AcE4K. 95
Fusion and Leakage in EPC/Chol Vesicles. 102
Effects of Transbilayer Distribution of Lipo-AcE4K 104
Freeze-Fracture Electron Microscopy 106
Lipid Mixing with Erythrocyte Ghosts. 106
DISCUSSION 110
CHAPTER 5 - SUMMARY 117
BIBLIOGRAPHY 121

LIST OF FIGURES

FIGURE 1.1 Structures of naturally occurring lipids used in this work. 3

FIGURE 1.2 Freeze-fracture electron micrographs of EPC liposomes. 5

FIGURE 1.3 Organization of lipid molecules in bilayer, hexagonal (H_{II}), and micelle phases and corresponding phosphorus-31 NMR spectra. 7

FIGURE 1.4 Factors influencing the bilayer to hexagonal (H_{II}) phase transition in membrane lipids. 11

FIGURE 1.5 Proposed mechanisms of fusion between lipid bilayers. 13

FIGURE 1.6 Transmembrane movement of a protonatable lipid in response to a pH gradient. 22

FIGURE 2.1 Effect of negative charge concentration in DOPC LUVs on lipid mixing with DOPE/DODAC (1:1) 32

FIGURE 2.2 Comparison of lipid mixing for DOPE/POPS (80:20) and DOPC/POPS (80:20) with DOPE/DODAC (1:1). 35

FIGURE 2.3 Effect of target vesicle acyl chain saturation on lipid mixing with DOPE/DODAC. 37

FIGURE 2.4 Size distributions of DOPE/DODAC (1:1) liposomes and 1:3 mixtures of DOPE/DODAC (1:1) with DSPC/POPS (80:20), DOPC/POPS (80:20) and POPC determined by quasi-elastic light scattering. 38

FIGURE 2.5 Freeze-fracture electron micrographs of DOPE/DODAC (1:1) liposomes mixed in a 1:3 lipid ratio with liposomes composed of DSPC/POPS (80:20), DOPC/POPS (80:20), and POPC. 40

FIGURE 2.6 Effect of cholesterol concentration on lipid mixing of DOPE/DODAC (1:1) and DSPC/Cholesterol. 42

FIGURE 2.7 Fusion of DOPE/DODAC (1:1) liposomes with erythrocyte ghosts. 44

FIGURE 2.8 Fluorescence micrographs showing the appearance of Rh-PE in erythrocyte ghosts upon lipid mixing with labeled DOPE/DODAC (1:1). 46

FIGURE 3.1 Structures of the synthetic aminolipids used in this study 52

FIGURE 3.2 Effect of pH on the TNS fluorescence of EPC/Chol (55:45) vesicles containing 0 mol% and 10 mol% AL1. 59

FIGURE 3.3 TNS fluorescence traces showing the effect of induction and dissipation of a pH gradient on AL1 in EPC/Chol (55:45) vesicles. 62

FIGURE 3.4 Effect of AL1 concentration (0–20 mol%) on fusion of EPC/Chol (55:45) vesicles by RET fluorescent probe dilution. 65

FIGURE 3.5 Effect of DOPE concentration on fusion rates of vesicles containing AL1. ... 67

FIGURE 3.6 Fusion of vesicles consisting of 0 and 5 mol% AL1 in EPC/DOPE/Chol (35:20:45). 68

FIGURE 3.7 ANTS/DPX contents-mixing assays for liposomes consisting of 5 mol% AL1 in EPC/DOPE/Chol (35:20:45) 69

FIGURE 3.8 ^{31}P-NMR and ^{2}H-NMR spectra of freeze–thawed MLVs prepared with 5 mol% AL1-d_4 in EPC/DOPE/Chol (35:20:45). 71

FIGURE 3.9 Freeze-fracture electron micrographs of 5 mol% **AL1** in EPC/DOPE/Chol (35:20:45). 73

FIGURE 3.10 Effect of aminolipid structure on fusion of EPC/DOPE/Chol (35:20:45) vesicles by RET fluorescent probe dilution. 75

FIGURE 4.1 Amino acid sequences of the hemagglutinin HA2 subunit N-terminal fusion peptide of influenza virus X31 strain (wt), E4 peptide, AcE4K. 81

FIGURE 4.2 Structure and synthesis of the Lipo-AcE4K lipopeptide. 84

FIGURE 4.3 Effects of pH and the presence of lipid vesicles on the circular dichroism of AcE4K and Lipo-AcE4K. 92

FIGURE 4.4 Tryptophan fluorescence emission spectra of showing the effects of pH and the presence of lipid vesicles. 94

FIGURE 4.5 Effect of pH on lipid mixing for 5 mol% Lipo-AcE4K in POPC LUVs. 96

FIGURE 4.6 Effects of Lipo-AcE4K concentration on lipid mixing and leakage in POPC LUVs. 98

FIGURE 4.7 Exchange of Lipo-AcE4K between vesicle populations and lipid mixing with membranes lacking lipopeptide 101

FIGURE 4.8 Lipid mixing and leakage in EPC/Chol (55:45) LUVs 103

FIGURE 4.9 Effect of transbilayer distribution of Lipo-AcE4K on lipid mixing in EPC/Chol (55:45) LUVs. 105

FIGURE 4.10 Freeze-fracture electron micrographs of EPC/Chol liposomes: effect of Lipo-AcE4K and pH. 107

FIGURE 4.11 Effect of method of lipopeptide incorporation into EPC/Chol (55:45) LUVs on lipid mixing with erythrocyte membranes. 109

FIGURE 4.12 Fluorescence micrographs showing the appearance of Rh-PE in erythrocyte membranes upon lipid mixing with 10 mol% Lipo-AcE4K in EPC/Chol (55:45). 111

ABBREVIATIONS

Lipids

AL1-AL6	synthetic aminolipids (structures given in Figure 3.1)
Chol	cholesterol
DODAC	*N,N*-dimethyl-*N,N*-di-9-octadecenylammonium chloride
DOPC	1,2- dioleoyl-*sn*-phosphatidylcholine
DOPE	1,2- dioleoyl-*sn*-phosphatidylethanolamine
DSG	distearoylglycerol
DSPC	1,2- distearoyl-*sn*-phosphatidylcholine
EPC	egg phosphatidylcholine
ESM	egg sphingomyelin
PA	phosphatidic acid
PC	phosphatidylcholine
PE	phosphatidylethanolamine
PG	phosphatidylglycerol
PI	phosphatidyinositol
POPC	1-palmitoyl-2-oleoyl-*sn*-phosphatidylcholine
POPS	1-palmitoyl-2-oleoyl-*sn*-phosphatidylserine
PS	phosphatidylserine
SM	sphingomyelin

Miscellaneous

AcE4K	synthetic peptide (sequence given in Figure 4.1)
ANTS	aminonaphthalenetrisulphonic acid
BCA	bicinchoninic acid
CD	circular dichroism
DCC	dicyclohexylcarbodiimide
DMAP	4-dimethylaminopyridine
DMSO	dimethylsulphoxide
DPA	dipicolinic acid

DPX	*p*-xylylene bis(pyridinium) bromide
E4	synthetic peptide (sequence given in Figure 4.1)
FID	free induction decay
HA	influenza hemagglutinin
HBS	HEPES buffered saline (typically 20mM HEPES, 150 mM NaCl)
HEPES	*N*-(2-hydroxyethyl)piperazine-N´-ethanesulphonic acid
H_{II}	hexagonal phase
HMA	HEPES/MES/acetate buffer
Lipo-AcE4K	synthetic lipopeptide (structure given in Figure 4.2)
LUV	large unilamellar vesicle
MES	2-(*N*-morpholino)ethanesulphonic acid (buffer)
MLV	multilamellar vesicle
NBD-PE	*N*-(7-nitro-2,1,3-benzoxadiazol-4-yl)-1,2-dioleoyl-*sn*-phosphatidylethanolamine
NHS	*N*-hydroxysuccinimide
NMR	nuclear magnetic resonance
pH_i	pH of vesicle interior
pH_o	pH of vesicle exterior
pK_a	acid dissociation constant
RET	resonance energy transfer
Rh-PE	*N*-(lissamine rhodamine B sulphonyl)-1,2-dioleoyl-*sn*-phosphatidylethanolamine
SUV	small unilamellar vesicle
TFA	trifluoroacetic acid
TLC	thin layer chromatography
TMC	transmonolayer complex
TNS	2-*p*-toluidinylnaphthalene-6-sulphonate
wt	wild type (refers to peptide sequence in Figure 4.1)
$\% \Delta F/\Delta F_{max}$	percent change in fluorescence (defined in Chapter 2)

ACKNOWLEDGEMENTS

This work would not have been possible were it not for the tremendous support of Dr. Pieter Cullis. I would like to thank him for accepting me into his laboratory, for providing an inspiring and enjoyable work environment, and for his generosity and perspicacious guidance throughout these studies.

I am also grateful to the many members of the Cullis group for their helpful input and support in completing this work. In particular, I would like to thank Dr. Kim Wong for his patient assistance with the freeze-fracture electron microscopy studies ("You call that focused!"). I am also greatly indebted to Dr. Myrna Monck, who made the lipopeptide studies a success by contributing countless hours in the laboratory (including the notorious preparative HPLC tag-team event) and by sharing her boundless enthusiasm for science. Thanks also to Nancy, Mike, Troy, and everyone else at UBC for making my time there enjoyable.

On a personal level, I would like to extend my warmest thanks to all my family and friends who provided invaluable support as well as much-needed distractions over the course of this work: Jennifer, Jean-Bernard, Brian, Bob, William & Richard, and, above all, my parents Yvonne and Paul.

CHAPTER 1

INTRODUCTION

Membrane fusion is an important phenomenon in many biological processes, including the intracellular delivery of lipids, proteins and metabolites by transport vesicles, endocytosis, exocytosis, cell division, cell–cell fusion, fertilization, and the infection of cells by enveloped viruses (Wilschut & Hoekstra, 1991). These fusion events involve proteins or protein complexes which bring the fusing membranes into close proximity and promote fusion through membrane destabilization. While a number of fusogenic proteins have been identified and characterized, the exact mechanisms of the fusion events remain poorly defined. Furthermore, the importance of the lipid composition of fusing membranes is not understood. The use of liposomes as models for biological membranes has provided insight into the possible roles of lipids in membrane fusion and has given rise to a number of applications for liposomes that are able to fuse with biological membranes.

The essence of membrane fusion is the formation of a continuous lipid bilayer from two closely apposed but separate lipid bilayers. This encompasses both the formation of a single membrane compartment from two previously distinct membrane-bound vesicles and the formation of a second vesicular compartment internal or external to a larger progenitor membrane. Intrinsic to these processes is the requirement for an intermediate non-bilayer lipid structure, in the sense that two bilayers cannot combine to form one bilayer without some local intermediate departure from bilayer structure. Early studies

demonstrating the ability of fusogens to induce fusion in biological membranes and to detect associated non-bilayer structures (Hope & Cullis, 1978) have led to the proposal of a number of structural intermediates of fusion. These proposed intermediates can be related to the polymorphic phase behaviour of lipids that are found in biological membranes.

Lipid Components of Biological Membranes

Biological membranes contain complex mixtures of lipid species. Their composition is highly differentiated, not only among organisms and among tissues of a given organism, but also among the membranes of cells and organelles of a given tissue and between monolayers of a given lipid bilayer. That lipid composition is important to the functional requirements of membranes has been demonstrated in a variety of processes including biological membrane fusion (Klappe *et al.*, 1986; Marquardt *et al.*, 1993).

Glycerol-based phospholipids are the predominant lipid species of eukaryotic membranes. These include phosphatidylcholine (PC), phosphatidylethanolamine (PE), phosphatidylinositol (PI) and cardiolipin. Sphingosine-based lipids, including sphingomyelin (SM), are also major components. Glycolipids, which are the dominant components of some plant membranes, have important roles as cell-surface antigens and membrane recognition factors in animals. Sterols can also be present at substantial levels; mammalian plasma membranes contain cholesterol (Chol) at molar concentrations equal to that of total phospholipid. Minor lipid components of membranes may include fatty

Glycerophospholipids

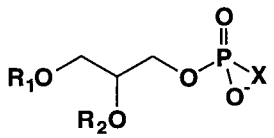

Acyl Chain	R_1,R_2
Palmitoyl (P)	
Oleoyl (O)	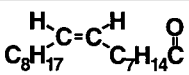
Stearoyl (S)	

Phospholipid Species	X
Phosphatidic Acid (PA)	**OH**
Phosphatidylcholine (PC)	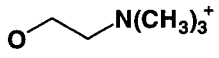
Phosphatidylethanolamine (PE)	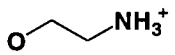
Phosphatidylserine (PS)	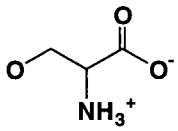
Phosphatidylglycerol (PG)	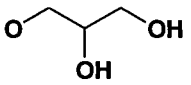

e.g., 1-Palmitoyl-2-oleoyl-*sn*-phosphatidylcholine (POPC: R_1=P, R_2=O)
1,2-Dioleoyl-*sn*-phosphatidylethanolamine (DOPE: R_1=R_2=O)

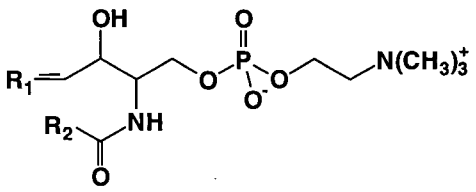

Sphingomyelin (SM)
(typically R_1= $C_{14}H_{29}$, R_2= oleoyl)

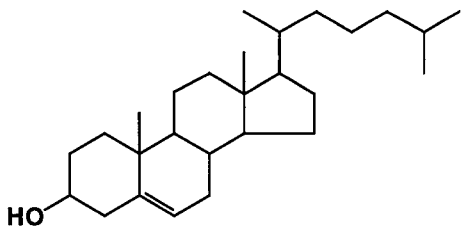

Cholesterol (Chol)

FIGURE 1.1 Structures of naturally occurring lipids used in this work.

acids, lyso-phospholipids, and diglycerides. The structures of the naturally occurring lipids used in this study are given in Figure 1.1.

Liposomes as Model Membranes

The physical characteristics of a particular lipid influence the properties of a membrane in which it is included. Of particular interest in this work are the effects of lipid composition on the stability of the bilayer phase and the propensity for membrane fusion. Upon hydration, many naturally occurring lipids form multilamellar vesicles (MLVs) which are liposomes composed of many concentric lipid bilayers (Figure 1.2). MLVs are poor models of biological lipid bilayers due to their high lamellarity. Other drawbacks include low levels of lipid hydration, low entrapment volumes, and unequal transbilayer distributions of solutes. Solute equilibration and decreased lamellarity can be achieved by subjecting MLVs to repeated freeze–thaw cycles (Mayer *et al.*, 1985).

MLVs can be transformed into unilamellar lipid vesicles by a number of techniques. Small unilamellar vesicles (SUVs) with diameters in the range of 30-50 nm are produced by sonication of MLVs or by extrusion of MLVs through polycarbonate filters of small, defined pore size (Szoka & Papahadjopoulos, 1980). Large unilamellar vesicles (LUVs) with 100-200 nm diameters can also be formed by extrusion as well as by a number of other techniques, including reverse phase evaporation (Szoka & Papahadjopoulos, 1978), detergent dialysis (Mimms *et al.*, 1981), and injection of lipids dissolved in organic solvents into aqueous buffers (Szoka & Papahadjopoulos, 1980). SUVs have highly

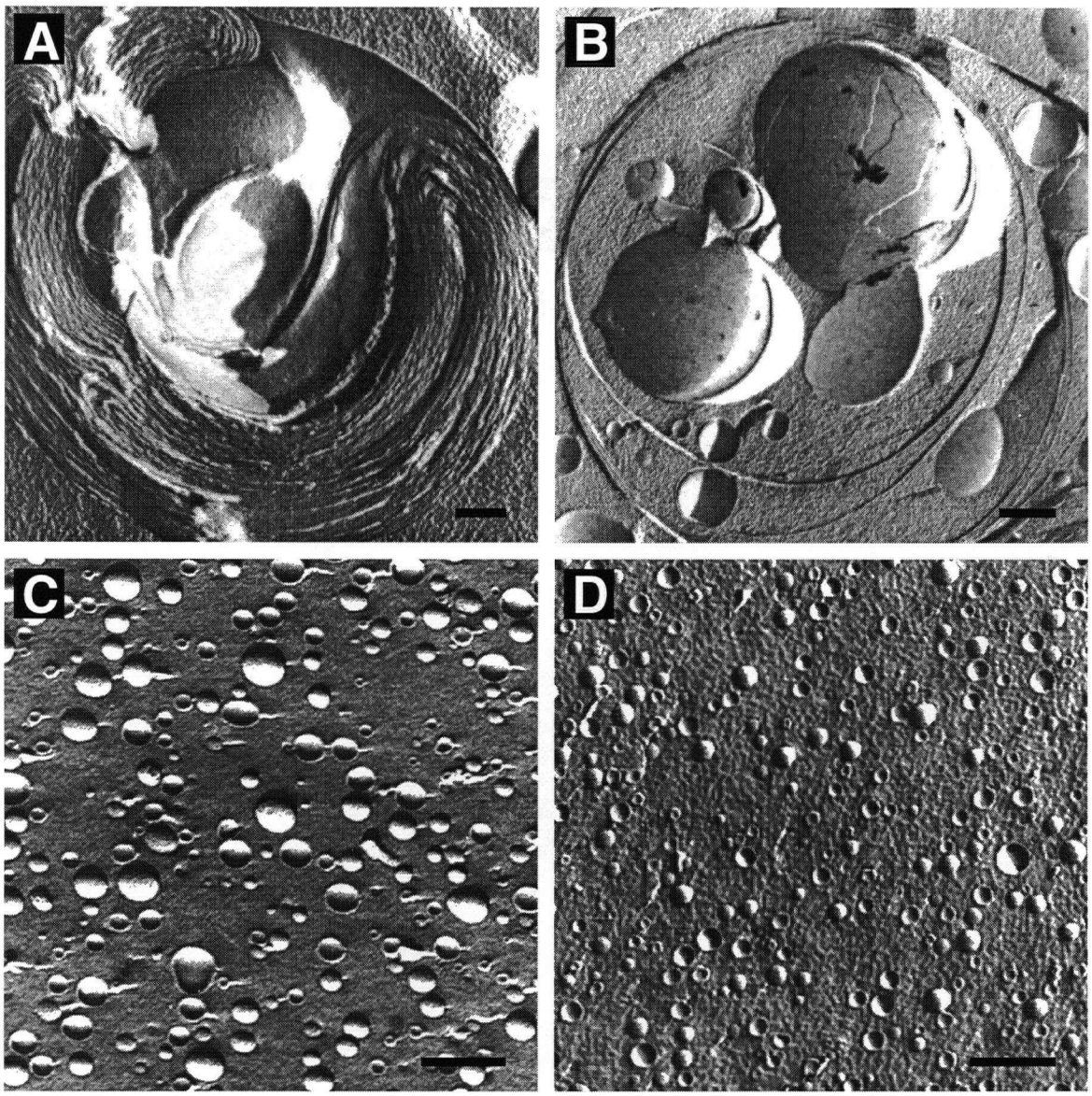

FIGURE 1.2 Freeze-fracture electron micrographs of EPC liposomes: MLVs (A) before and (B) after five freeze–thaw cycles, (C) LUVs and (D) SUVs extruded through polycarbonate filters of 100 nm and 50 nm pore size, respectively. Lipid concentration was approximately 50 mM and original magnification was 20,000X (bars represent 200 nm).

curved bilayer surfaces with considerable intrinsic strain and high permeability as well as low entrapment volumes. LUVs have bilayers with lower membrane curvatures with lower permeability and significantly higher volumes of entrapment. As such, LUVs are useful models of biological membranes where a single bilayer surrounds a cell, an organelle, or an intracellular vesicle.

LIPID POLYMORPHISM

Pure Lipids

Some of the lipid species that are found in biological membranes preferentially adopt non-bilayer phases when dispersed as a single species in aqueous media. The phase preference of a given lipid depends on the chemical structure of the lipid, temperature and a variety of extrinsic chemical influences. The polymorphic properties of lipids have been extensively reviewed (Cullis & de Kruiff, 1979; Gruner *et al.*, 1985: Lindblom & Rilfors, 1989; Seddon, 1990). Among the non-bilayer phases available to natural lipids are the micellar phase and the hexagonal (H_{II}) phase. For comparison, the arrangement of lipid molecules in the bilayer, micellar and H_{II} phases are illustrated in Figure 1.3.

Among the lipids which are found in biological membranes, those which will form micelles upon hydration exist only as minor components. However, lipids that can adopt H_{II} phase are present at substantial levels, usually at least 30 mole percent of total lipid. Formation of H_{II} phase can also be induced by the chemical environment of some lipids. While aqueous dispersions of unsaturated PE spontaneously adopt H_{II} structure,

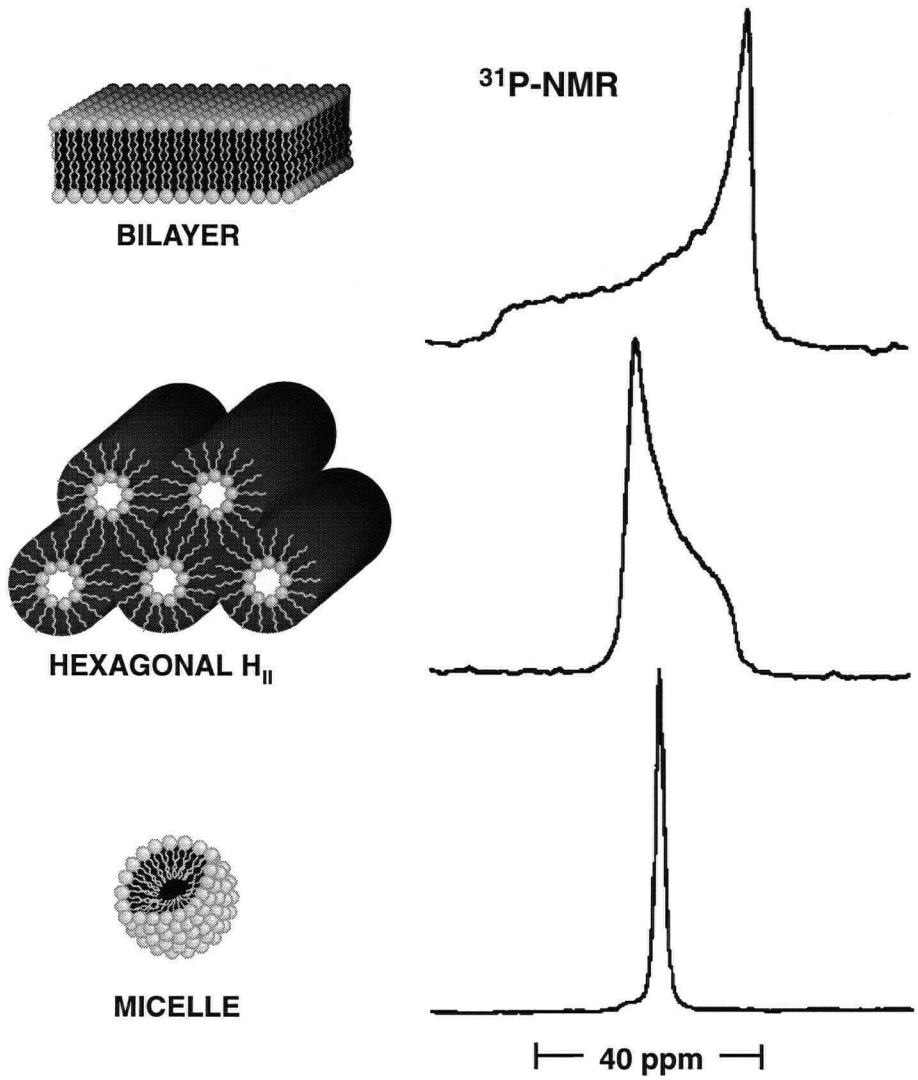

FIGURE 1.3 Organization of lipid molecules in bilayer, hexagonal (H_{II}), and micelle phases and corresponding phosphorus-31 NMR spectra. Hydrophobic regions are shown in black and aqueous space is in white.

unsaturated PA and PS exist in bilayers unless the headgroup charge is neutralized either by low pH or the presence of multivalent cations, such as Ca^{2+}.

The morphologies of pure lipids are related to their molecular geometries, or "shape", and in particular to the relative surfaces areas occupied by the hydrophilic headgroup and the hydrophobic hydrocarbon chains. A model describing this relationship has been detailed (Israelachvilli *et al.*, 1980; Cullis *et al.*, 1986a). Lipid molecules for which the headgroup and hydrocarbon structures subtend equal areas in a membrane (e.g. PC) approximate cylinders and pack into stable bilayers. Those lipids for which the headgroup area is large relative to the hydrocarbon (e.g., lysolipids, detergents) have inverted cone geometries and form micelles. Conversely, those with relatively small headgroups have conical geometries and form inverted micelles or H_{II} structures (e.g., PE). Accordingly, increasing the effective area occupied by the hydrocarbon chains by increasing chain length, increasing unsaturation, or increasing temperature promotes the formation of H_{II} phase. While the shape model is a simplification of complex molecular forces, it offers excellent correlation between experimentally observed phase preferences and the molecular geometries of lipids.

Lipid Mixtures

The morphologies of mixed lipid systems offer greater insight into the role of lipid diversity in biological membranes. The properties of a wide variety of binary and tertiary lipid mixtures have been documented (Seddon, 1990; Cullis *et al.*, 1991). Generally, it has been found that H_{II}-preferring lipids, such as unsaturated PE, form stable bilayers upon

addition of 20 to 50 mole percent of a bilayer-forming lipid, including PC, PS or SM. The addition of cholesterol to membrane-stabilized PE mixtures containing PC or SM induces the H_{II} phase to reform. These observations are consistent with the concept of cholesterol exhibiting a conical geometry, compatible with H_{II} phase. Alternatively, micelle-forming species can form bilayers when mixed with H_{II}-preferring lipids, as has been demonstrated in detergent–PE systems (Madden & Cullis, 1982).

The polymorphic phase behaviour of lipid mixtures suggests the possible involvement of the lipidic structures formed by these mixtures in the formation of the non-bilayer intermediates of membrane fusion.

Factors Modulating Lipid Polymorphism

The physical and chemical environment of lipid dispersions can have profound effects on lipid polymorphism and, by extension, lipid shape or morphology. The neutralization of headgroup charge by variation of pH or the presence of polyvalent ions (e.g., Ca^{2+}) can lead to destabilization of the lamellar phase and formation of hexagonal phase (Tilcock *et al.*, 1988). A similar effect is seen in systems containing insufficient water to fully hydrate lipids that form bilayers under water-saturated conditions. Under such conditions, the headgroup size is effectively smaller, leading to the formation of H_{II} phase (Cullis *et al.*, 1986a). H_{II} phase can also be promoted by increasing temperature which results in increased hydrocarbon chain motion. DOPE, for example, adopts bilayer structures below 10°C and H_{II} phase at higher temperatures (Tilcock *et al.*, 1982a). Increasing hydrocarbon

chain unsaturation also favors H_{II} formation (Tilcock & Cullis, 1982b). The factors that modulate the phase behavior of membrane lipids are summarized in Figure 1.4.

LIPID POLYMORPHISM AND FUSION

The factors that promote H_{II} phase are also capable of inducing membrane fusion in liposomal systems. Evidence for this association comes largely from phosphorus-31 NMR spectroscopy and freeze-fracture electron microscopy of liposomes.

Detection of Non-Bilayer Structures

The addition of Ca^{2+} to MLVs with high levels of DOPS results in a change in the ^{31}P-NMR lineshape from one which corresponds to bilayer structures to one which is associated with H_{II} phase (Hope & Cullis, 1978; Cullis & de Kruiff, 1979). The bilayer spectrum exhibits a high field peak and low field shoulder separated by approximately 40 ppm. In the H_{II} phase, additional motional averaging due to lateral diffusion around the narrow tubes of this structure results in a ^{31}P-NMR lineshape with reversed asymmetry which is narrower by a factor of two. Formation of H_{II} phase is also observed upon the addition of fusion-promoting, or "fusogenic", lipids such as diacylglycerides or fatty acids to stable bilayers (Hope & Cullis, 1981). The promotion of H_{II} phase by increasing temperature and decreasing hydration have also been demonstrated by ^{31}P-NMR (Tilcock *et al.*, 1982a; Tilcock & Cullis, 1987).

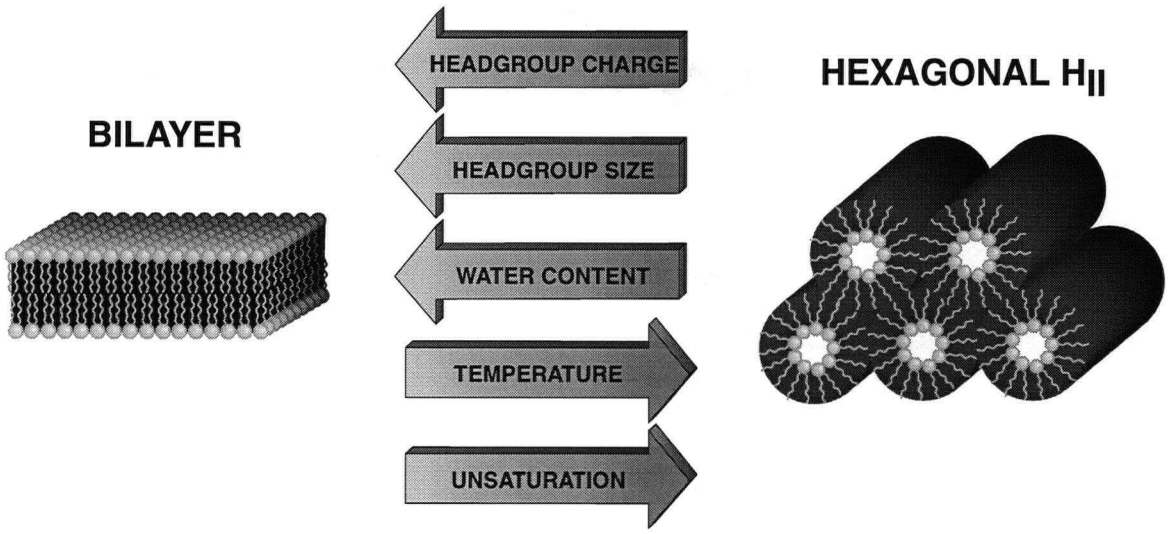

FIGURE 1.4 Factors influencing the bilayer to hexagonal (H_{II}) phase transition in membrane lipids.

Factors that contribute to the formation of H_{II} phase can also induce membrane fusion in LUVs. This fusion is accompanied by the appearance of "lipidic particles" on the fractured surfaces of the fused vesicles (Cullis & Hope, 1978; Verkleij *et al.*, 1980). It has been proposed that these structures arise from lipids in a non-bilayer arrangement that constitute the intermediate structures in membrane fusion.

Non-Bilayer Structures as Intermediates in Fusion

Lipidic particles were initially interpreted as inverted micelles sandwiched between two bilayers and as depicted in Figure 1.5(a). A second possible interpretation is the "stalk" intermediate described by Markin, Chernomordik and co-workers (Markin *et al.*, 1984; Chernomordik *et al.*, 1985) involving the formation of a semi-toroidal lipid structure formed by coalescence of the outer monolayers of fusing membranes (Figure 1.5(b)). The proposed mechanism for fusion involves an increase in the radius of the stalk to form a *trans* monolayer contact (TMC), followed by rapid radial expansion of the TMC giving rise to an area difference between the *cis* and *trans* monolayers. The resulting tension would lead to rupture of the TMC and membrane fusion.

A detailed theoretical comparison of the free energies associated with inverted micelle intermediates and stalks has been carried out by Siegel (1993). It was shown that for a variety of lipid compositions which exhibit fusion, the formation of a stalk intermediate is clearly energetically favored. However, Siegel showed that the expansion of the TMC as proposed would lead to energetically unfavorable structures due to the accompanying

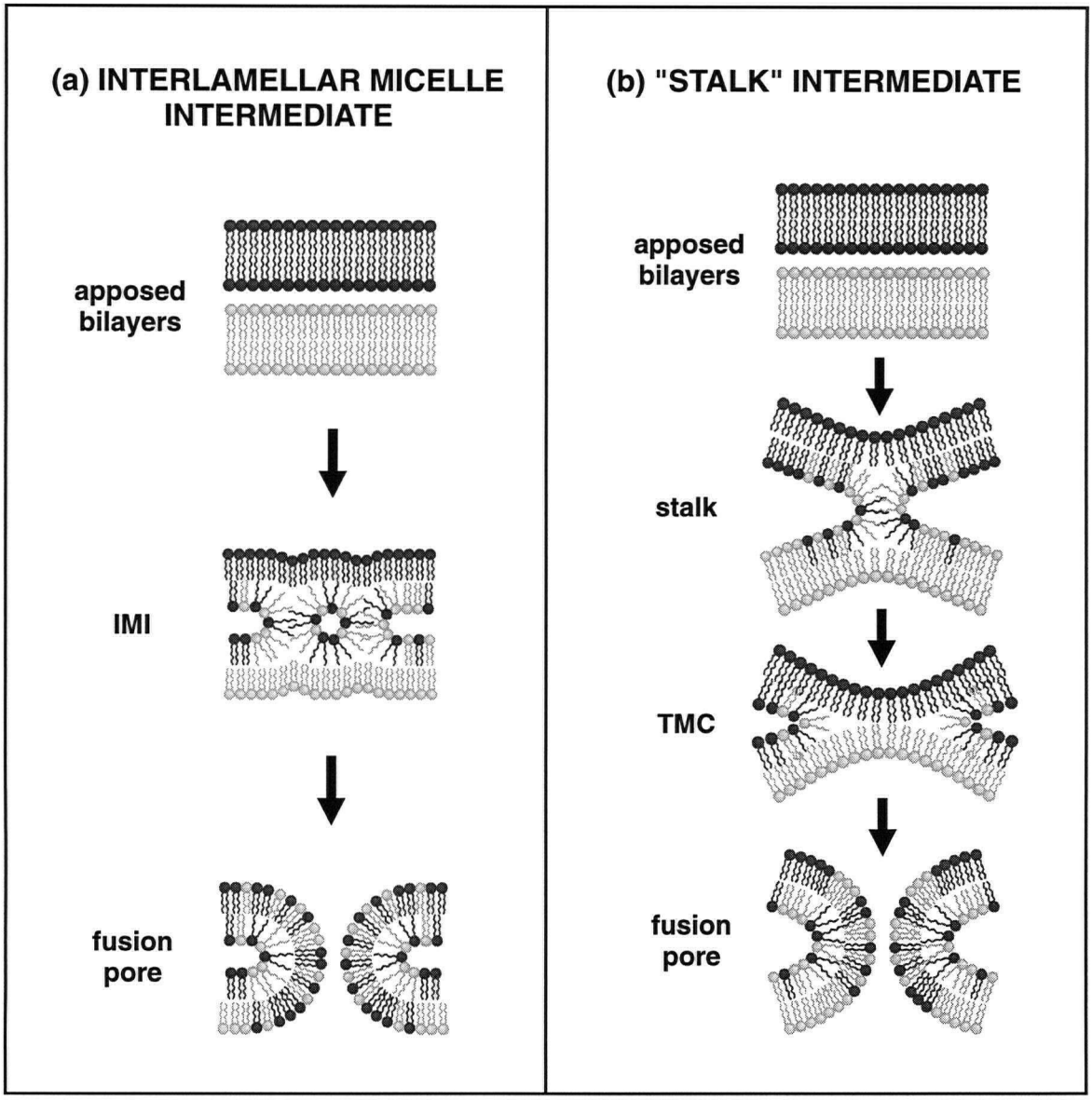

FIGURE 1.5 Proposed mechanisms of membrane fusion indicating key intermediate structures. (a) Two apposed membranes form an interlamellar micelle intermediate (IMI), or lipidic particle, which leads directly to the formation of an interlamellar attachment, or fusion pore. (b) The *cis* monolayers of the apposed membranes mix to form a stalk intermediate which expands radially to a *trans* monolayer contact (TMC) arrangement. Expansion of the TMC leads to rupture as a result of curvature and interstitial stresses and creates a fusion pore.

rapid increase in hydrophobic interstitial volume, and that rupture of the TMC with a small radius to form a fusion pore is preferred. This is consistent with the observation that the addition of trace hydrocarbons greatly affects fusion rates by reducing the free energy associated with the hydrophobic interstices (Walter & Siegel, 1993). Based on these results, a modified mechanism for fusion involving a stalk intermediate leading rapidly to fusion-pore formation has been proposed.

While these energy considerations are useful in comparing the lipid structures which have been proposed as fusion intermediates, there is an insufficient understanding of the actual energy-intensive events involved in the proposed fusion mechanisms, specifically, membrane rupture and pore formation. Furthermore, it is probable that the presence of fusogenic proteins affect the energies of these proposed structures or, possibly, give rise to alternate intermediate lipid structures in the fusion of biological membranes. As a result, it remains difficult to definitively assign the non-bilayer lipid structures which may be involved in membrane fusion.

QUANTITATIVE ASSAYS FOR FUSION IN LIPOSOMES

The methods for observing membrane fusion discussed to this point only give information about bulk lipid morphology and lipid structures following the addition of fusogens. To study the dynamic fusion process and to quantify the extent of membrane fusion occurring in liposomal systems, a variety of assays have been developed. It is important that the results of these assays be interpreted with the understanding that membrane fusion is a

multi-step process, and that the measurement of a single parameter is unlikely to be sufficient to completely describe the fusion process.

Quantifiable processes that occur during the fusion of lipid vesicles include vesicle aggregation, lipid mixing, contents mixing and vesicle leakage. Liposomal aggregation can be directly measured by orthogonal light-scattering or absorbance; however, such data alone is of limited use since, while the formation of vesicle complexes is a minimum requirement for fusion to occur, not all aggregation processes lead to membrane fusion (e.g. Mg^{2+} aggregation of PS LUVs, Wilschut *et al.*, 1985). More usually, factors influencing aggregation rates are determined through kinetic analysis of lipid mixing or contents mixing data using mass action models as described by Ellens *et al.* (1984) and Bental *et al.* (1987). Not surprisingly, these studies have shown that increases in aggregation rates are accompanied by corresponding increases in rates of lipid mixing, suggesting that the factors causing membrane destabilization influence both processes.

Lipid Mixing Assays

Lipid mixing arising from the fusion of lipid vesicles has been studied by a variety of techniques, including differential scanning calorimetry, spin-labelled lipid dilution, excimer fluorescence, fluorescence dequenching, and resonance energy transfer (RET) fluorescence assays (for a review, see Hoekstra & Düzgüneş, 1993).

The method which is most often employed is a dual fluorescent probe dilution assay using two headgroup-labelled PE probes, *N*-(7-nitro-2,1,3-benzoxadiazol-4-yl)-1,2-dioleoyl-*sn*-phosphatidylethanolamine (NBD-PE), and N-(lissamine rhodamine B sulphonyl)-1,2-

dioleoyl-*sn*-phosphatidylethanolamine (Rh-PE). When vesicles containing both of these labels fuse with unlabelled vesicles, the dilution of the fluorescent probes results in loss of RET between the probes and increased fluorescence for NBD-PE. This assay is widely applicable and has a number of advantages over other methods. The probes are added to the lipid compositions of interest at concentrations less than one mole percent and do not significantly affect membrane properties. Exchange of these labelled lipids between vesicles does not occur even in highly aggregated systems, and fluorescence increases only upon mixing of membrane lipids (Hoekstra, 1982).

Contents Mixing Assays

A number of soluble fluorescent probes have been used to quantify the mixing of aqueous contents resulting from lipid vesicle fusion (for a review, see Düzgüneş & Wilschut, 1993). The most widely applicable of these involves entrapment of the fluorophore aminonaphthalenetrisulfonic acid (ANTS) in one vesicle population and the quencher *p*-xylylene bis(pyridinium) bromide (DPX) in the second population (Ellens *et al.*, 1984). Liposomal fusion then leads to a decrease in ANTS fluorescence due to DPX quenching. Contents mixing can be distinguished from vesicle leakage with this assay, since leakage results in insufficient DPX concentrations to provide quenching. Vesicle leakage during membrane fusion can also be measured by entrapping both ANTS and DPX in a single vesicle population and mixing these with empty liposomes. The advantage of the ANTS/DPX assay over other contents mixing assays is that ANTS fluorescence is unchanged over a broad range of pH.

Historically, it has been asserted that in order to firmly establish the occurrence of membrane fusion, evidence of lipid mixing alone is insufficient, and aqueous contents mixing must also be demonstrated. This assertion is supported by evidence that, in some lipid systems, mixing of the lipids present in the outer monolayers of lipid vesicles occurs more rapidly than mixing of inner monolayer lipids and vesicle contents; in the extreme case lipid mixing can be arrested at a state of "hemi-fusion" (Leventis *et al.*, 1986; and Kemble *et al.*, 1994). However, very few model membrane systems exhibit contents mixing in the absence of extensive vesicle leakage. More typically, either contents mixing and leakage occur on comparable timescales, or rapid leakage precludes the observation of contents mixing. Furthermore, recent evidence that fusion in biological systems, and in particular the fusion of enveloped viruses (Gunther-Ausborn *et al.*, 1995), can also result in extensive leakage of solutes suggests that the requirement for contents mixing may be inappropriate.

STUDIES ON INDUCED MEMBRANE FUSION

The ability to induce the fusion of liposomal membranes with biological membranes either *in vitro* or *in vivo* has a number of potentially important applications. The encapsulation of drugs within liposomes has been extensively investigated and has begun to achieve widespread clinical use. Liposomal encapsulation offers improved drug delivery to disease sites, lower toxicity, and extended drug circulation lifetimes (Chonn & Cullis, 1995). The therapeutic activity of these liposomal drugs would be greatly enhanced if fusion of the liposomal membranes with the cells of target tissues could be achieved.

More recently, the use of liposomes to deliver non-conventional drugs including genes, antisense oligonucleotides, and recombinant proteins has become an active area of research. This work is largely based on the success achieved to date in the *in vitro* transfection of cells using liposomal preparations as discussed below. Again, this technology would greatly benefit from the ability to induce liposomal fusion in a controlled fashion.

This thesis comprises work on three different approaches to inducing membrane fusion. In each approach, fusion follows destabilization of the lipid bilayer by charge neutralization of one of the membrane components either through contact with membranes of opposite charge or by a change in pH. The results are rationalized in terms of the formation of non-bilayer lipid fusion intermediates promoted by the fusogenic components which function differently in each case.

Cationic Liposomes and Cellular Transfection

The ability to deliver DNA into cells is important both for understanding gene and protein function and regulation, and for applications in genetic engineering such as the production of therapeutically useful proteins. Techniques for gene transfer include co-precipitation of DNA with inorganic salts or polycations, cell membrane permeation by solvents or detergents, disruption of cell membranes by osmotic shock or electroporation, and liposome-mediated DNA delivery. Interest in the development of gene transfer techniques has greatly increased with the possibility of human gene therapy. The principal barrier to

the development of *in vivo* therapeutic gene transfer is the delivery of genetic material in sufficient concentrations to appropriate sites of expression.

Cationic amphiphiles have achieved widespread use as gene transfer agents. DNA complexes with cationic lipids and complexes formed by adding DNA to liposomes prepared from cationic detergents or lipids mixed with neutral lipids have proven highly efficient for the transfection of cultured cells (for a review see Behr, 1994). The techniques involve the formation of lipid–DNA or liposome–DNA complexes through charge interactions, followed by incubation of these complexes with the cells to be transfected. An excess of the positively charged lipid component relative to negative charge on the DNA is required, apparently to promote interactions between the complexes and the anionic residues on the cell surface. The mode by which the complexes gain entry to the cytoplasm has been the subject of extensive studies, and it is increasingly evident that this process occurs by endocytosis followed by release of the complex by destabilization of the endosomal membrane (Farhood *et al.*, 1995; Wrobel & Collins, 1995). However, release of the DNA from the lipid complexes and its eventual delivery to the nucleus are inefficient and poorly characterized processes (Zabner at al., 1995).

A comparison of the reported DNA–cationic lipid systems is difficult. The chemical structure of the cationic lipids and the cell types that have been used to gauge transfection efficiencies are disparate. However, some systematic studies on the effects of cationic lipid structure have been made (Felgner *et al.*, 1987; Ito *et al.*, 1990; Leventis & Silvius, 1990; Gao & Huang, 1991). One observation is that greater levels of transfection are

achieved with lipids bearing cationic charges close to the lipid-water interface. In addition, transfection efficiency as a function of neutral lipid composition for DNA–cationic liposome complexes (Felgner *et al.*, 1987; Stamatatos *et al.*, 1988; Düzgüneş *et al.*, 1989; Farhood *et al.*, 1992; Zschörnig *et al.*, 1992; Bennett *et al.*, 1995) have demonstrated that unsaturated phosphatidylethanolamines are the preferred neutral lipids for mixture with cationic lipids or detergents.

Very little is known about the influence of the composition of target cellular membranes on the extent of fusion achieved by a given DNA-cationic lipid formulation. Such information may be useful in understanding the variability in transfection among various cell lines. To model the effects of the lipid composition of target membranes, we have studied the ability of cationic LUVs composed of DOPE/DODAC (1:1) to fuse with LUVs of varying composition in the absence of DNA. The results are presented in Chapter 2. The effects of negative surface charge concentration, phospholipid headgroup, acyl chain saturation, and the addition of cholesterol were studied. In addition, fusion of DOPE/DODAC (1:1) with erythrocyte ghosts and the ability of serum to inhibit such fusion were demonstrated.

Transbilayer Lipid Asymmetry and Membrane Fusion

The concentrations of various lipid species on the cytosolic and plasma or lumenal monolayers of biological membranes is highly regulated. Among the possible functional roles this transbilayer lipid asymmetry may have is to regulate membrane fusion. For example, PE and PS are found mainly on the cytosolic monolayer of eukaryotic plasma

membranes, and PC and SPM constitute the major lipids of the outer monolayer (Houslay & Stanley, 1982). Hope *et al.* (1983) demonstrated that liposomes approximating the lipid composition of the inner monolayer fused in the presence of Ca^{2+} while liposomes modeled on the outer monolayer were resistant to fusion. In addition, erythrocytes that have lost this transbilayer lipid asymmetry are prone to fusion (Tullius *et al.*, 1989). Furthermore, myoblasts, which readily fuse to form myotubes, have higher concentrations of PE and PS on the outer monolayer of the plasma membrane than erythrocytes (Session & Horowitz, 1983), and the concentrations of these lipids increase prior to fusion (Santini *et al.*, 1990).

The influence of transbilayer lipid asymmetry on the propensity for membrane fusion has also been demonstrated in liposomal systems. In lipid vesicles composed in part of lipids bearing weak acid or weak base headgroups, asymmetry can be induced by imposing a pH gradient across the membrane (Figure 1.6). Neutral lipid species can partition into the hydrophobic region of the bilayer much more readily than their charged counterparts, and accumulation of the charged form on one monolayer can be readily achieved (Hope & Cullis, 1987). If the lipid is one which promotes non-bilayer structures, its accumulation

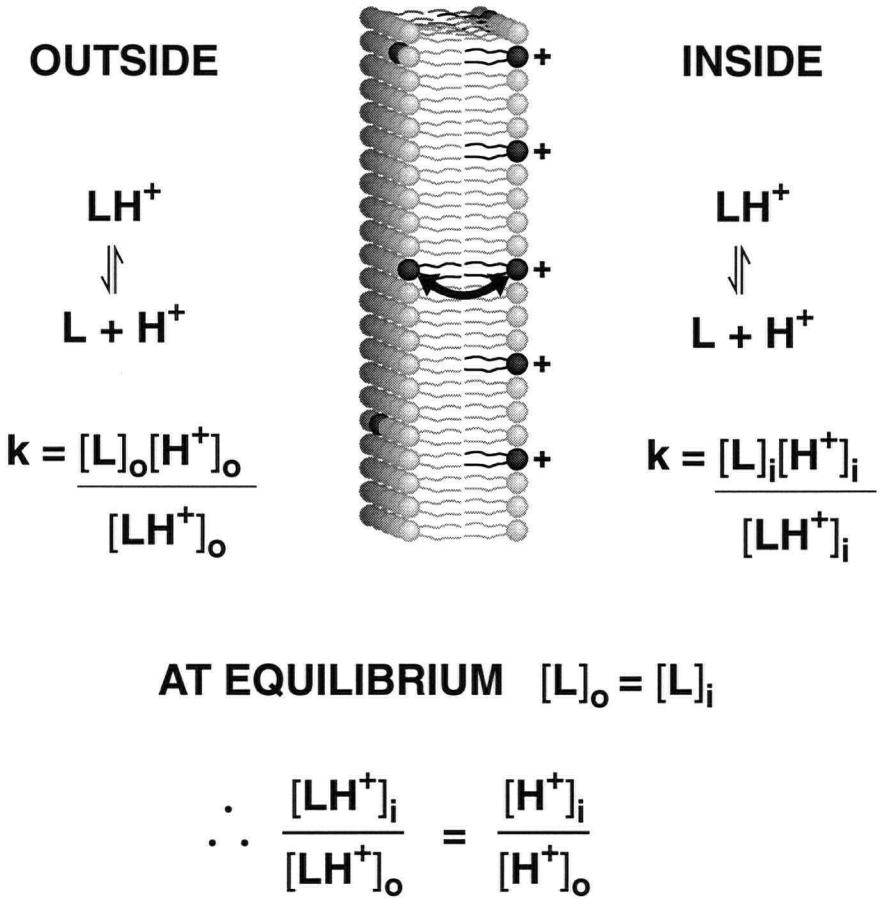

FIGURE 1.6 Transmembrane movement of a protonatable lipid in response to a pH gradient. The neutral form of the lipid (L) is readily transported across the lipid bilayer such that at equilibrium the ratio of the charged form (LH^+), inside versus outside, is determined by the proton gradient.

on the outer monolayer of LUVs will promote membrane fusion. Conversely, transport of such a lipid to the inner monolayer of vesicles will prevent fusion with other membranes.

A liposomal system exhibiting transbilayer lipid asymmetry-modulated membrane fusion was reported by Eastman *et al.* (1992). Vesicles composed of 10 mol% DOPA in DOPC/DOPE/PI (25/60/5) fused upon the addition of 8 mM Ca^{2+}. However, it was shown that by lowering the external pH of these vesicles DOPA was transported to the inner monolayer and that the rate of fusion upon the addition of Ca^{2+} was reduced.

As discussed in Chapter 3, the application of cationic lipids for promoting membrane fusion has been extended to synthetic aminolipids which are positively charged only at low pH. The transbilayer distribution of these synthetic lipids can be controlled by pH gradients, and at neutral pH they are capable of inducing membrane fusion in the absence of anionic lipids or other neutralizing species. Evidence for the involvement of non-bilayer intermediates promoted by the neutral forms of the aminolipids is given. A systematic variation in aminolipid structure was performed, along with optimization of the extent of membrane fusion achieved by formulating the aminolipids with other lipid species.

Liposomal Fusion Induced by Viral Fusion Peptides

Cellular infection by enveloped viruses is a multi-step process in which fusion between the viral envelope and either the plasma membrane or an endosomal membrane of the cell is a essential component (Stegmann *et al.* 1989; White *et al.*, 1991). The process is mediated by viral glycoproteins which are responsible for binding to receptors on target

cells, bringing the membranes into close proximity, and promoting the fusion of the viral envelope with the cellular membrane, leading to release of the viral capsid into the cytosol. The fusion proteins of a number of enveloped viruses have been identified and extensively characterized.

A common feature of the viral fusion proteins is the presence of a short hydrophobic peptide which has the potential to interact with the membrane of a target cell. It is believed that these "fusion peptides" penetrate cellular membranes and play a role in membrane destabilization and fusion. The functional role of fusion peptides has been investigated by site-directed mutagenesis of fusion proteins (Gething *et al.*, 1986; Bosch *et al.*, 1989) and by physical characterizations of synthetic peptides with corresponding amino acid sequences and of their interactions with lipid bilayers (Brasseur *et al.*, 1990; Düzgüneş & Shavnin, 1992; Nieva *et al.*, 1994).

Influenza hemagglutinin (HA) is the best characterized viral fusion protein to date (for a review see Hughson, 1995). The protein spike of the influenza envelope is a homo-trimer of HA molecules, each consisting of an HA1 subunit bearing a sialic acid-binding site and an HA2 subunit containing the transmembrane domain. The fusion peptide is a stretch of about 20 amino acids found at the N-terminus of the HA2 subunit. At neutral pH the fusion peptide remains buried within the trimer, near the viral membrane. Crystallographic results suggest that upon exposure to the low pH of the endosome HA undergoes a major conformational change which results in the exposure of the fusion

peptide at the distal end of the viral spike where it can penetrate the endosomal membrane (Bullough *et al.*, 1994).

The membrane-destabilizing properties of synthetic fusion peptides derived from the HA2 N-terminal sequences of various influenza strains have been given considerable attention (Burger *et al.*, 1991; Clague *et al.*, 1991; Rafalski et al, 1991; Ishiguro et al, 1993; Murata *et al.*, 1993). Peptide–bilayer interactions can lead to membrane destabilization, measured by hemolysis or leakage of lipid vesicles, and membrane fusion, determined by lipid mixing assays. In general, the peptides adopt amphipathic α-helical structures and penetrate lipid bilayers at the pH corresponding to that required for fusion of the native virus with the endosomal membrane. For peptides derived from the X31 and A/PR/8/34 strains the helical structure only forms upon neutralization of the acidic residues. However, the rank in importance of the degree of α-helical structure formed by the peptide, its overall hydrophobicity, and the orientation it adopts with respect to the lipid bilayer remains contentious.

Artificial amphipathic α-helical peptides which mimic the behaviour of viral fusion peptides have been synthesized and anchored to lipid bilayers by either a N-terminal palmitoyl moiety (Kato *et al.*, 1991) or a C-terminal cysteine linked to a bifunctional PE derivative (Puyal *et al.*, 1994). These lipopeptides provide a means to study to what extent membrane fusion between lipid vesicles can be induced by a short membrane-bound peptide. In the first case, the membrane-destabilizing properties of the peptide were

reduced by the lipid anchor. In the second case destabilization was reportedly enhanced, but the lipid-mixing data did not distinguish membrane fusion from vesicle aggregation.

In Chapter 4, the use of a synthetic peptide derived from influenza hemagglutinin covalently coupled to a lipid anchor to induce membrane fusion is demonstrated. In contrast to the aminolipids described in Chapter 3, the synthetic lipopeptide destabilizes lipid bilayers only at low pH. The structure of the peptide and its interactions with the lipid bilayer as a function of pH are reported. Again, the importance of membrane lipid composition and the transbilayer distribution of the fusogenic agent is demonstrated. The extent of fusion between liposomes and biological membranes induced by the membrane-bound peptide was also assessed.

CHAPTER 2

MEMBRANE FUSION WITH CATIONIC LIPOSOMES: EFFECTS OF TARGET MEMBRANE LIPID COMPOSITION

The extent of fusion achieved by cationic liposomes composed of DODAC/DOPE (1:1) with other lipid vesicles was studied as a function of target membrane composition. While cationic liposomes are currently in widespread use as DNA transfection agents, the interactions of cationic liposomes with biological membranes are not well characterized. We have investigated the effects of varying the negative charge concentration, the lipid composition, and the degree of acyl chain unsaturation in target membranes in order to better understand these interactions. Fusion of cationic liposomes with biological membranes is also demonstrated.

MATERIALS AND METHODS

Lipids and Chemicals.

DODAC was provided by Inex Pharmaceuticals Corporation (Vancouver, BC). POPC was purchased from Northern lipids (Vancouver, BC). EPC, NBD-PE, Rh-PE, and all other synthetic lipids were supplied by Avanti Polar Lipids (Alabaster, AL). Mouse serum was obtained from Caltag Laboratories (South San Francisco, CA). Cholesterol, all buffers, and miscellaneous chemicals were purchased from Sigma Chemical Co. (St. Louis, MO).

Preparation of Liposomes.

Chloroform solutions of lipids were dried by vortex mixing under a nitrogen stream followed by the removal of residual solvent under high vacuum for 1 hour. Lipids were hydrated in HEPES buffered saline (HBS: 20 mM HEPES, 150 mM NaCl, pH 7.5) to give 20 mM MLV suspensions. Five freeze–thaw cycles were used to ensure homogeneous mixture. The MLVs were extruded 10 times through two 100 nm pore-size polycarbonate filters (Costar, Cambridge, MA) in a pressure extruder (Lipex Biomembranes, Vancouver, BC) to produce LUVs. All preparations were extruded at temperatures above the gel-to-liquid-crystalline phase transition. The size distributions of the liposomes were determined by quasi-elastic light scattering on a Nicomp 270 Sub-micron Particle Sizer using manufacturer's software to calculate Gaussian fits to the correlation data. Lipid concentrations were determined by phosphate assay as described by Bartlett (1959). All liposome preparations were diluted with HBS to 10 mM total lipid prior to assays.

Preparation of Erythrocyte Membranes.

Sealed human erythrocyte ghosts were prepared by the method of Steck and Kant (1974). Briefly, 4 ml of packed cells were washed 3 times with HEPES buffered saline (HBS; 5 mM HEPES, 150 mM NaCl, pH 7.5), centrifuging each time for 5 minutes at 750 g with a swinging-bucket rotor. Washed cells were diluted two-fold with HBS, lysed in 300 ml of 5 mM HEPES, 1 mM $MgCl_2$, pH 7.5, and pelleted at 20,000 g for 20 minutes. Ghosts were removed from above the hard, protease-rich pellet and resuspended in 200 ml of HEPES buffered saline containing 1 mM $MgCl_2$. The suspension was repelleted, washed

twice more, and finally resuspended in 10 ml of HBS. Phospholipid concentration was determined by phosphate assay. The absence of glyceraldehyde-3-phosphate dehydrogenase activity (Steck & Kant, 1974) was used to confirm the formation of sealed right-side-out ghosts.

Lipid Mixing Fusion Assays.

The extent of membrane fusion as measured by lipid mixing was monitored by the RET assay described in Chapter 1. DOPE/DODAC (1:1) LUVs containing 0.5 mol% of both NBD-PE and Rh-PE were prepared in HBS, pH 7.5. Labelled vesicles were diluted to 50 μM lipid with HBS in a 3 ml quartz cuvette. Fluorescence was monitored with excitation at 465 nm, emission at 535 nm, and an emission cut-off filter at 530 nm. Temperature was maintained at 25°C with a circulating water bath. At 30 seconds, target LUVs of a desired composition or erythrocyte ghosts were added in a labelled to unlabelled lipid ratio of 1:3 to give a total lipid concentration of 0.2 mM. Fluorescence was monitored over five minutes.

Each lipid mixing time course was normalized by subtracting the initial fluorescence (F_0) and dividing by the fluorescence achieved by infinite probe dilution determined by the addition of 25 μl of 100 mM Triton X-100 (F_{max}). The percent change in fluorescence was calculated as

$$\% \frac{\Delta F}{\Delta F_{max}} = 100 \times \left(\frac{F - F_0}{F_{max} - F_0} \right)$$

These calculated values were not corrected for the effects of membrane composition or Triton X-100 on NBD-PE fluorescence.

Freeze-Fracture Electron Microscopy and Size Analysis.

LUVs of four different lipid compositions were prepared in HBS, pH 7.5: DOPE/DODAC (1:1), DSPC/POPS (80:20), DOPC/POPS (80:20), and POPC. Cationic liposomes were mixed with each of the three target vesicle preparations in a ratio of 1 to 3 at a total lipid concentration of 10 mM. After 5 minute incubations at 25°C, samples were mixed 1:1 with glycerol and quickly frozen. Platinum–carbon replicas were prepared as described previously (Fisher & Branton, 1974).

Fluorescence Microscopy.

Lipid mixing of DOPE/DODAC (1:1) LUVs with erythrocyte ghosts was demonstrated by fluorescence microscopy using the dual fluorescent label DOPE/DODAC preparation described above for the lipid mixing assay. These LUVs contain Rh-PE at a self-quenching concentration, and the appearance of fluorescence in the ghost membranes can be used to detect membrane fusion. Labelled liposomes and ghosts were mixed in a 1:3 lipid ratio at a total lipid concentration of 1 mM in HBS, pH 7.5. After a 5 minute incubation at 25°C, 5 µl samples were mounted under large coverslips to achieve rapid immobilization, and micrographs were taken using both phase contrast and a red fluorescence filter. A sample in which the DOPE/DODAC liposomes were mixed with 1% mouse serum prior to incubation with erythrocyte ghosts was also used.

RESULTS

DOPE/DODAC LUVs.

LUVs composed of DOPE/DODAC (1:1) were used throughout these studies. Pure DOPE does not form bilayers when dispersed in aqueous buffer, but rather adopts a highly hydrophobic hexagonal (H_{II}) phase. Addition of as little as 15 mol% DODAC to DOPE can induce the formation of bilayer phase in water. However, membranes composed of DOPE and cationic lipids can be destabilized in the presence physiological levels of salt (Stamatatos *et al.*, 1988). In our system, at least 30 mol% DODAC is required to form liposomes with DOPE in HBS, and even at this level rapid increase in vesicle size is observed (data not shown). With 1:1 DOPE/DODAC, the liposomes are more stable and undergo limited size increases over a period of several hours (see light-scattering data and freeze-fracture below). In all experiments described here, the DOPE/DODAC (1:1) vesicles were prepared on the day the experiment was performed.

Effect of Negative Charge on Lipid Mixing.

To determine the effect of negative charge concentration in target liposomes on the extent of membrane fusion, we examined lipid mixing between DOPE/DODAC (1:1) LUVs and DOPC LUVs containing POPS in the range of 0 to 50 mol% (Figure 2.1). A small increase in fluorescence was observed with DOPC vesicles in the absence of negative charge ($\Delta F/\Delta F_{max} \sim 6\%$). This increase was approximately doubled by the addition of 10 mol% POPS to the target vesicle population. At 20 mol% POPS extensive lipid mixing

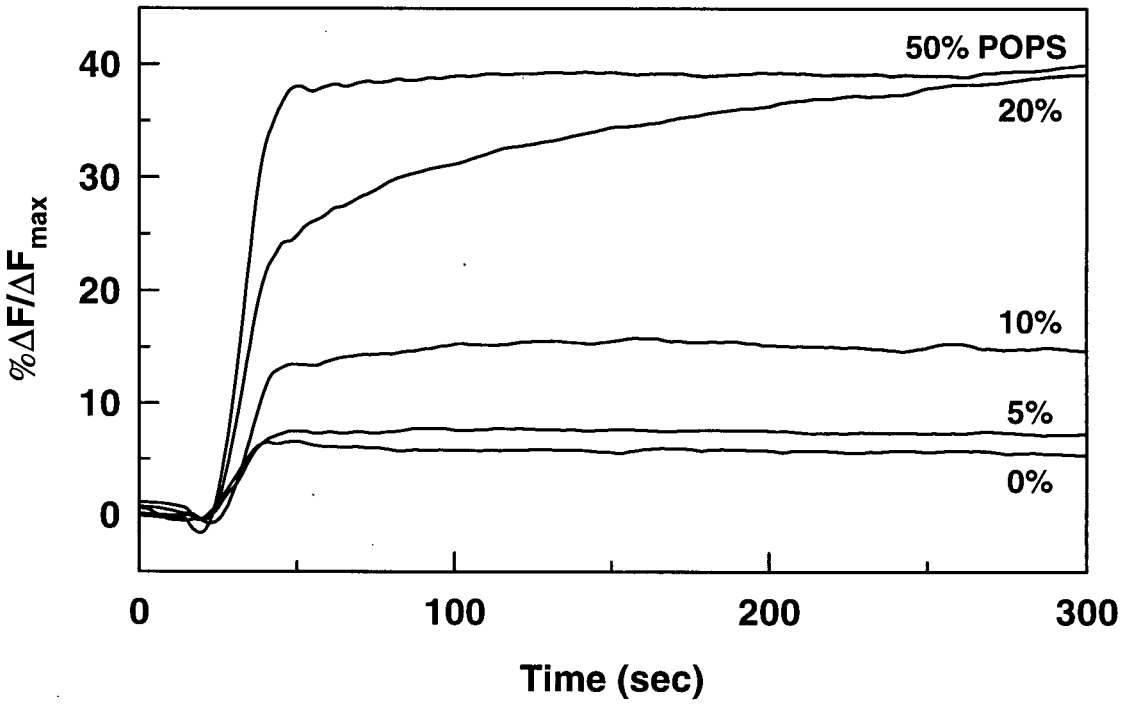

FIGURE 2.1 Effect of negative charge concentration in DOPC LUVs on lipid mixing with DOPE/DODAC (1:1). At 30 seconds, DOPC/POPS liposomes prepared with POPS concentrations ranging from 0 to 50 mol% were added to DOPE/DODAC liposomes labeled with 0.5 mol% each of NBD-PE and Rh-PE. Ratio of anionic to cationic liposomes was 3:1, and total lipid concentration was 0.2 mM. NBD-PE fluorescence was normalized to the value obtained by the addition of Triton X-100 detergent as described in Materials and Methods.

occurred and continued to occur for the duration of the assay, reaching a value of $\Delta F/\Delta F_{max}$ ~ 40% at five minutes. This result was used as a benchmark in subsequent experiments in which the lipid compositions of the target vesicles were varied while maintaining POPS content at 20 mol%.

When vesicles composed of equimolar DOPC and POPS were added to DOPE/DODAC (1:1), the increase in fluorescence was very rapid over the first few seconds and then arrested at an apparent maximum of $\Delta F/\Delta F_{max}$ ~ 40%. This value probably corresponds to the maximum possible extent of lipid mixing between these vesicle populations. We were unable to extrude a lipid preparation composed of DOPC/POPS/DOPE/DODAC (60:15:12.5:12.5) to verify this. The attenuation of NBD-PE fluorescence by high concentrations of negatively charged POPS can account for the relatively low level of fluorescence observed.

The fluorescence assay used here has been previously shown to be insensitive to vesicle aggregation (Düzgüneş *et al.*, 1987) and specifically measures dilution of fluorescent lipid probes. However, the assay does not distinguish between fusion and hemifusion (lipid mixing of only the outer monolayers of apposed vesicles), and it does not provide any information on the fate of the contents of the two vesicle populations, i.e. whether the contents mixing occurs or membrane destabilization gives leakage of the vesicle contents. Previous attempts to use contents mixing assays with cationic liposome systems have failed (Düzgüneş *et al.*, 1989). We had similar difficulties with the DOPE/DODAC (1:1) system. The available contents mixing probes (calcein, aminonaphthalene trisulfonic acid,

and dipicolinic acid) are all multivalent anions that destabilize the cationic liposomes at millimolar concentrations in HBS. Without being able to encapsulate these probes, we have relied on lipid mixing, particle size analysis and electron microscopy to determine the extent of membrane fusion.

Effects of Phospholipid Headgroup.

Substitution of DOPE for DOPC in negatively charged target vesicles (20 mol% POPS) resulted in much more rapid lipid mixing with DOPE/DODAC vesicles (Figure 2.2). The lipid mixing was followed by the formation of large aggregates that gave rise to increased noise and a slow decrease in the fluorescence as the aggregates precipitated. The increased lipid mixing is attributed to the mutual membrane destabilization caused by charge neutralization between DOPE/DODAC and DOPE/POPS vesicles compared to destabilization of only the DOPE/DODAC membranes when incubated with a DOPC/POPS target. DOPE/POPS liposomes containing 10 to 50 mol% POPS all gave similar lipid mixing behaviour (only 20 mol% shown), although higher levels of aggregation were observed at the lower levels of POPS. Replacing DOPC with DOPA or DOPG also gave very rapid lipid mixing with DOPE/DODAC (not shown), but these target vesicles are composed entirely of negatively charged lipids which is likely to be of greater influence than their phospholipid headgroup geometries.

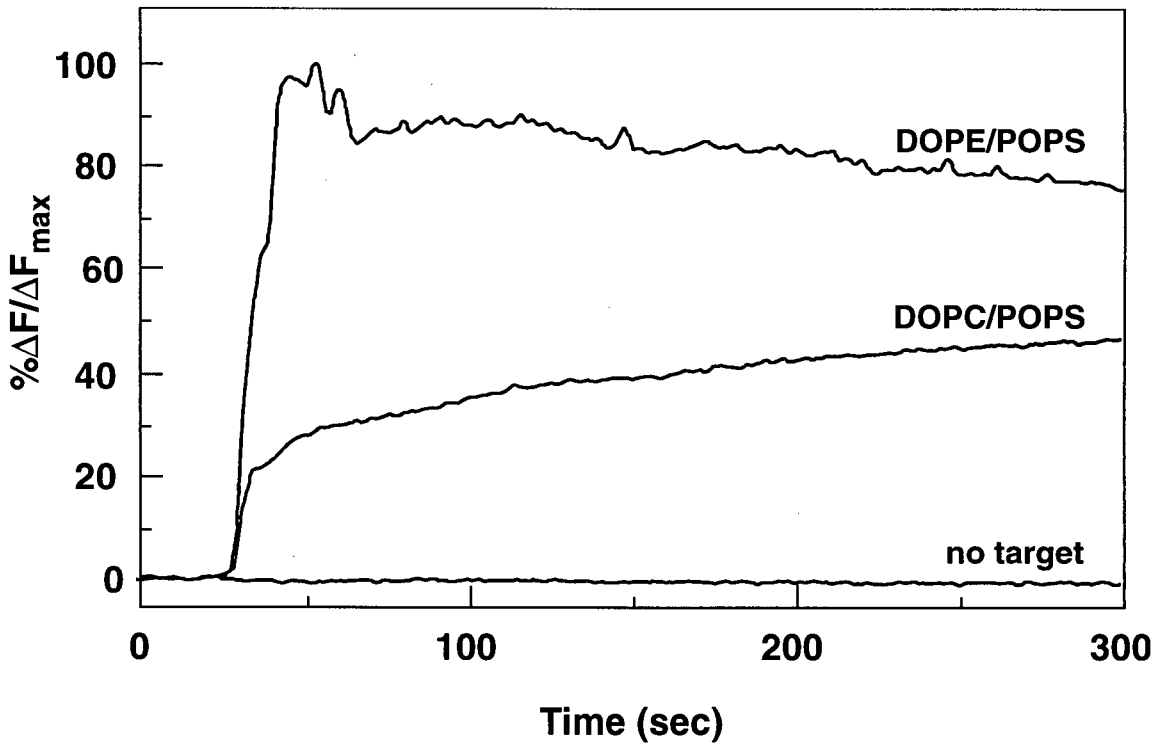

FIGURE 2.2 Comparison of lipid mixing for DOPE/POPS (80:20) and DOPC/POPS (80:20) with DOPE/DODAC (1:1). The control fluorescence timecourse was recorded without adding target liposomes.

Effects of Acyl Chain Saturation.

To determine the effects of fatty acyl chain saturation in the target membranes on lipid mixing with DOPE/DODAC (1:1), we prepared target vesicles composed of 20 mol% POPS in various synthetic PCs. It was expected that increased chain saturation would give reduced lipid mixing since increasing chain order should stabilize the target bilayers. This was the case for POPC/POPS (80:20), which gave a much lower rate and extent of lipid mixing compared to DOPC/POPS (Figure 2.3). However, the disaturated PCs, DPPC and DSPC, gave higher levels of lipid mixing than DOPC. These unexpected results can be attributed to the phase behaviour of the disaturated lipids. DPPC and DSPC both exist in the gel state at 25°C while DOPC and POPC are liquid-crystalline at this temperature. Membranes composed of gel state lipids can contain defects between planar lipid domains, and the presence of hydrophobic regions at these defects may be responsible for increased membrane destabilization and lipid mixing with DOPE/DODAC LUVs. Higher levels of lipid mixing with these disaturated systems relative to DOPC occur even in the absence of negatively charged POPS (data not shown).

The mixtures of DOPE/DODAC and target vesicles described above were subjected to size analysis by quasi-elastic light scattering (Figure 2.4). The results indicate very different interactions for DOPE/DODAC (1:1) with DSPC/POPS (80:20) compared to those observed with DOPC/POPS (80:20). Addition of negatively charged LUVs containing the disaturated lipid DSPC to DOPE/DODAC gave particles larger than could be measured by light scattering. In contrast the bis-monounsaturated lipid DOPC gave a

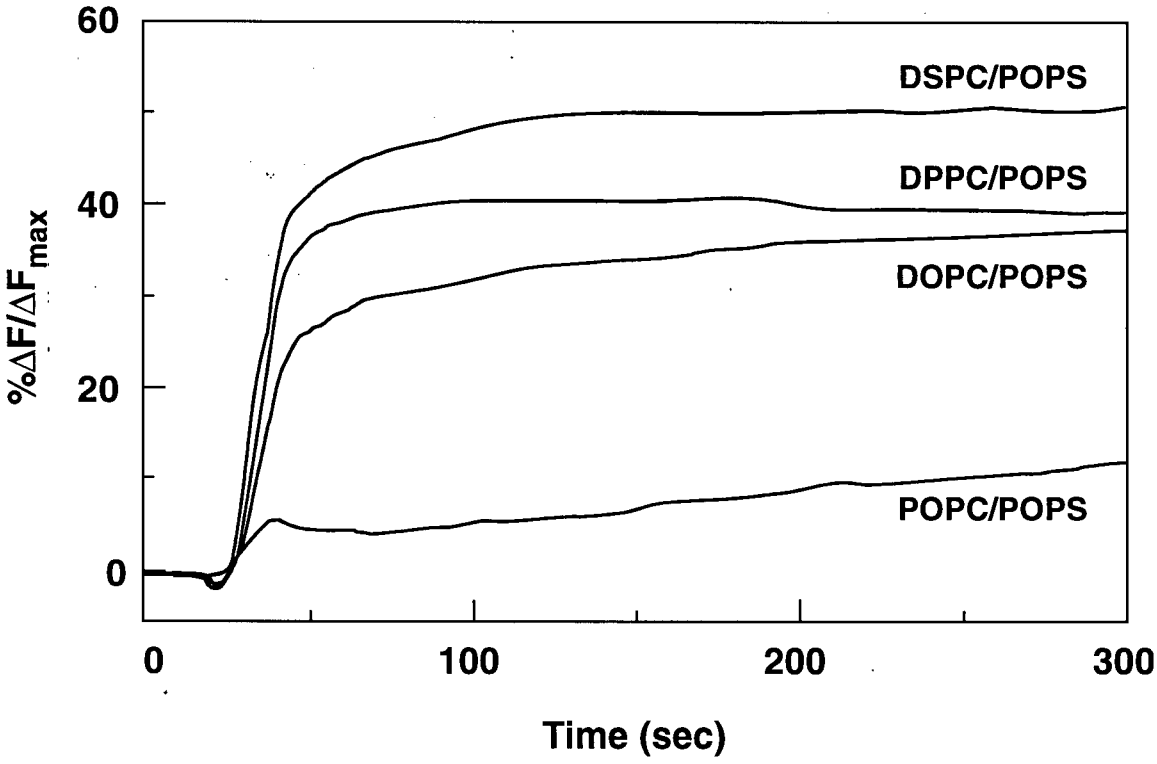

FIGURE 2.3 Effect of target vesicle acyl chain saturation on lipid mixing with DOPE/DODAC. DOPC, POPC, DPPC, and DSPC vesicles were all prepared with 20 mol% POPS and added to DOPE/DODAC (1:1) liposomes at 30 seconds.

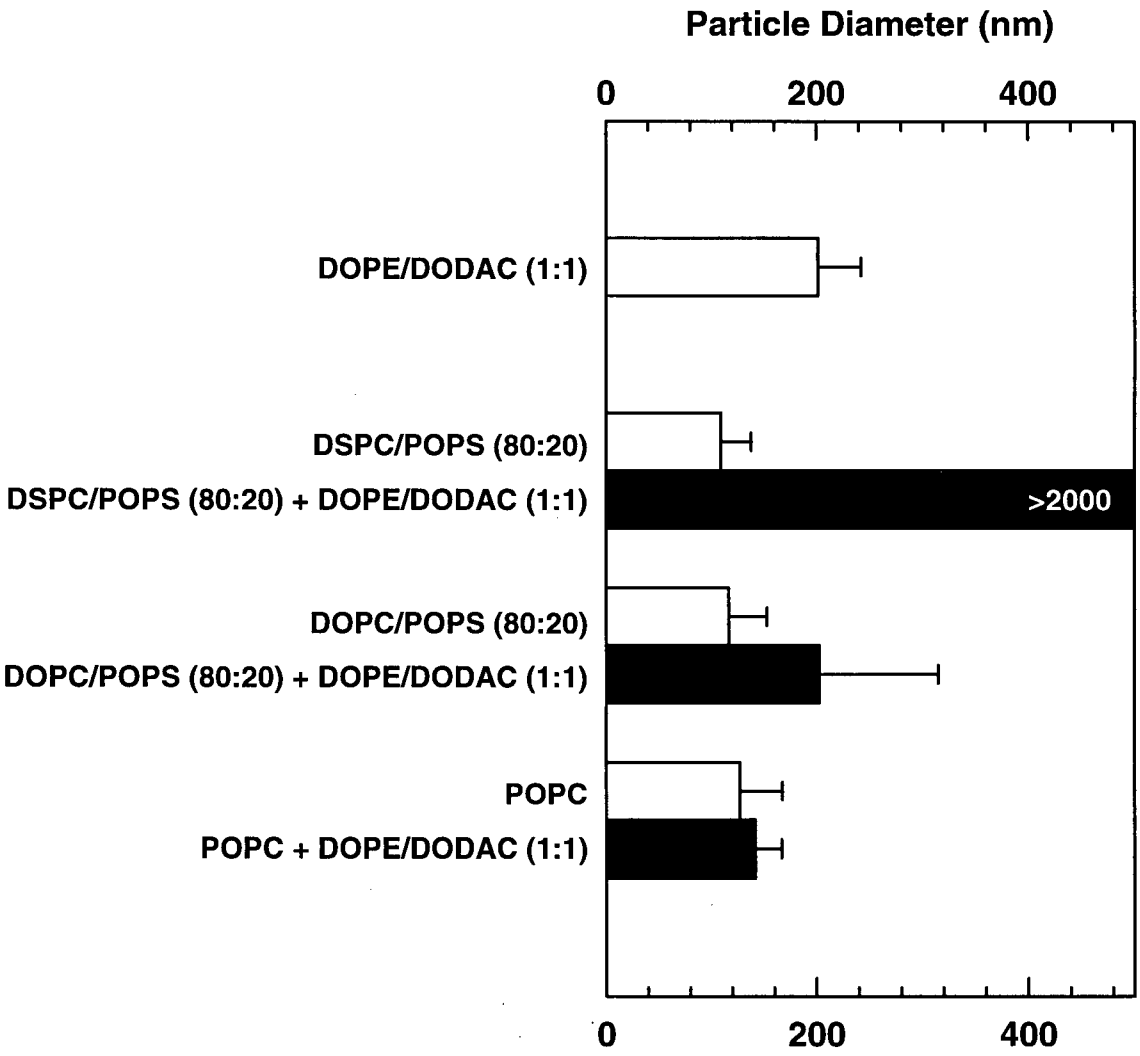

FIGURE 2.4 Size distributions of DOPE/DODAC (1:1) liposomes and 1:3 mixtures of DOPE/DODAC (1:1) with DSPC/POPS (80:20), DOPC/POPS (80:20) and POPC determined by quasi-elastic light scattering. Data accumulation was begun 5 minutes after addition of target vesicles and continued for five minutes with a photopulse rate of 350-400 kHz.

smaller, measurable size increase of about 75% with an accompanying increase in size distribution. POPC vesicles without any negatively charged lipid gave no significant size increase when mixed with DOPE/DODAC. The size of the DOPE/DODAC (1:1) liposomes prior to addition of target vesicles is also given. Note that while the cationic liposomes are larger than expected for the given extrusion conditions due to their instability in HBS, they were combined with target vesicles in a ratio of 1:3 as for the lipid mixing assays. Therefore, the size increase observed for the mixture with DOPC/POPS is not simply a result of mixing vesicle populations of two different sizes. This is demonstrated by the POPC control, where no such increase is observed.

The effect of lipid saturation in target vesicles on fusion with DODAC/DOPE LUVs was also determined by freeze-fracture electron microscopy (Figure 2.5). Addition of DSPC/POPS (80:20) vesicles to DOPE/DODAC resulted in very large aggregated structures with complex networks of continuous membrane. This correlates well with the high degree of membrane fusion indicated by the lipid mixing assay and the formation of very large particles as determined by light scattering. Addition of DOPC/POPS (80:20) target vesicles to DOPE/DODAC (1:1) gave numerous, distinct, large lipid vesicles (approaching 1 μm) indicating extensive fusion of liposomes without the formation of large aggregates, again in agreement with lipid mixing and light scattering results. The surfaces of these large vesicles are mostly smooth with some small indentations. These indentations, called "lipidic particles", have previously been observed in fusing liposomal systems and have been attributed to the existence of non-bilayer fusion intermediates

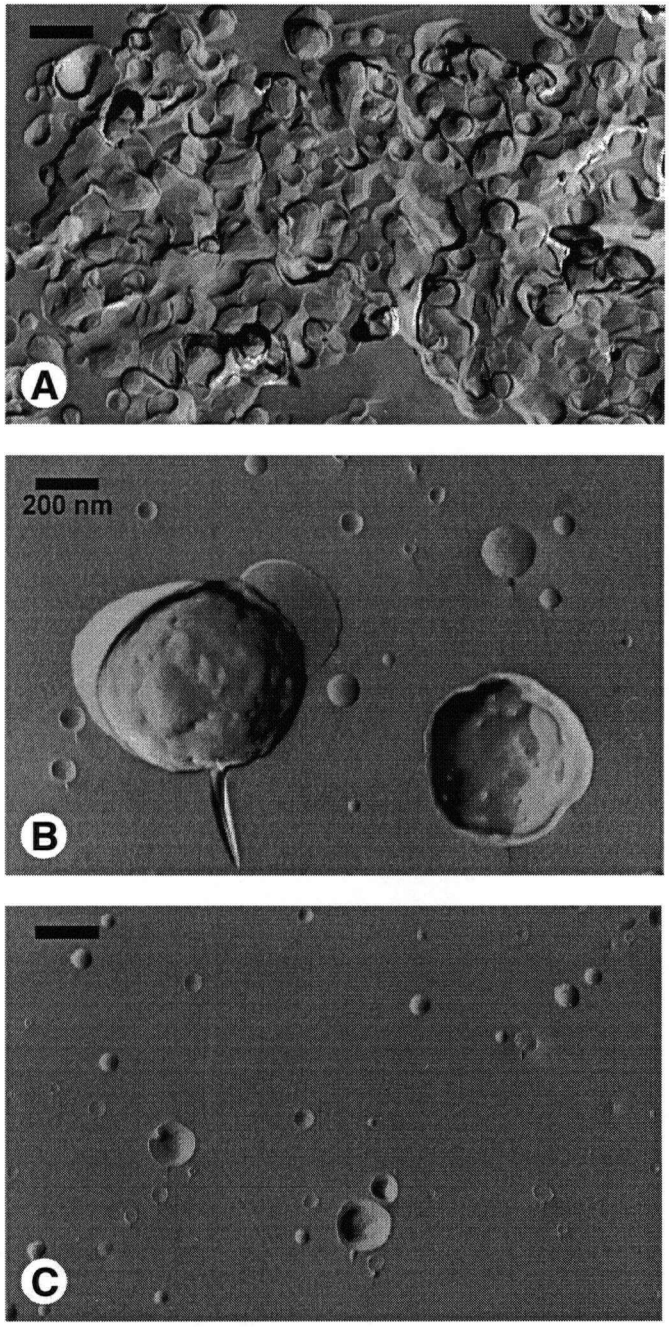

FIGURE 2.5 Freeze-fracture electron micrographs of DOPE/DODAC (1:1) liposomes mixed in a 1:3 lipid ratio with liposomes composed of (**A**) DSPC/POPS (80:20), (**B**) DOPC/POPS (80:20), and (**C**) POPC. Total lipid concentration was 10 mM. Samples were incubated for 5 minutes at 25°C and mixed 1:1 with glycerol prior to preparation of platinum–carbon replicas. Original magnification was 20,000x, and bars represent 200 nm.

(Verkleij *et al.*, 1980). The freeze-fracture micrograph of the control mixture of POPC liposomes with DOPE/DODAC (1:1) indicated no membrane fusion with mostly 100 nm LUVs and some larger vesicles (~200 nm) which can be attributed to DOPE/DODAC vesicles (see size analysis).

Effect of Cholesterol on Disaturated Lipid Vesicles.

The presence of cholesterol in DSPC or DPPC membranes results in the disappearance of the gel state and the formation of an ordered liquid-crystalline phase (Bloom *et al.*, 1991). At 25°C, this ordered lamellar phase can be detected with the addition of 3-4 mol% cholesterol, and at concentrations greater than 25 mol% no gel state domains remain. To demonstrate that the existence of the gel phase lipid was responsible for the extensive lipid mixing observed for the disaturated phospholipid target vesicles, we studied the effect of adding increasing levels of cholesterol to DSPC vesicles while maintaining the level of negatively charged POPS at 20 mol% (Figure 2.6). Addition of 5 to 10 mol% cholesterol gave small increases in lipid mixing, but at 20 mol% cholesterol, the level of fluorescence attained was diminished and at 45 mol% cholesterol it was reduced to less than half. Interestingly, the decreases in lipid mixing observed at the higher levels of cholesterol appeared to be accompanied by an increase in vesicle aggregation as evidenced by the decrease in the fluorescence over time and by the turbid appearance of the sample.

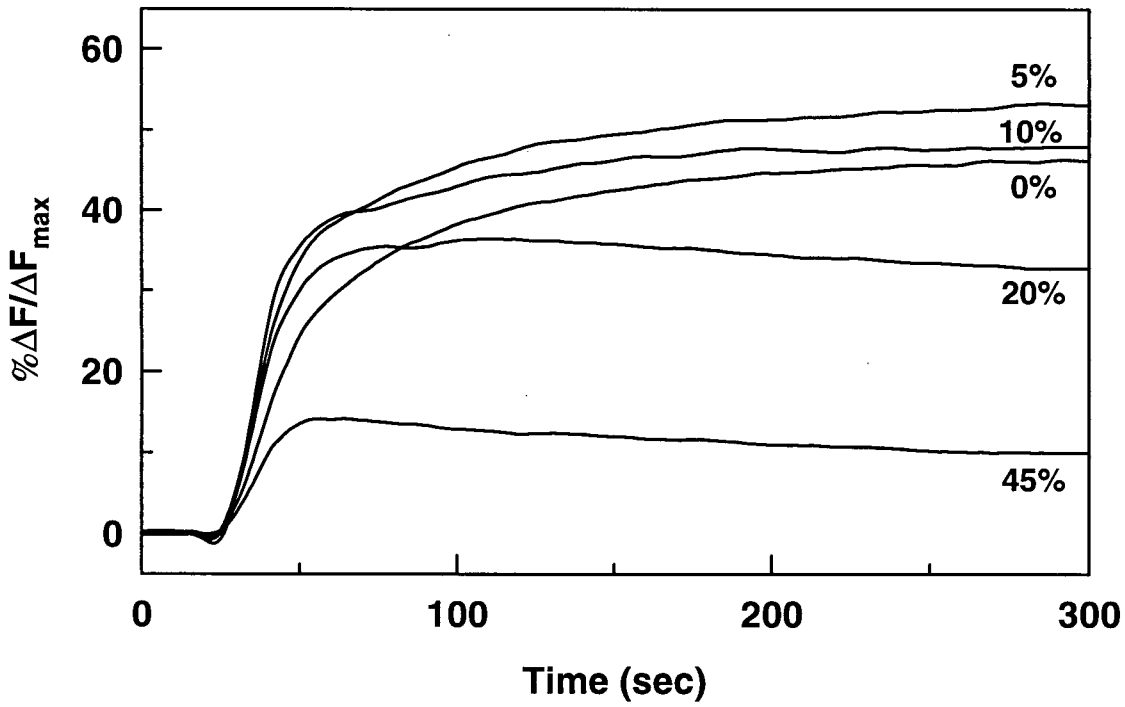

FIGURE 2.6 Effect of cholesterol concentration on lipid mixing of DOPE/DODAC (1:1) and DSPC/Cholesterol. At 30 seconds, DSPC/Chol liposomes prepared with Chol concentrations ranging from 0 to 45 mol% were added to fluorescently labeled DOPE/DODAC liposomes.

Lipid Mixing with Erythrocyte Ghosts.

The destabilization of DOPE/DODAC vesicles by the addition of liposomes containing negatively charged phospholipids is a crude model to study the interaction of cationic liposomes with biological membranes. The outer leaflets of cell membranes normally have very low levels of negatively charged phospholipids (Houslay & Stanley, 1982). The negative surface charge of cells arises primarily from the presence of acidic residues on membrane proteins and glycolipids. It is assumed that the observed interactions of cationic liposomes with cells involve charge attraction to anionic residues near the cell surface.

Erythrocyte ghosts were added to DOPE/DODAC (1:1) liposomes in HBS to demonstrate lipid mixing of this cationic lipid system with a biological membrane (Figure 2.7). An initial drop in NBD-PE fluorescence occurred due to light scattering of the relatively large ghosts. Fluorescence then increased over the duration of the assay, reaching a value of $\Delta F/\Delta F_{max}$ ~ 40 % at five minutes. The high rate of fusion observed is presumably due to anionic residues present on the exterior of the erythrocyte membrane. The importance of these negatively charged residues was demonstrated by mixing DOPE/DODAC liposomes with vesicles composed of EPC/ESM/Chol (1:1:2) which approximates the lipid composition of the outer leaflet of the erythrocyte membrane (Houslay & Stanley, 1982). Very little lipid mixing was observed.

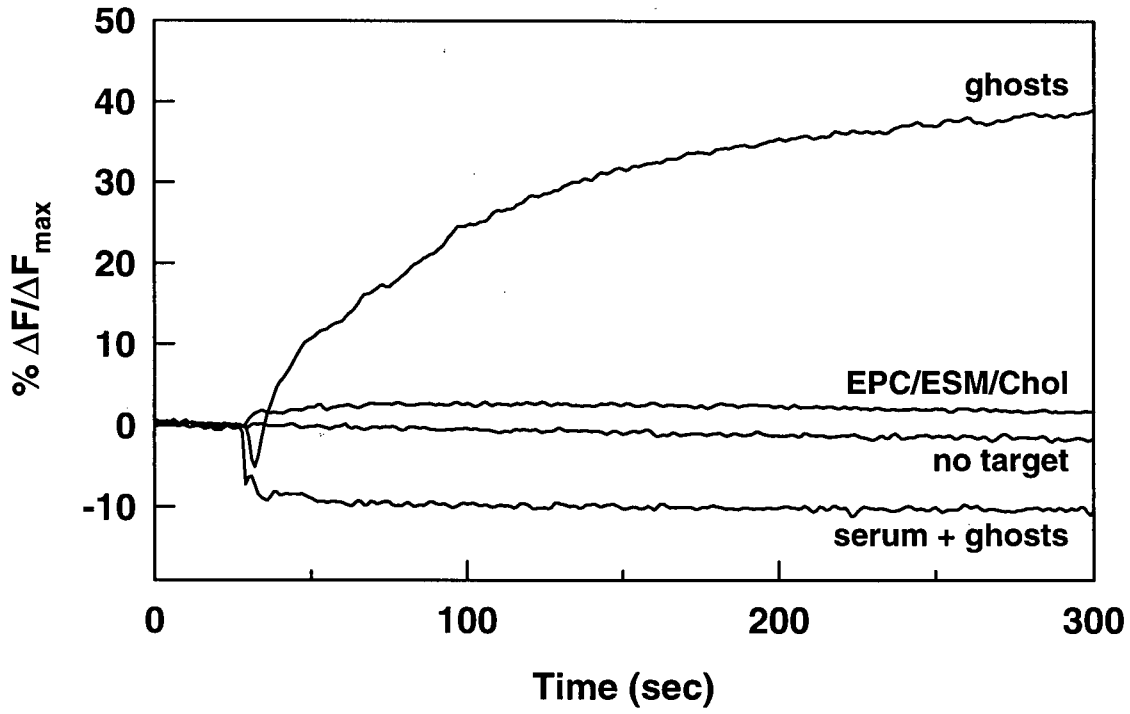

FIGURE 2.7 Fusion of DOPE/DODAC (1:1) liposomes with erythrocyte ghosts. Fluorescently labeled liposomes and ghosts were mixed in a 1:3 lipid ratio (0.2 mM total lipid) at 30 seconds either in the absence or presence of 1% (v/v) mouse serum. For comparison, EPC/ESM/Chol (1:1:2) was assayed as a model of the lipid composition of the outer leaflet of the erythrocyte membrane. Also shown is a control without the addition of ghosts or target vesicles.

The high level of lipid mixing between DOPE/DODAC (1:1) and erythrocyte ghosts is in contrast to previous reports that cationic liposomes do not fuse with the plasma membranes of cultured cells *in vitro* and that endocytosis of lipid/DNA complexes is necessary for transfection (Wrobel & Collins, 1995). However, the presence of as little as 1% serum eliminates lipid mixing between DOPE/DODAC and erythrocyte ghosts (Figure 2.7), presumably due to interactions of serum proteins with the cationic liposomes. Serum, which is normally included in the medium of cultured cells, would therefore be expected to inhibit fusion of cationic liposomes with cell membranes.

Lipid mixing of fluorescently labelled DOPE/DODAC (1:1) liposomes and erythrocyte ghosts as well as the effects of serum were also observed by confocal fluorescence microscopy (Figure 2.8). Prior to lipid mixing, the Rh-PE is present in the DOPE/DODAC at self-quenching concentrations (Arbuzova *et al.*, 1993). Five minutes after the addition of erythrocyte ghosts, many of the ghosts exhibit Rh-PE fluorescence. In the presence of 1% serum, however, no labeling of ghosts occurs.

DISCUSSION

Fusion of cationic liposomes composed of DOPE/DODAC (1:1) with a population of target membranes is dependent on the concentration of negative charge in the target. The negative charge has several probable roles. First it promotes close contact between the two membrane surfaces by charge attraction. This results in a mutual surface-charge neutralization which reduces the hydrophilic nature of the apposed membranes and

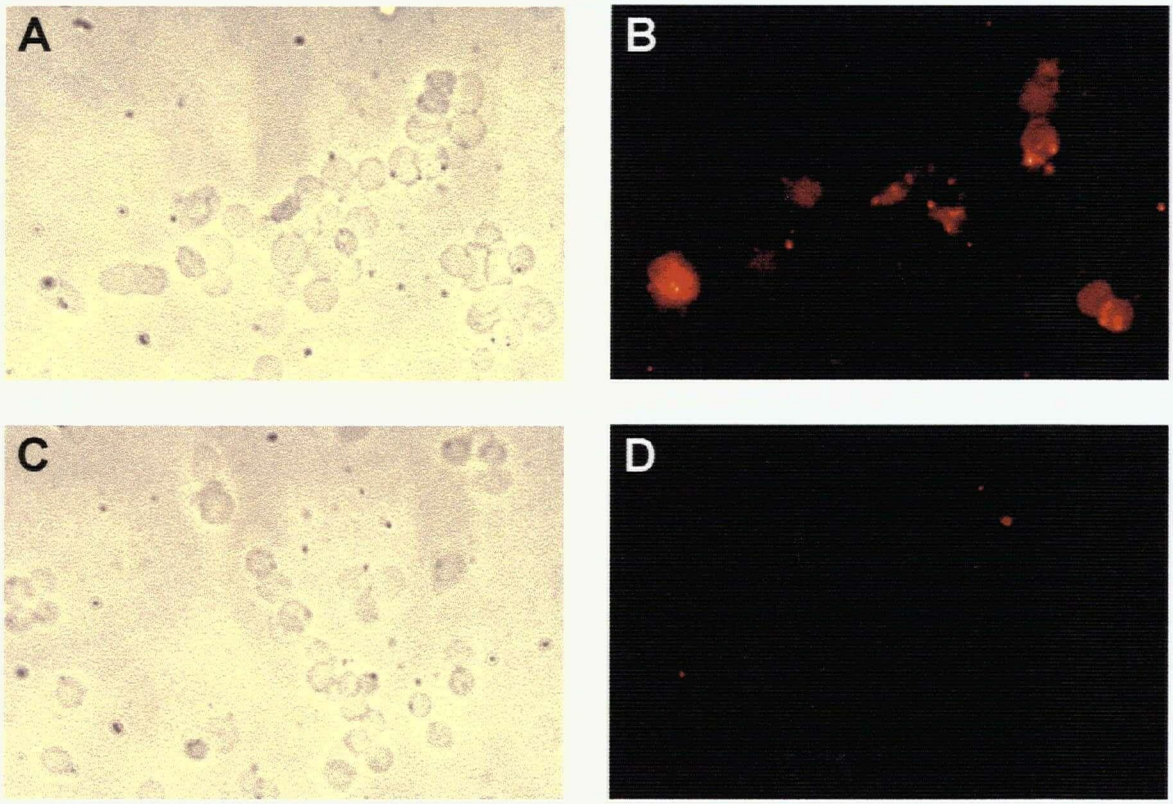

FIGURE 2.8 Fluorescence micrographs showing the appearance of Rh-PE in erythrocyte ghosts upon lipid mixing with labeled DOPE/DODAC (1:1). Liposome and ghosts were mixed in a 1:3 lipid ratio (1 mM total lipid): (**A**) phase contrast and (**B**) Rh-PE fluorescence in HBS; (**C**) phase contrast and (**D**) Rh-PE fluorescence when liposomes were pre-incubated with 1% (v/v) mouse serum prior to addition of ghosts. Original magnification, 200x.

promotes intimate contact by the loss of water previously bound through hydrogen bonding. Finally, the neutralization of the DODAC promotes membrane destabilization by virtue of the preference of DOPE to adopt non-bilayer structures, in the same way that addition of multivalent anions or high salt concentrations destabilize these systems.

While in our model systems, the negative charge is provided by an anionic phospholipid, it appears that the negative charges associated with cell membranes such as acidic residues on glycolipids or proteins can also fulfill this role. Erythrocyte membranes do not have negatively charged phospholipids exposed on the outer leaflet, yet they readily fuse with DOPE/DODAC liposomes in the absence of serum. If, in the presence of serum, fusion of cationic liposomes with cellular membranes occurs only after endocytosis, as appears to be the case, destabilization of the cationic liposomes might be promoted by anionic residues of the endosomal membrane or soluble components of the matrix.

Destabilization of DOPE/DODAC liposomes was promoted by the presence of high concentrations of DOPE in the target membranes, which is again attributed to the preference of this lipid to adopt hexagonal phase. Lipid mixing was also promoted by the disaturated lipids, DPPC and DSPC, which do not form hexagonal structures. This unexpected effect is attributed to the presence of defects in LUVs composed of saturated PCs at temperatures below the gel-to-liquid-crystalline transition temperature. As shown by Nayar *et al.*(1989), these defects can be visualized by freeze-fracture electron microscopy as interfaces between planar regions on the LUV surface. The ability of cholesterol to inhibit gel phase formation and the corresponding loss of lipid mixing with

DODAC/DOPE LUVs suggests a role for the hydrophobic defects present in gel state LUVs in the fusion events. Whether these defects promote vesicle aggregation through increased van der Waal's attractions or actually promote the formation of non-bilayer intermediates cannot be established without further experiments. However, as stated in Capter 1, previous studies have shown that membrane destabilization leading to increased aggregation rates is accompanied by corresponding increases in lipid mixing rates.

A complete understanding of the processes by which DNA complexes with cationic liposomes achieve cellular transfection must include an understanding of the role of the cellular membranes in these processes, and how their interactions with cationic liposomes are influenced by membrane composition. It is clear from this work that destabilization by and fusion with cationic liposomes depends not only on charge attraction leading to contact with the target membrane but also on the composition of the target membranes which determines the propensity of the target membrane to undergo fusion.

CHAPTER 3

MODULATION OF MEMBRANE FUSION BY ASYMMETRIC TRANSBILAYER DISTRIBUTIONS OF AMINOLIPIDS

In this chapter, membrane fusion induced by synthetic aminolipids which rapidly redistribute across lipid bilayers in response to imposed pH gradients is demonstrated. At low pH, these compounds are positively charged and form stable bilayers in various lipid mixtures, but at neutral pH they promote H_{II} phase and lipid mixing in the absence of multivalent salts or additional neutralizing species. The ability of the neutral form to rapidly cross lipid bilayers in response to pH gradients permits the control of membrane fusion by lipid asymmetry.

This work is based on previous studies showing that unsaturated diglycerides are extremely potent fusogens (Das & Rand, 1986) and that uncharged lipids are more able to adopt or induce non-bilayer structures than their charged forms (Cullis *et al.*, 1986). In particular, it was reasoned that a diglyceride substituted with an amino function should be highly fusogenic at pH values above the pK_a of the conjugate acid of the amine, while at lower pH values the presence of headgroup charge would be more compatible with bilayer structure. Further, the presence of the amino function should allow the aminolipid to be sequestered on the inner monolayer of LUVs with an acidic interior, as has been previously demonstrated with stearylamine (Hope & Cullis, 1987).

We have synthesized a number of aminolipids that have behaviours consistent with these expectations. These synthetic compounds exhibit varying degrees of fusogenicity which

correlate with their chemical structure and acid-base properties. Of particular interest is a preparation of 5 mol% 1,2-dioleoyl-3-N,N-dimethylaminopropane (AL1) in LUVs consisting of EPC/DOPE/Chol (35:20:45). In these systems, it is shown that AL1 can be sequestered on the inner monolayer by a pH gradient (pH_i = 4.0, pH_o = 7.5), and dissipation of the pH gradient results in the outward movement of AL1 and extensive liposomal fusion.

MATERIALS AND METHODS

Lipids and Chemicals

EPC, DOPE, NBD-PE, and Rh-PE were obtained from Avanti Polar Lipids (Alabaster, AL). ANTS and DPX were purchased from Molecular Probes (Eugene, OR). Oleic acid, cholesterol, nigericin, potassium 2-*p*-toluidinylnaphthalene-6-sulphonate (TNS), and all buffers were supplied by Sigma Chemical Co. (St. Louis, MO). 3-*N,N*-Dimethylamino-1,2-propanediol, oxalyl chloride, acetyl chloride, butyric acid, and decanoyl chloride were purchased from Aldrich Chemical Co. (Milwaukee, WI), and 9,10-d_2-oleic acid was supplied by Cambridge Isotope Laboratories (Woburn, MA). Organic solvents were all HPLC grade and were used without redistillation.

Synthesis of ±-1,2-dioleoyl-3-N,N-dimethylaminopropane (AL1)

This compound was prepared by the method of Leventis and Silvius (1990). Three ml (35 mmol) of oxalyl chloride was added to 1.0 g (3.5 mmol) oleic acid dissolved in 10 ml benzene and stirred at room temperature for 1 h. After removal of solvent and excess

oxalyl chloride under vacuum, the acid chloride was dissolved in 5 ml diethyl ether, and a further 5 ml of ether containing 0.20 g (1.7 mmol) of 3-*N,N*-dimethylamino-1,2-propanediol and 0.15 g pyridine was added. The resulting mixture was stirred at room temperature for 30 minutes before quenching with 1 ml methanol and removing solvents under vacuum. The crude product was dissolved in 50 ml hexane and washed with 2 x 25 ml 0.1 M potassium hydroxide in methanol/water (1:1) followed by 25 ml 0.1 M aqueous sodium chloride. Drying over anhydrous sodium sulphate and removal of hexane under vacuum gave a slightly yellow oil. Column chromatography on silica gel (70-230 mesh), eluting with ethyl acetate, gave 0.92 g (84%) of pure product (TLC, $R_f = 0.5$). The structure of the product was confirmed by 200 MHz ^{1}H-NMR. Similar procedures were used to prepare the deuteriated analogue, ±-1,2-bis(9',10'-dideuteriooleoyl)-3-*N,N*-dimethylamino-propane (AL1-d_4) and ±-1,2-didecanoyl-1-*N,N*-dimethylaminopropane (AL6). See Figure 3.1 for structures.

Synthesis of ±-1-oleoyl-2-hydroxy-3-N,N-dimethylaminopropane (AL2) and asymmetric ±-1,2-diacyl-3-N,N-dimethylaminopropanes (AL3-AL5)

Oleoyl chloride (3.5 mmol), prepared as above, was dissolved in 5 ml THF and added to a five-fold excess of 3-*N,N*-dimethylamino-1,2-propanediol (2.0 g, 17 mmol) and 0.15 g

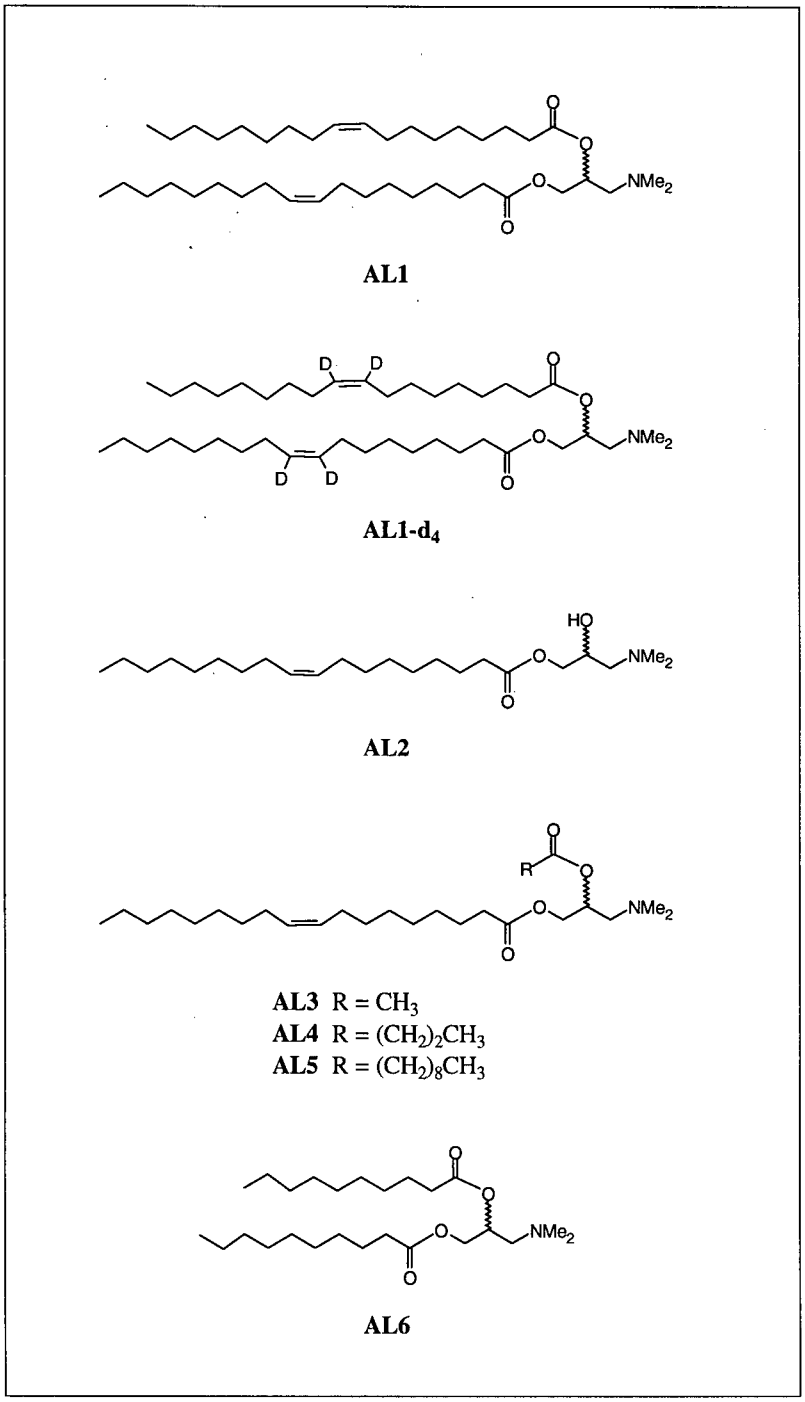

FIGURE 3.1 Structures of the synthetic aminolipids used in this study. All compounds are based on 3-*N*,*N*-dimethylamino-1,2-propanediol and are optical racemates as indicated by the jagged bond at the two position of the aminoglycol backbone.

pyridine in 25 ml THF at 0 °C. Crude 1-monooleoyl-2-hydroxy-3-N,N-dimethylamino-propane (AL2) was isolated as above and purified by column chromatography on silica gel using ethyl acetate/methanol (3:1) as eluant (R_f 0.4). Subsequent acylation with one equivalent of acetyl chloride, butyryl chloride, or decanoyl chloride with reaction conditions, extraction procedures, and purification as described above produced AL3, AL4, and AL5, respectively.

Preparation of LUVs

Chloroform solutions of lipids were dried by vortexing under nitrogen followed by removal of residual solvent under high vacuum for 1 hour. The resulting lipid films were hydrated by vortex-mixing with appropriate buffers to produce MLVs. Five freeze-thaw cycles were used to achieve homogeneous mixtures. The MLVs were extruded ten times through two 100 nm pore-size polycarbonate filters to produce LUVs.

Determination of pK_a for Aminolipids in Lipid Vesicles

To determine the pH at which the synthetic aminolipids AL1-AL6 in liposomal membranes lose their positive charge, LUVs containing 0 and 10 mol% of each aminolipid in EPC/Chol (55:45) were prepared in 5 mM HEPES, 5 mM ammonium acetate, 5 mM KCl, 1 μM nigericin at pH 7.5. Preparations were diluted to 25 μM total lipid in 5 mM HEPES, 5 mM ammonium acetate, 5 mM KCl, 2 mM TNS at pHs ranging from 3.0 to 10.0. The surface charge was monitored by determining the TNS fluorescence at each pH,

which was measured on a Perkin Elmer LS-50 spectrofluorometer using excitation and emission wavelenths of 321 nm and 445 nm, respectively.

Determination of Lipid Asymmetry by TNS Fluorescence

The transport of AL1 to the inner monolayer of vesicles and the subsequent redistribution to the outer monolayer was demonstrated by TNS fluorescence using a procedure adapted from Eastman *et al.* (1991). EPC/Chol (55:45) vesicles were prepared with 0 and 10 mol% AL1 in either 300 mM citrate, pH 4.0, or 20 mM HEPES, 150 mM NaCl, pH 7.5. For the samples prepared at low pH, the external buffer was exchanged for 300 mM sucrose, 1 mM citrate, pH 4.0, on Sephadex G-25 columns. All samples were diluted to 30 mM total lipid. TNS fluorescence time courses were performed over 200 seconds as follows. At 10 seconds, 10 µl of lipid was added to 3 ml of buffer containing 20 mM HEPES, 150 mM NaCl, 5 µM TNS, at pH 7.5. At 100 seconds, 30 µl of 10 µM nigericin was added.

Lipid-Mixing Fusion Assay

Fusion was monitored by the decrease in resonance energy transfer (RET) resulting from fluorescent probe dilution as described in Chapter 1. LUVs of a desired composition were prepared in 300 mM citrate, pH 4.0. Similar vesicles containing 0.5 mol% of both NBD-PE and Rh-PE were also prepared. External buffer was exchanged for 1 mM citrate, 300 mM sucrose, pH 4.0, on Sephadex G-25 columns before diluting preparations to 10 mM lipid. For fusion assays, 20 µl fluorescently labelled vesicles and 60 µl unlabelled

vesicles were added to 3.92 ml of 20 mM HEPES, 150 mM NaCl, pH 7.5. After 5 minutes of incubation at room temperature, a 3 ml aliquot was added to a cuvette, and the fluorescence was monitored over time. Excitation and emission wavelengths were 465 nm and 535 nm, respectively, and a 530 nm emission cutoff filter was used. To dissipate the gradient and induce fusion, 100 µl of 3.0 M ammonium acetate was added at 30 seconds.

Each lipid mixing time course was normalized using three control curves: (i) an assay excluding unlabelled vesicles (F_{nu}) to account for the effect of pH-gradient dissipation on fluorescence due to lipid charge interactions; (ii) a maximum-fluorescence trace (F_{max}) measured after adding 100 µl of 25 mM Triton X-100; and (iii) a zero-fusion trace (F_0) in which no ammonium acetate was added. The percent change in fluorescence (% $\Delta F/\Delta F_{max}$) was then calculated as

$$\% \frac{\Delta F}{\Delta F_{max}} = 100 \times \left(\frac{F - F_{nu}}{F_{max} - F_0} \right)$$

for each point in the fluorescence time course. Liposomes containing both fluorescent probes at one quarter the concentration used in the assay gave $\Delta F/\Delta F_{max} = 80\%$, and fusion results presented were not corrected to reflect the increase observed upon addition of Triton X-100.

Contents-Mixing Fusion and Leakage Assays

Liposomes were prepared with either 25 mM ANTS, 300 mM citrate, pH 4.0, or 100 mM DPX, 300 mM citrate, pH 4.0. External buffer was exchanged with 1 mM citrate, 300

mM sucrose, pH 4.0, as described above, and the preparations were diluted to 10 mM total lipid. To detect contents-mixing, 40 µl of the ANTS preparation was combined with 120 µl of the DPX preparation and made up to 4 ml with 20 mM HEPES, 150 mM NaCl, pH 7.5. The quenching of ANTS by DPX was monitored by measuring ANTS fluorescence of a 3 ml aliquot over 30 minutes. Excitation and emission wavelengths were 360 nm and 530 nm, respectively, and a 490 nm emission cutoff filter was used. To dissipate pH gradients and induce fusion, 100 µl of 3.0 M ammonium acetate was added at 30 seconds. Maximum quenching was determined by repeating the assay with an equivalent amount of liposomes containing 6 mM ANTS, 75 mM DPX, 300 mM citrate, pH 4.0. Zero quenching was measured using only ANTS liposomes. Leakage upon dissipation of the pH gradient was determined by comparing the result obtained above with the ANTS/DPX liposomes with a similar assay in which 50 µl of 100 mM Triton X-100 was added at 30 seconds.

^{31}P-NMR and ^{2}H-NMR Spectroscopy:

Freeze-thawed MLVs of 5 mol% AL1-d_4 in EPC/DOPE/Chol (35:20:45) were prepared in 20 mM HEPES, 20 mM ammonium acetate, 150 mM NaCl, at pH 4.0 and pH 7.5 in deuterium depleted water. Sample concentrations were approximately 200 mM total lipid. High resolution ^{31}P spectra were recorded at 81.02 MHz on a Bruker MSL200 spectrometer, using a 2.8 µs pulse and 1 s repeat. Temperature was maintained at 23 °C with a liquid nitrogen flow system. The FID was accumulated over 1000 scans and transformed with 50 Hz line-broadening. ^{2}H-NMR broadline spectra were recorded at

46.175 MHz on a home-built 300 MHz spectrometer using a 5 μs 90° pulse, 50 μs interpulse spacing, 30.5 μs ring-down delay, and a 300 ms repetition time. A quadrupole echo sequence with eight step phase cycling was used to accumulate 200000 scans. The resulting FID was transformed with 100 Hz line-broadening.

Freeze-Fracture Electron Microscopy

LUVs consisting of 5 mol% AL1 in EPC/DOPE/Chol (35:20:45) were prepared as above in 300 mM sodium citrate at pH 4.0 with a total lipid concentration of 100 mM. External buffer was exchanged for 1 mM citrate, 300 mM sucrose, pH 4.0 on a Sephadex G-25 column before diluting the preparation to approximately 10 mM lipid with 20mM HEPES, 150 mM NaCl, pH 7.5. After removal of a control sample, the pH gradient was dissipated by addition of 3 M ammonium acetate, pH 7.5, to a final concentration of 100 mM. Platinum/carbon replicas were prepared as described previously (Fisher & Branton, 1974) for samples at 4, 15, and 30 minutes after dissipation of the gradient, as well as the control with the pH gradient present.

RESULTS

Effects of pH on Aminolipid Charge

The aminolipids would be expected to be more fusogenic in their neutral forms which predominate at pH values above the pK_a of the protonatable amino group. In order to sequester the aminolipid to the acidic interior, the lipid must be charged at the interior pH. The apparent pK_a's of the various aminolipids in a lipid bilayer were determined by

measuring the relative surface charges as a function of pH by TNS fluorescence. A pH titration curve of 10 mol% AL1 in EPC/Chol (55:45) vesicles is shown in Figure 3.2. Fluorescence was measured in the absence of pH gradients. Fitting the data to the Henderson-Hasselbach equation indicates an apparent pK_a of 6.58 for the conjugate acid of AL1. At pH 4.0, virtually all of the aminolipid is in the charged form, while at pH 7.5 approximately 90% is in the neutral form. These results suggest that the acid–base properties of AL1 are ideal for the induction of asymmetry by a pH gradient (pH_i = 4.0, pH_o = 7.5). In addition, the prevalence of the neutral form at pH 7.5 should provide the bilayer destabilization desired to induce membrane fusion.

The apparent pK_a of AL1 situated in the lipid bilayer is much lower than is expected for a tertiary amino group (pKa 9~10 in solution). This difference arises largely as a result of the apolar environment of the lipid bilayer. However, another important consideration is the influence of the surface potential induced by the positively charged aminolipid on the proton concentration near the bilayer surface. The surface potential will itself be pH dependent, such that deviations of the apparent pK_a from the intrinsic pK_a will be greatest

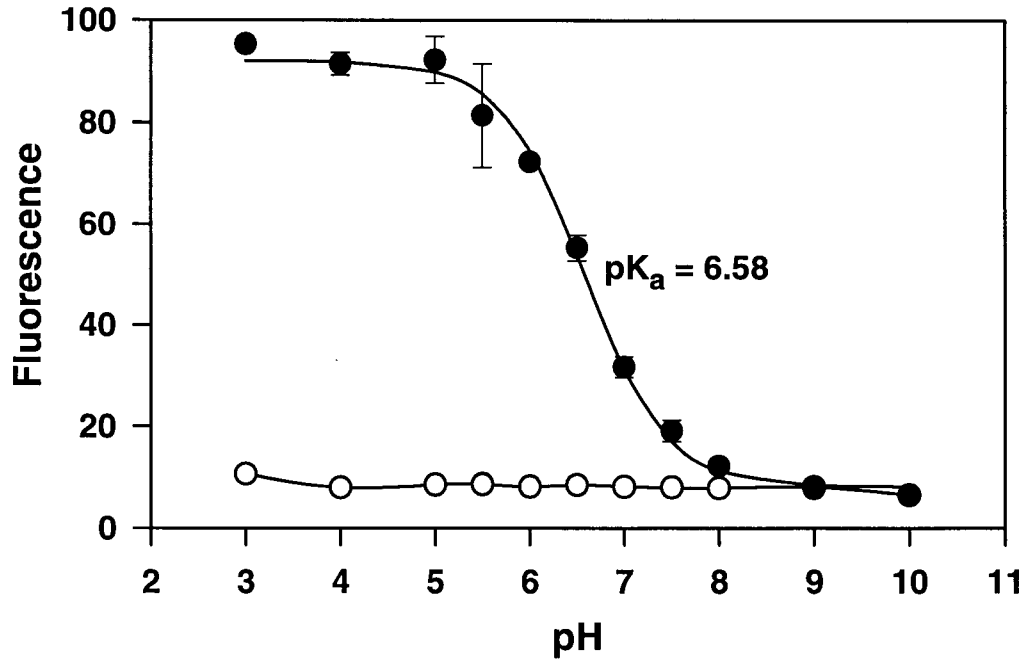

FIGURE 3.2 Effect of pH on the TNS fluorescence of EPC/Chol (55:45) vesicles containing 0 mol% (○) and 10 mol% (●) AL1. Liposomes were prepared in 5 mM HEPES, 5 mM ammonium acetate, and 1 μM nigericin at pH 4.0. Preparations were diluted to 25 μM total lipid in the same buffer containing 2 μM TNS at various pH's. Data shown represent mean values and standard deviations from duplicate experiments. Error bars are smaller than symbols unless indicated.

at low pH. Using methods provided by McLaughlin (1977) and from the ionic strength and surface concentration of AL1 used in the pH titration, we estimated a surface potential of 43mV at the equivalence point, corresponding to an intrinsic $pK_a = 7.30$.

A comparison of results derived from similar pH titration curves for the synthetic aminolipids AL2-AL6 is given in Table 3.1. The effects of chemical structure on the acid–base characteristics of the amines when incorporated into liposomes are manifested as changes in the apparent pK_a values observed and in the fraction of aminolipid species remaining charged at pH 7.5. These changes likely stem from the depth of penetration of the amine headgroup into the lipid bilayer as influenced by the relative hydrocarbon chain content and the polarity of the headgroup. Compound AL2, having only a single oleoyl chain and an unsubstituted hydroxy group, has an apparent pK_a of 7.57 compared to 6.58

Aminolipid	Apparent pK_a	% Charged at pH 7.5
AL1	6.58	11
AL2	7.57	54
AL3	6.79	16
AL4	6.66	13
AL5	6.73	14
AL6	6.81	17

TABLE 3.1 Apparent acid dissociation constants (pK_a) and percent charged species at pH 7.5 for aminolipids AL1-AL6. Data were derived from TNS fluorescence titrations as shown in Figure 3.2. Curves for each aminolipid were fit to Henderson-Hasselbach equations by iteratively varying pK_a and maximum and minimum fluorescence.

for AL1 with two oleoyl chains. Therefore, at pH 7.5 the AL2 headgroup remains greater than 50% charged. Esterification of the hydroxyl at the 2- position with acetate to give AL3 reduces the apparent pK_a to 6.79, and the fraction of charged species at pH 7.5 is only 16% compared to 11% for AL1. The remaining compounds, AL4–AL6, also have sufficient hydrocarbon content to have apparent pK_a 's and relative charges at pH 7.5 approaching those of AL1. The influence of the structural differences of these aminolipids on their fusogenic capacity is discussed below.

Asymmetry of Aminolipids in Liposomes

The effect of a pH gradient on the transbilayer distribution of the synthetic aminolipids was demonstrated by monitoring the changes in surface charge of vesicles comprised of aminolipids and EPC/Chol (55:45) by TNS fluorescence. Vesicles with internal pH of either 4.0 or 7.5 were injected into pH 7.5 buffer to give the fluorescence time-courses shown in Figure 3.3. Trace (a) is the fluorescence of 10 mol% AL1 in the absence of a gradient, internal and external pH 7.5. Trace (b) is the same lipid composition with an initial internal pH of 4.0. The pH gradient produced upon the addition of these vesicles to buffer at pH 7.5 results in an immediate attenuation of fluorescence relative to trace (a). When the pH gradient is dissipated by the addition of nigericin, the fluorescence in (b) increases to the value observed in (a). Nigericin is used to dissipate the gradient in this case, since TNS fluorescence is highly sensitive to shielding of the membrane surface charge by salts. Preparations containing no aminolipid either in the absence (c) or presence (d) of a pH gradient exhibited the same surface charge as those containing 10

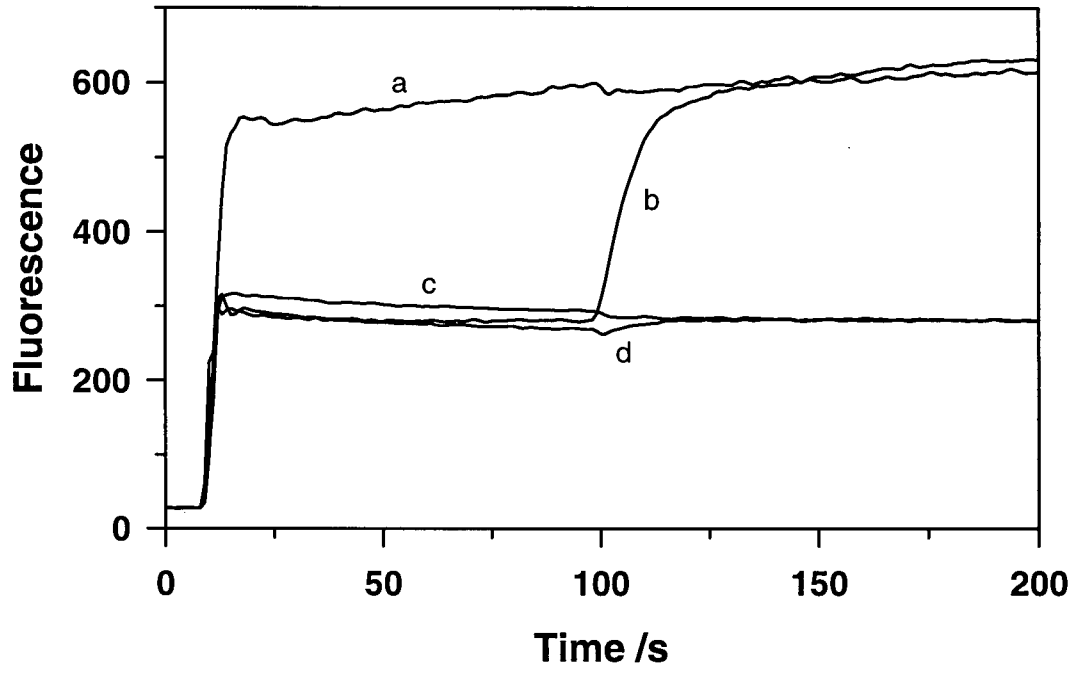

FIGURE 3.3 TNS fluorescence traces showing the effect of induction and dissipation of a pH gradient on AL1 in EPC/Chol (55:45) vesicles. At 10 seconds, liposomes prepared with either 10 mol% (a,b) or 0 mol% (c,d) AL1 were added to buffer containing 20 mM HEPES, 150 mM NaCl, 5 μM TNS, pH 7.5, to a final lipid concentration of 0.1 mM. Internal buffer was either 20 mM HEPES buffer, 150 mM NaCl, pH 7.5 (a,c) or 300 mM citrate, pH 4.0 (b,d). At 100s, nigericin was added to a final concentration of 0.1 μM.

mol% AL1 with a pH gradient. Note that the differences in fluorescence observed for liposomes containing AL1 reflect only the approximately 10% of the aminolipid which remains charged at pH 7.5. Also, the ionic strengths of both the internal and external buffers used in this experiment are much higher than was used in the pK_a determination above, which would result in decreased surface potential, a less significant proton gradient at the membrane surface, and a higher apparent pK_a.

Comparison of these traces clearly shows that the imposition of a pH gradient (pH_i = 4.0, pH_o = 7.5) causes rapid and complete loss of positive surface charge, and therefore AL1, from the outer monolayer. Subsequent dissipation of the gradient results in the redistribution of the aminolipid between the bilayers accompanied by an increase in surface charge. Similar behaviour was observed for the aminolipids AL2-AL6 (data not shown).

Fusion of Liposomes Containing AL1

The dissipation of the pH gradient across the membranes of vesicles with acidic interiors can also be achieved by the addition of ammonium ions which cross the membrane in the form of neutral ammonia to become protonated in the vesicle interior, thus raising the internal pH. As demonstrated above, for LUVs containing aminolipids primarily on the inner monolayer, the loss of the pH gradient causes a loss of transbilayer asymmetry accompanied by neutralization of the aminolipid. Lipid mixing resulting from this redistribution was monitored by a loss in RET between the fluorescently labelled lipids, NBD-PE and Rh-PE. When vesicles containing both of these labels fuse with unlabelled

vesicles, the dilution of the fluorescent probes results in increased fluorescence for NBD-PE. Appreciable exchange of these labelled lipids between vesicles does not appear to occur even in aggregated systems, and fluorescence increases only upon mixing of membrane lipids (Hoekstra, 1982).

The use of this fluorescent probe dilution assay to demonstrate lipid mixing in LUVs containing 0–20 mol% AL1 is depicted in Figure 3.4. Unlabelled and labelled vesicles (3:1) consisting of EPC/Chol (55:45) without AL1 showed no increase in fluorescence upon dissipation of the pH gradient. With 10 and 20 mol% AL1, only small increases in $\Delta F/\Delta F_{max}$ are observed (less than 2% over 5 minutes). This represents very limited lipid mixing. Complete lipid mixing under these conditions would give a $\Delta F/\Delta F_{max}$ of about 80%, as determined by preparing vesicles with the fluorescent labels at one quarter of the assay concentration. The low rates of increase in fluorescence observed indicate that the ability of AL1 to induce pH gradient-controlled fusion in EPC/Chol vesicles is limited. For AL1 concentrations greater than 20 mol% in EPC/Chol vesicles, rapid and complete aggregation was observed following extrusion at pH 4.0, making it impossible to study lipid asymmetry and fusion in such systems.

The rates of lipid mixing achieved with vesicles containing AL1 were improved by the addition of DOPE to the lipid preparation. DOPE provides additional membrane destabilization by virtue of its preference for hexagonal H_{II} phase. Fusion assays for EPC/DOPE/Chol vesicles containing 10 mol% AL1, where increasing levels of DOPE

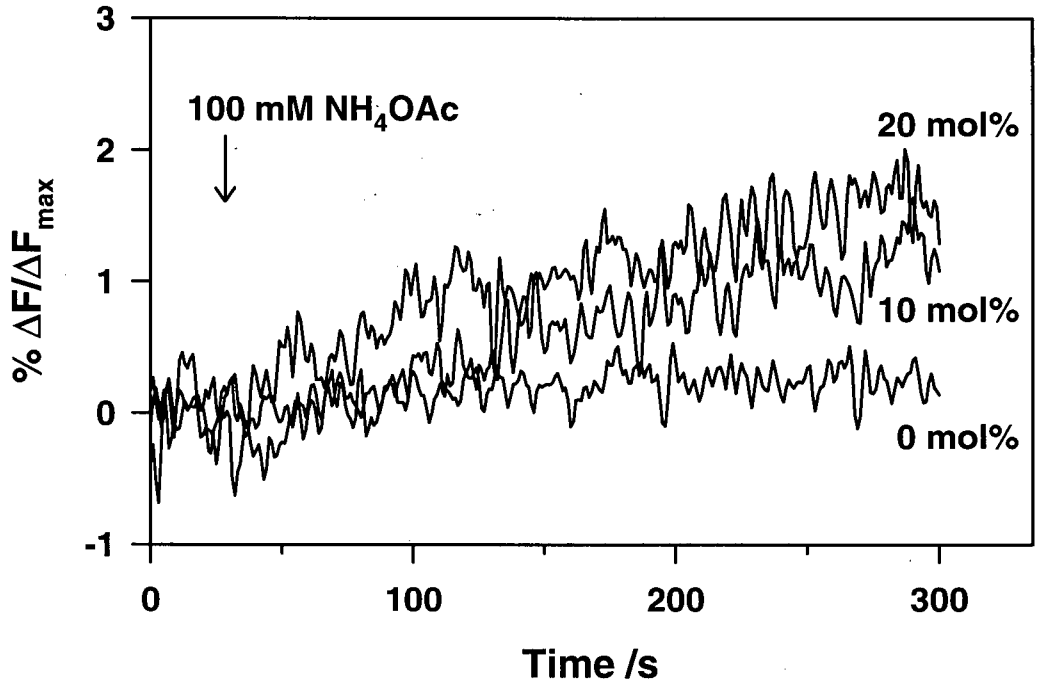

FIGURE 3.4 Effect of AL1 concentration (0–20 mol%) on fusion of EPC/Chol (55:45) vesicles by RET fluorescent probe dilution. Vesicles of each composition were prepared with and without 0.5 mol% each of NBD-PE and Rh-PE, an internal buffer of 300 mM sodium citrate, pH 4.0, and an external buffer of 20 mM HEPES, 150 mM NaCl, pH 7.5. The labeled and unlabeled vesicles were mixed in a 1:3 ratio and diluted to 0.20 mM total lipid. The pH gradient was dissipated by the addition of ammonium acetate to a final concentration of 100 mM at 30 seconds.

replace the EPC, are shown in Figure 3.5. Increases in lipid mixing rates were evident with increasing DOPE concentration up to a ratio of 35:20:45 (EPC/DOPE/Chol). This formulation gave a $\Delta F/\Delta F_{max}$ greater than 5% after 5 minutes. However, at this level of DOPE, some aggregation of vesicles was observed at low pH. Higher levels of DOPE again gave rapid aggregation.

The best rates of lipid mixing were observed when the AL1 concentration was reduced to 5 mol% in EPC/DOPE/Chol (35:20:45), as shown in Figure 3.6. At pH 4.0, this formulation produces stable vesicles which remain stable when the external pH is increased to 7.5. Dissipation of the pH gradient results in a nearly linear increase in $\Delta F/\Delta F_{max}$ over the first five minutes to a value greater than 10%. As expected for a liposomal fusion event, the rate of lipid mixing decreases with time, but lipid mixing clearly continues for the duration of the 15 minute assay.

The liposomal fusion observed in this lipid system by fluorescent lipid probe-dilution could not be confirmed by the ANTS/DPX contents-mixing assay (Ellens *et al.*, 1984). Dissipation of the pH gradient with ammonium acetate gave a rapid attenuation of ANTS fluorescence both in the presence and absence of DPX liposomes (Figure 3.7). This pH sensitivity may result from a change in the interaction of ANTS with AL1 or the inner liposomal monolayer upon neutralization and redistribution the aminolipid. After this initial loss of fluorescence and up to thirty minutes, there was no further decrease in ANTS fluorescence indicating fusion with DPX liposomes. In fact, the mixing assay gave a slight increase in fluorescence relative to the control assay with no DPX liposomes,

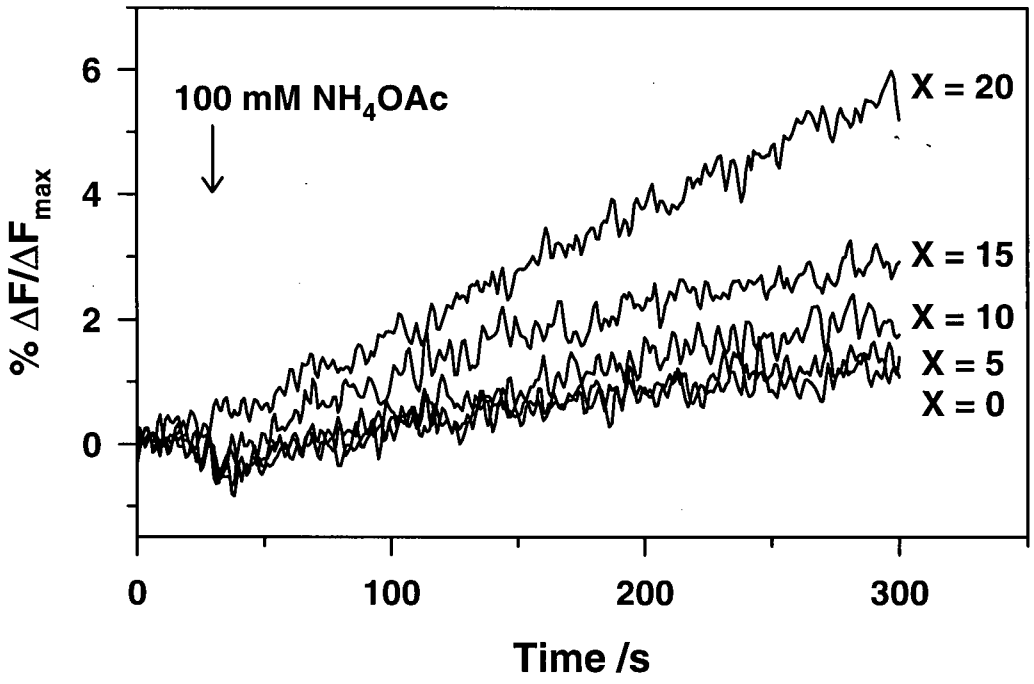

FIGURE 3.5 Effect of DOPE concentration on fusion rates of vesicles containing AL1. LUVs were prepared with EPC/DOPE/Chol (55-X:X:45, X = 0, 5, 10, 15, 20), 10 mol% AL1, with or without 0.5 mol% each of NBD-PE and Rh-PE, an internal buffer of 300 mM sodium citrate, pH 4.0, and an external buffer of 20 mM HEPES, 150 mM NaCl, pH 7.5. Fusion assays were carried out as described in Materials and Methods.

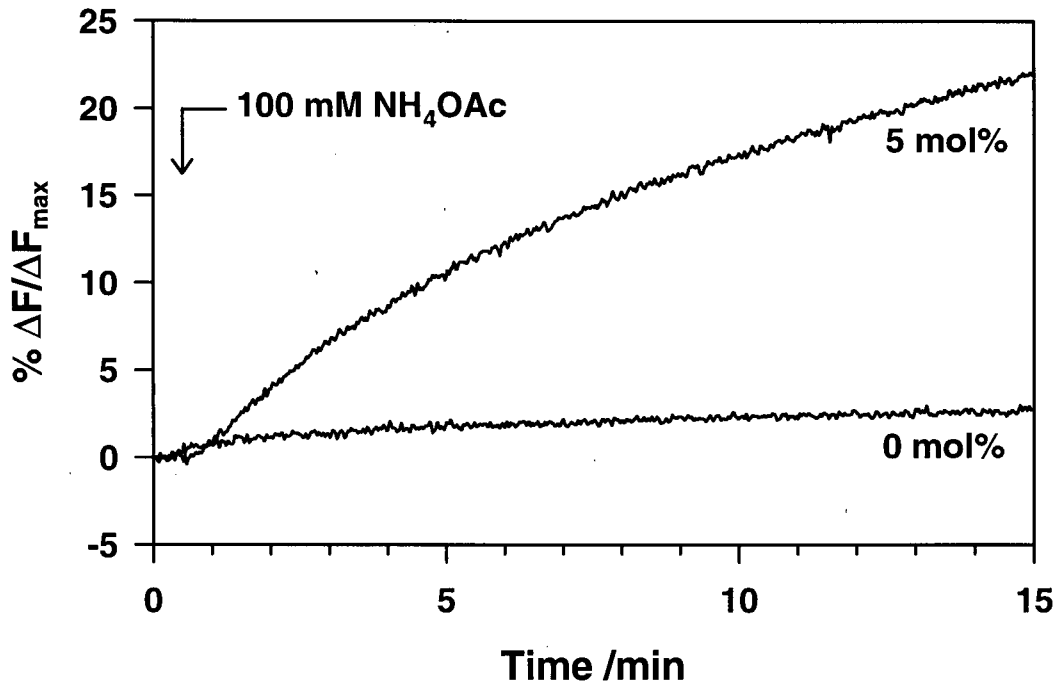

FIGURE 3.6 Fusion of vesicles consisting of 0 and 5 mol% AL1 in EPC/DOPE/Chol (35:20:45). LUVs were prepared with or without 0.5 mol% each of NBD-PE and Rh-PE, an internal buffer of 300 mM sodium citrate, pH 4.0, and an external buffer of 20 mM HEPES, 150 mM NaCl, pH 7.5. Fusion assays were carried out as described in Materials and Methods.

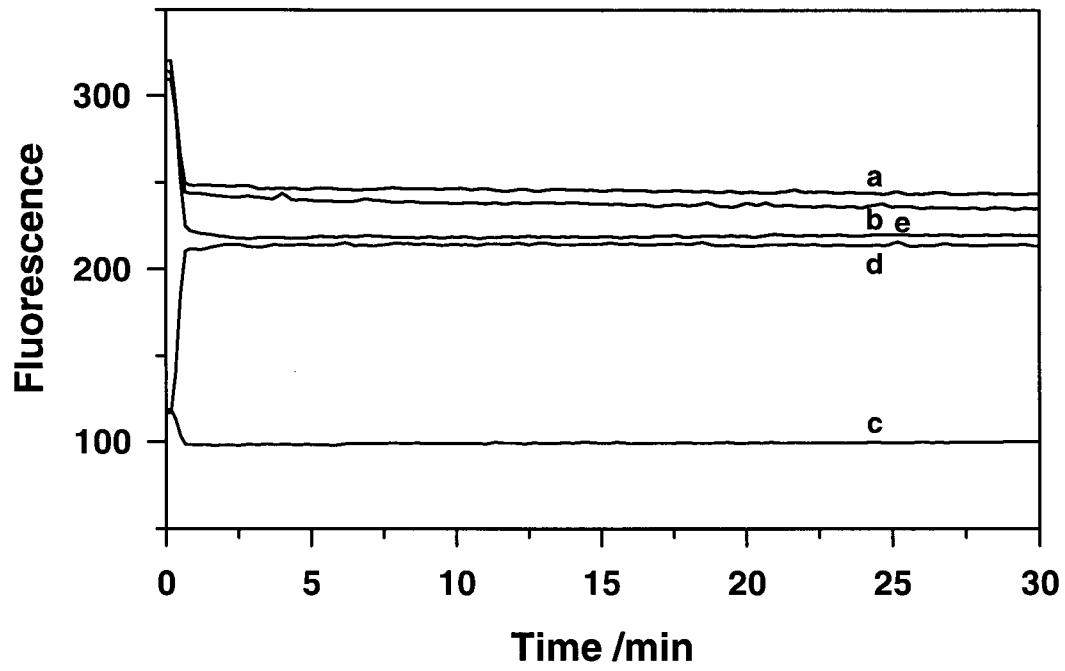

FIGURE 3.7 ANTS/DPX contents-mixing assays for liposomes consisting of 5 mol% AL1 in EPC/DOPE/Chol (35:20:45). (**a**) LUVs containing 300 mM citrate, pH 4.0, and either 25 mM ANTS or 100 mM DPX were mixed in a ratio of 1:3 (ANTS:DPX) in 20 mM HEPES, 150 mM NaCl, pH 7.5, to a final lipid concentration of 0.4 mM. The pH gradient was dissipated by the addition of ammonium acetate to a concentration of 100 mM at 30 seconds, and ANTS fluorescence was monitored over 30 minutes. (**b**) Control curve with no DPX liposomes, representing zero contents mixing. (**c**) Liposomes containing 6 mM ANTS and 75 mM DPX, representing maximum contents-mixing. (**d**) Same as **c** with the addition of Triton X-100 to a final concentration of 1.6 mM, representing maximum leakage. (**e**) Same as **a** with the addition of Triton X-100, to demonstrate fluorescence equal to **d**.

which is the opposite of the expected result. On the other hand, dissipation of the gradient for liposomes containing both ANTS and DPX gave, after the initial attenuation, no increase in fluorescence over 30 minutes, suggesting that leakage of liposomal contents also does not occur. Therefore, while liposomal fusion could not be confirmed with this contents-mixing assay, the lipid-mixing which was shown to occur appears not to be a result of membrane rupture. The terbium–dipicolinic acid (Tb/DPA) assay which has also been used for contents mixing cannot be applied for liposomes with acidic interiors (Ellens *et al.*, 1985).

^{31}P-NMR and ^{2}H-NMR Spectroscopy

The changes in phospholipid morphology which accompany the bilayer destabilization leading to fusion of vesicles containing AL1 were investigated by high resolution phosphorus-31 NMR. MLVs were prepared by incorporating 5 mol% of the deuterium chain-labelled analogue AL1-d_4 into EPC/DOPE/Chol (35:20:45) MLVs. The use of MLVs in this experiment avoids the loss of useful information caused by rapid tumbling of LUVs on the NMR timescale. Differences in morphology of the phospholipids, EPC and DOPE, at pH 4.0 and pH 7.5 are evident in the spectra shown in Figure 3.8(a). At pH 4.0, a typical bilayer signal with an upfield peak and a downfield shoulder is observed. At pH 7.5, the bilayer signal is reduced slightly and a hexagonal H_{II} signal is seen as a more intense downfield shoulder. The pH-induced destabilization of these vesicles clearly involves morphological changes for at least some of the phospholipid in the bilayer. The accompanying changes in the phase behaviour of AL1-d_4 can be seen in the quadrupolar

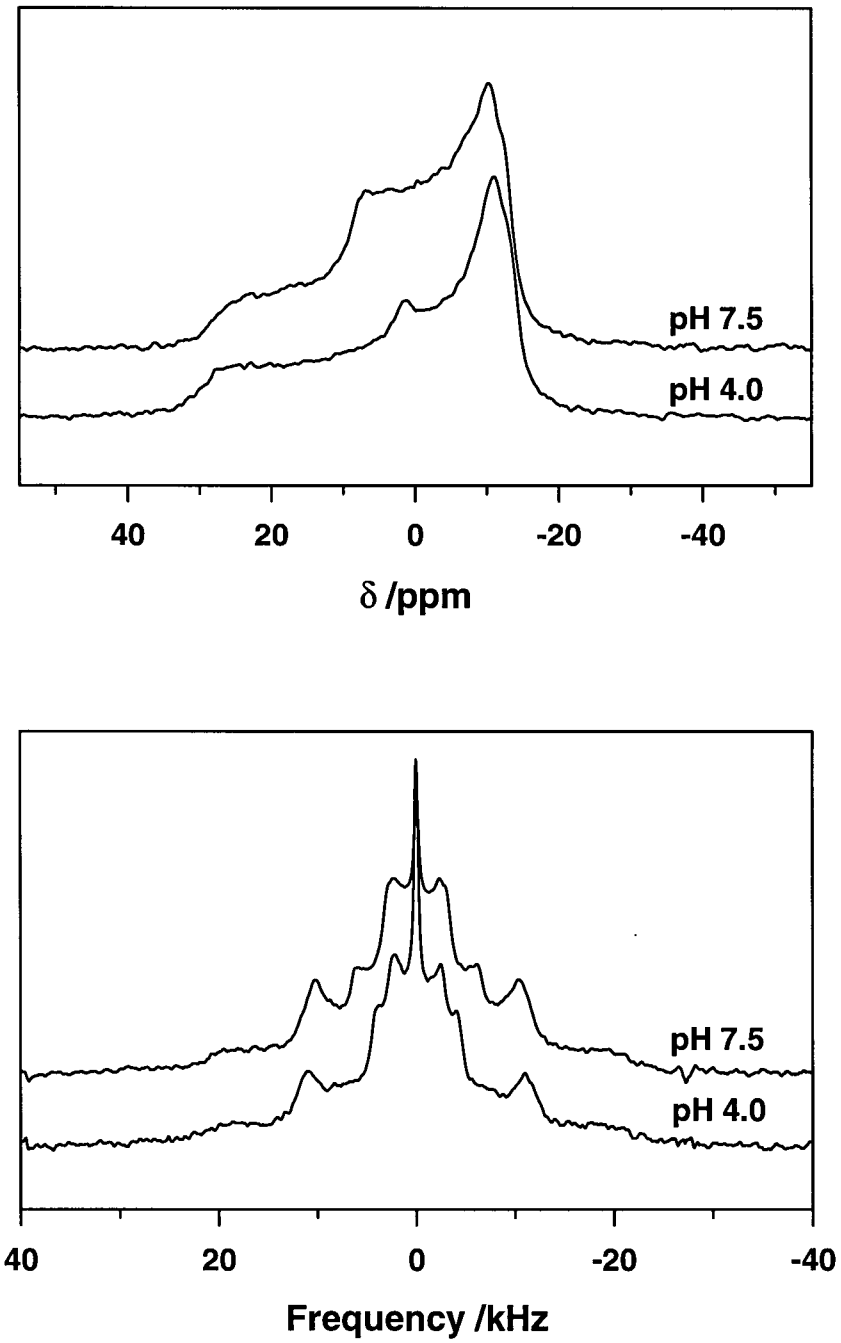

FIGURE 3.8 (a, top) ^{31}P-NMR and (b, bottom) ^{2}H-NMR spectra of freeze–thawed MLVs prepared with 5 mol% AL1-d_4 in EPC/DOPE/Chol (35:20:45) buffered with 20 mM HEPES, 20 mM ammonium acetate, 150 mM NaCl at pH 4.0 and pH 7.5.

deuterium spectra given in Figure 3.8(b). At pH 4.0, the ^2H spectrum shows deuterium splittings for the olefinic deuterons in the range expected for oleoyl chains on a lipid incorporated into a bilayer. The shoulders on the peaks arise from the non-identical chains on the 1 and 2 positions of the aminoglycol backbone, and the strong central isotropic signal probably results from the presence of smaller vesicles. In the sample prepared at pH 7.5, the bilayer signal persists, although it appears to be slightly less ordered, judging from the decrease in quadrupolar splittings. The aminolipid clearly remains associated with the bilayer. In addition, there is a distinct signal with a splitting of about 12 kHz, which we believe arises from the portion of the aminolipid in hexagonal H_{II} phase. The appearance of this signal is again consistent with the destabilization of the bilayer leading to membrane fusion.

Freeze-Fracture Electron Microscopy

Additional evidence of the fusion of vesicles consisting of 5 mol% AL1 in EPC/DOPE/Chol (35:20:45) is given by the freeze-fracture electron micrographs in Figure 3.9. Vesicles with the aminolipid sequestered on the inner monolayer prior to dissipation of the pH gradient ($pH_i = 4.0$, $pH_o = 7.5$) appear as well-defined individual spheres. Four minutes after the dissipation of the gradient by ammonium acetate, large aggregates and fused vesicles are already visible. This fusion process continues, and by 30 minutes, much of the lipid in the sample is found in very large fused vesicles.

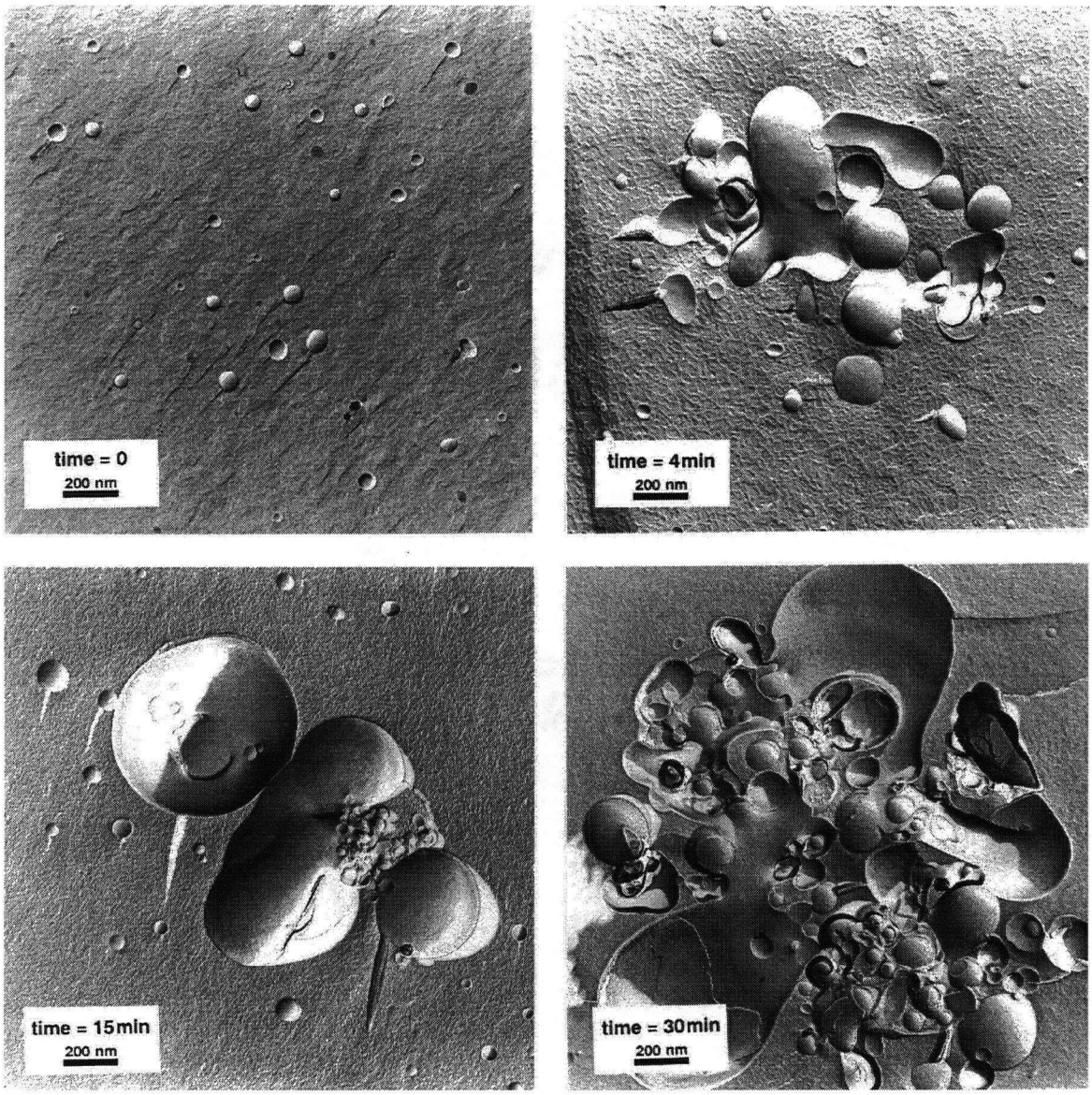

FIGURE 3.9 Freeze-fracture electron micrographs of 5 mol% AL1 in EPC/DOPE/Chol (35:20:45), with a pH gradient (time = 0, internal 300 mM sodium citrate, pH 4.0; external 20 mM HEPES, 150 mM NaCl, pH 7.5), and 4, 15, and 30 minutes after dissipation of the gradient by the addition of ammonium acetate to a final concentration of 100 mM. Lipid concentration was approximately 10 mM and original magnification was 20,000X.

Effects of Aminolipid Structure

A comparison of the fusogenic capacity of the aminolipids AL1-AL6 was made by assaying for lipid mixing with vesicles consisting of 5 mol% of each aminolipid in EPC/DOPE/Chol (35:20:45), shown in Figure 3.10. AL2, which has a single oleoyl chain, gives very little lipid mixing at pH 7.5 compared to liposomes without aminolipid. This lack of fusogenic activity probably results not only from the relatively high pK_a of AL2 which remains half-charged at this pH, but also from the small surface area occupied by the single hydrocarbon chain relative to the aminolipids with two chains. Bilayer destabilization requires a substantial imbalance between the size of the polar headgroup of the fusogenic lipid and its hydrophobic moiety. Esterification of the 2-position with acetate (AL3) produces a substantial increase in fusion rate, and lengthening this second chain to butyryl (AL4) or decanoyl (AL5) again gives small increases, with rates approaching that achieved with AL1. Compound AL6 with two decanoyl chains gave only limited lipid mixing, despite its comparably low pK_a. Clearly the fusion induced by these compounds relies not only on the formation of the neutral form, but also on their hydrocarbon structure.

DISCUSSION

Previous results from this laboratory have demonstrated that Ca^{2+} induced fusion between LUVs can be regulated by the transbilayer distribution of anionic phospholipids such as PA (Eastman *et al.*, 1992). The results presented here show that the regulatory effects of

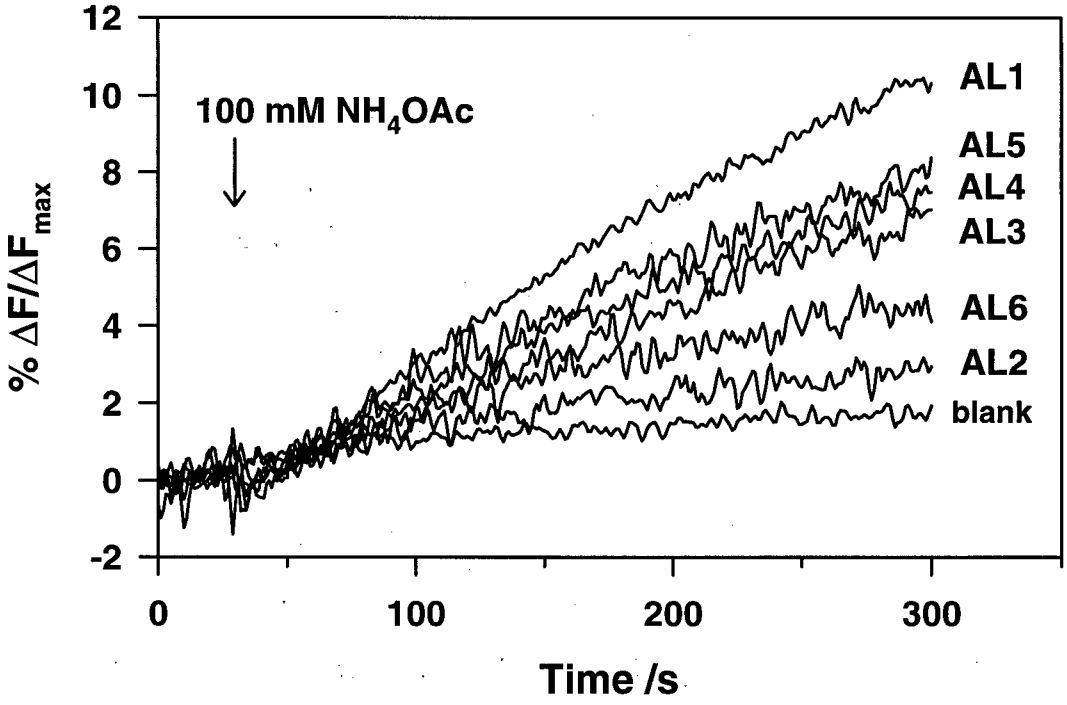

FIGURE 3.10 Effect of aminolipid structure on fusion of EPC/DOPE/Chol (35:20:45) vesicles by RET fluorescent probe dilution. Liposomes were prepared with 5 mol% of the indicated aminolipid (AL1-AL6), an internal buffer of 300 mM sodium citrate, pH 4.0, and an external buffer of 20 mM HEPES, 150 mM NaCl, pH 7.5. Fusion assays were carried out as described in Materials and Methods.

lipid asymmetry on fusion can be extended to LUV systems containing synthetic aminolipids in the absence of Ca^{2+} or other fusion-stimulating agents. Three points of interest are the ability of pH gradients to induce asymmetry of aminolipids, the mechanism of fusion that results upon relaxation of this asymmetry and the practical utility of this behaviour.

For anionic lipids such as PA, only the protonated, neutral form is able to move across the bilayer (Eastman *et al.*, 1991). In LUVs with a pH gradient, net transport then proceeds from the low pH side of the bilayer to the high pH side. In the case of aminolipids such as AL1, the deprotonated form is neutral and membrane-permeable, resulting in net transbilayer transport from high pH to low pH. As the pK_a of an amino function near the bilayer surface can be 7 or lower, net inward transport to an acidic interior can be achieved at physiological external pH values. The inward transport of AL1 and the other aminolipids studied is extremely rapid at pH 7.5 and 20 °C. This is in contrast to the behaviour of PA and other phospholipids which require elevated temperatures and low external pH values for rapid transbilayer movement. The rapid transport of the aminolipids AL1-AL6 can be attributed to the lack of the large, polar phosphate group of the phospholipids and to their pK_a's which are such that an appreciable fraction of the neutral, membrane-permeable form is present at pH 7.5.

With regard to the mechanism of aminolipid-induced fusion, the behaviour of AL1, when present in the outer monolayer of LUVs at pH values above the aminolipid pK_a, is consistent with the highly fusogenic character of diacylglycerols (Das & Rand, 1986),

owing to the propensity of these compounds to induce non-bilayer structures, such as the hexagonal H_{II} phase. This is supported in the NMR data by the appearance of an H_{II} component in the EPC/DOPE/Chol/AL1 multilamellar system at pH 7.5 which is not observed at pH 4.0. Thus the results presented here are also consistent with a fusion process which relies on the ability of component lipids to adopt transitory non-bilayer structures such as inverted micelles (Cullis & Hope, 1978), interlamellar attachment sites (Siegel *et al.*, 1989) or "stalks" (Siegel, 1993).

The rate of membrane fusion has been shown to depend on the hydrocarbon structure of the aminolipid as well as its pK_a. Aminolipids AL2–AL6 gave rates of lipid mixing dependent upon the length and number of hydrocarbon chains in their structures. Compounds with longer hydrocarbon chains gave higher rates of lipid mixing, even when the pK_a remained relatively constant. None of these compounds matched the lipid mixing rate observed with AL1, a result which highlights the importance of long, unsaturated chains to membrane destabilization. This interpretation of the structural effects on the destabilizing properties of the aminolipids assumes that all of the fusogens remain associated with the liposomal membranes. However, this may not be the case for AL2-AL6. Critical micelle concentrations for phosphatidylcholine species with hydrocarbon structures corresponding to those of AL2-AL6 are in the range of $5x10^{-6}$ to $1x10^{-8}$ (Marsh, 1990), suggesting the possibilty of appreciable monomer concentrations at the assay lipid concentration of 20 μM (10 mol% of 0.2mM).

The ability to control the transbilayer asymmetry of the aminolipids described in this work using pH gradients and to thereby control membrane fusion has a number of potential applications. For example, the ability of liposomes to deliver encapsulated materials, such as DNA, to the interior of target cells requires fusion with the plasma membrane or, following endocytosis, the endosomal membrane. While cationic liposomes are now widely used for highly efficient nucleic acid transfections of mammalian cells *in vitro* (Malone *et al.*, 1989), extending this technology to *in vivo* targeted delivery of liposomally encapsulated drugs and gene therapy has encountered problems of rapid clearance of liposomes, cellular toxicity, hemolysis, and accelerated clotting responses caused by the cationic lipids (Senior *et al.*, 1991). These problems appear to occur above a threshold plasma concentration of positive charge and are not largely dependent on the nature of the cationic species.

The aminolipids described in this work may offer considerable advantages over cationic fusogenic lipids bearing permanent positive charges. Farhood *et al.* (1992) have shown that lipids bearing tertiary amines have lower cytotoxicity than quaternary amine analogues. Here we show that the low pK_a of AL1 and related compounds permit them to be maintained on the inner surface of the of acidic vesicles with an exterior physiological pH. This may result in longer circulation residence times by reducing plasma protein interactions which lead to clearance by the macrophages of the reticuloendothelial system.

In addition, the mechanism of cell entry for the system described here would be different from that proposed for cationic liposomes which require high concentrations of polyanions

(e.g., DNA) or oppositely charged membranes to give fusion (Düzgüneş *et al.*, 1989; Stamatatos *et al.*, 1988). AL1 is capable of destabilizing a lipid membrane and causing lipid mixing when present on the outer monolayer at physiological pH. In combination with liposomal targeting methods and passive gradient dissipation, fusion of liposomes with target plasma membranes might be achieved.

In summary, we have demonstrated the modulation of membrane fusion via pH gradient-induced asymmetric distributions of synthetic aminolipids. The protonatable lipids are charged and bilayer-stable at pH 4.0 when incorporated at 5 mol% into liposomes consisting of EPC/DOPE/Chol (35:20:45). The aminolipids can be rapidly sequestered to the inner monolayer of LUVs by increasing the external pH to 7.5 with retention of membrane stability. Dissipation of the pH gradient results in neutralization of the amino headgroups and redistribution of the aminolipids to the outer monolayer. In the neutral form, the aminolipids destabilize the membrane and cause membrane fusion by a process consistent with the formation non-bilayer lipid intermediates.

CHAPTER 4

pH-INDUCED DESTABILIZATION OF LIPID BILAYERS BY A LIPOPEPTIDE DERIVED FROM INFLUENZA HEMAGGLUTININ

To study the properties of a membrane-anchored peptide derived from the HA2 N-terminal fusion peptide, we have synthesized the peptide AcE4K. The amino acid sequence is based on the peptide E4 studied by Wilschut and co-workers (Rafalski *et al.*, 1991), which corresponds to the HA2 N-terminal sequence of an X31 mutant produced by Gething *et al.* (1986). The amino acid sequences of AcE4K, E4, and the "wild-type" (wt) are given in Figure 4.1. The more recent study cited above showed that under mildly acidic conditions E4 caused somewhat lower rates of contents leakage from lipid vesicles compared to wt. However, E4 exhibited a number of potentially advantageous properties: higher solubility at neutral pH, a more highly α-helical structure at low pH, and a greater response to changes in pH in terms of its propensity to insert into a lipid bilayer. In synthesizing AcE4K we acetylated the N-terminus and added a lysine residue to the C-terminus to permit a facile coupling to a reactive DSG lipid anchor via the lysine sidechain.

In this chapter, the membrane-destabilizing properties of the lipopeptide Lipo-AcE4K induced by low pH are reported. Lipo-AcE4K is incorporated into stable POPC and EPC/Chol (55:45) liposomes at up to 10 mol% at pH 7.5. Acid-induced changes in peptide structure and lipid bilayer interactions are determined by circular dichroism (CD) spectropolarimetry and tryptophan fluorescence. Leakage of vesicle contents and lipid

wt: GLFGAIAGFIENGWEGMIDG...

E4: GLF**E**AIAGFIENGWEGMIDG

AcE4K: **Ac-** GLF**E**AIAGFIENGWEGMIDG**K**

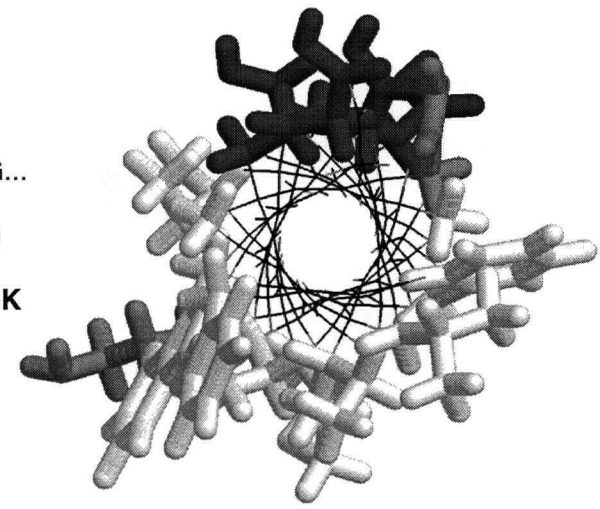

FIGURE 4.1 Amino acid sequence of the hemagglutinin HA2 subunit N-terminal "fusion peptide" of influenza virus X31 strain (wt), sequence of the E4 peptide prepared by Rafalski et al. (1991) containing a glutamic acid substitution at position 4, and sequence of the peptide AcE4K used in this study, including N-terminal acetylation and the addition of lysine-21 at the C-terminus. A representation of AcE4K as an α-helix with acidic sidechains shown in black and hydrophobic residues in white demonstrates the potential amphipathic nature of the peptide in this conformation.

mixing are shown by quantitative fluorescence assays and freeze fracture electron microscopy. In addition, fusion of liposomes bearing Lipo-AcE4K with erythrocyte ghosts is demonstrated by lipid mixing and confocal fluorescence microscopy.

MATERIALS AND METHODS

Lipids and Chemicals.

Crude AcE4K peptide was initially obtained from the laboratory of Dr. Ian Clark-Lewis, Biomedical Research Laboratory, University of British Columbia. Subsequently, purified peptide was purchased from Multiple Peptide Systems (San Diego, CA). 1,2-Distearoyl-*sn*-glycerol (DSG) was obtained from Genzyme Corp. (Boston, MA). POPC, EPC, NBD-PE, and Rh-PE were supplied by Avanti Polar Lipids (Alabaster, AL). ANTS and DPX were purchased from Molecular Probes (Eugene, OR). Succinic anhydride, DMAP, NHS, DCC, cholesterol and all buffers were purchased from Sigma Chemical Co. (St. Louis, MO). All organic solvents were HPLC-grade and were used without redistillation.

Preparation of AcE4K and Lipo-AcE4K.

After lyophilization, the peptide was purified by reverse-phase HPLC on a Synchropak (Synchrom, Inc.) C8 semi-preparative HPLC column using a 40%-70% linear gradient of acetonitrile in water (0.1% TFA) with a flow rate of 6 ml/minute over 20 minutes. The peptide elutes at approximately 55% acetonitrile. The composition of the peptide was verified by amino acid analysis, mass spectrometry, and HPLC. Purity was estimated to be greater than 95%.

The synthesis of the lipopeptide is illustrated in Figure 4.2. One gram of DSG (1.6 mmol) (**1**), 0.2 g succinic anhydride (2 mmol), and 0.24 g 4-dimethylaminopyridine (2 mmol) were dissolved in 10 ml of CH_2Cl_2 and stirred at room temperature for one hour. The resulting acid (**2**) was isolated by removing solvent by rotary evaporation followed by purification by silica gel chromatography using 10% ethyl acetate in hexane as eluant. Two hundred milligrams of this material (0.28 mmol) and 32 mg of *N*-hydroxysuccinimide (0.28 mmol) were dissolved in 5 ml of CH_2Cl_2 and 57 mg of 1,3-dicyclohexylcarbodiimide (0.28 mmol) was added with stirring. The reaction was allowed to proceed for one hour at room temperature after which the mixture was filtered to remove precipitate, and the solvent was removed by rotary evaporation yielding the activated lipid (**3**). A mixture of 5.6 mg of the peptide AcE4K (2.5 μmol), 4.1 mg of **3** (5.0 μmol) and 15 mg of triethylamine in 1 ml of dimethylsulfoxide (DMSO) was heated to 65°C to achieve co-dissolution of the lipid and peptide and incubated for one hour. After cooling, the lipopeptide (**4**) was precipitated by the addition of 5 ml of diethyl ether and centrifuged at 750 x g for 5 minutes. The pellet was washed three times with 2 ml of diethyl ether repeating the centrifugation with each wash. The lipopeptide was dried under vacuum and its identity was confirmed by mass spectrometry. Purity as determined by peptide-to-lipid ratio using ^{1}H-NMR was found to be greater than 95%.

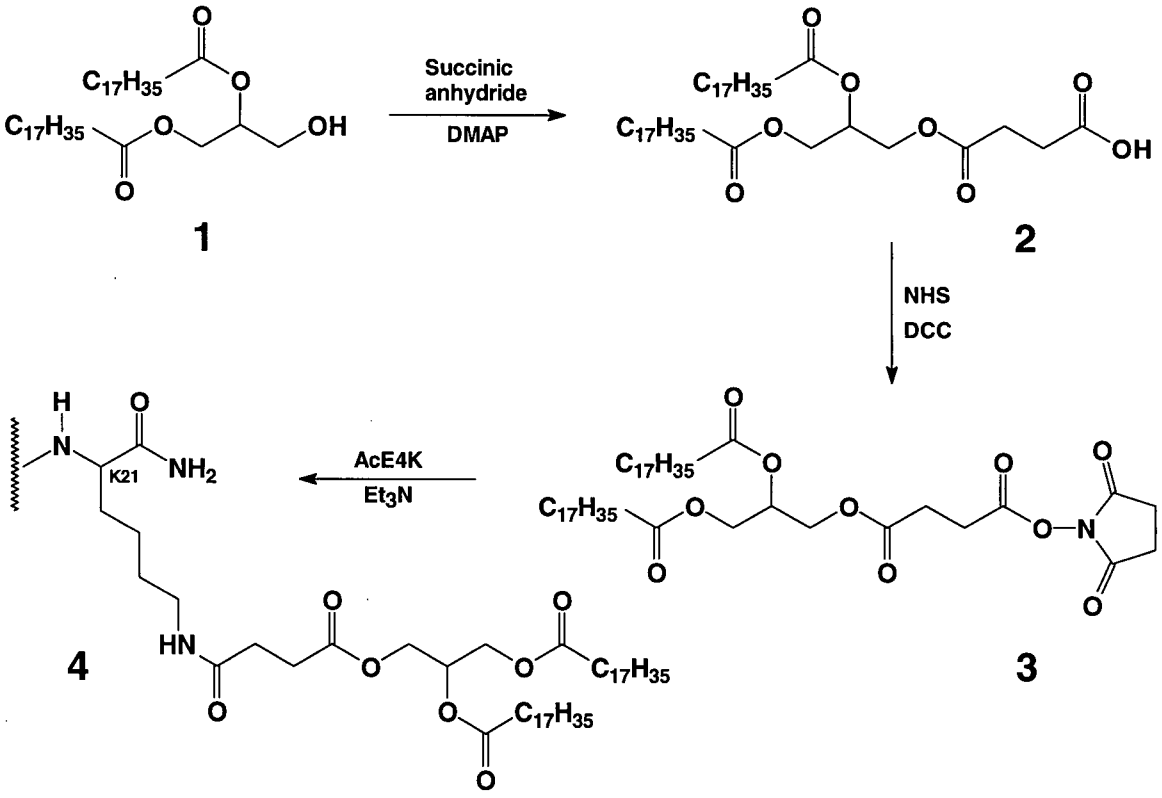

FIGURE 4.2 Structure and synthesis of the Lipo-AcE4K lipopeptide (**4**). The activated lipid (**3**) reacts exclusively with the primary amine on the C-terminal lysine (K21) of the peptide.

Preparation of Liposomes.

Chloroform solutions of lipids were dried by vortex mixing under nitrogen followed by the removal of residual solvent under high vacuum for 1 hour. When lipopeptide was incorporated into the liposome preparations, it was added to the dried lipids as a 1 mM solution in DMSO along with an equal volume of benzene-methanol (95:5) prior to freeze-drying for 5 hours. Lipids were hydrated with appropriate buffers to concentrations ranging from 5 to 20 mM lipid. Five freeze–thaw cycles were used to ensure homogeneous mixture of the MLV suspensions. The MLVs were extruded 10 times through two 100 nm pore-size polycarbonate filters (Costar, Cambridge, MA) in a high-pressure extruder (Lipex Biomembranes, Vancouver, BC) to produce LUVs. Lipid concentrations were determined by phosphate assay as described by Bartlett (1959). Depending on the lipid formulation, the mean diameter of the LUVs ranged from 100 to 135 nm as measured by quasi-elastic light scattering.

Circular Dichroism.

AcE4K was initially dissolved in 10 mM phosphate buffer, pH 7.5, at a concentration of 0.5 mM. Subsequently, 200 µl samples were prepared by diluting this stock to a peptide concentration of 25 µM in 10 mM phosphate buffer at either pH 5.0 or pH 7.5. CD spectra from 200 to 250 nm were recorded on a Jasco J720 spectropolarimeter using a 1 mm quartz cuvette and accumulations of five scans. To obtain spectra in the presence of lipid bilayers, we used POPC LUVs at a concentration of 2.5 mM lipid (lipid/peptide ratio = 100) prepared in 10 mM phosphate buffer adjusted to either pH 7.5 or pH 5.0. Under

these conditions the CD spectra of the peptide could be measured with minimal difficulties arising from absorbance and scattering due to the lipid. The spectra were corrected by subtracting control spectra of lipid and buffer, as appropriate.

For the lipopeptide, LUVs were prepared with 1% Lipo-AcE4K in POPC at a phospholipid concentration of 2.5 mM in 10 mM phosphate buffer adjusted to either pH 5.0 or pH 7.5. CD spectra were obtained as above. The very low solubility of the lipopeptide prevented measurement in the absence of lipid.

Tryptophan Fluorescence.

Tryptophan fluorescence spectra were recorded with an excitation wavelength of 280 nm over an emission range of 300 to 400 nm on a Perkin Elmer LS50 fluorometer using a 1 cm quartz cuvette thermostatted at 25°C. For the free peptide, 30 µl of 100 µM aqueous peptide solution was added to 2.97 ml of 10 mM phosphate buffer at pH 7.5 or pH 5.0, either with or without POPC LUVs (0.1 mM phospholipid, lipid/peptide ratio = 100). Spectra of the lipopeptide incorporated into liposomes were obtained using the Lipo-AcE4K/POPC LUVs described above diluted to 0.1 mM POPC, 1.0 µM Lipo-AcE4K. The spectra were corrected by subtracting scans of phosphate buffer or LUVs, as appropriate.

Preparation of Erythrocyte Membranes.

Sealed erythrocyte ghosts were prepared by the method of Steck and Kant (1974). Briefly, 4 ml of packed cells was washed 3 times in HEPES buffered saline (HBS: 5 mM HEPES,

150 mM NaCl, pH 7.5), with centrifugation each time for 5 minutes at 750 x g in a swinging-bucket rotor. Washed cells were diluted 2-fold with HBS, lysed in 300 ml of 5 mM HEPES, 1 mM $MgSO_4$, pH 7.5, and pelleted at 20,000 g for 20 minutes. Ghosts were removed from above the hard, protease-rich pellet and resuspended in 200 ml of HBS containing 1 mM $MgCl_2$. The suspension was repelleted, washed twice more, and finally resuspended in 10 ml of HBS. Phospholipid concentration was determined by phosphate assay. The absence of glyceraldehyde-3-phosphate dehydrogenase activity (Steck & Kant, 1974) was used to confirm the formation of sealed right-side-out ghosts.

Lipid Mixing Fusion Assays.

The extent of membrane fusion as measured by lipid mixing in the presence of Lipo-AcE4K was monitored by the RET assay described in Chapter 1. LUVs of a desired lipid composition containing 0.5 mol% of both NBD-PE and Rh-PE were prepared in HMA buffer (10 mM HEPES, 10 mM MES, 10 mM sodium acetate, 100 mM NaCl), pH 7.5. Lipo-AcE4K was either included in the lipid preparation as described above or added to labelled vesicles from a 2 mM solution in DMSO. Labelled vesicles were mixed with either unlabelled LUVs or erythrocyte ghosts in a lipid ratio of 1:3 at a total lipid concentration of 0.2 mM. Typically, 15 µl 10 mM labelled LUVs and 45 µl of 10 mM unlabelled LUVs or 300 µl of erythrocyte ghosts were made up to 3 ml in a 1 cm quartz cuvette with a HMA buffer, pH 7.5. Fluorescence was monitored at 25°C over 5 minutes with excitation at 465 nm, emission at 535 nm, and an emission cut-off filter at 530 nm.

During the assays, 1 M HCl was added to decrease the pH to a desired value. (HMA buffer has a linear pH response to acid volume over the pH range 4.0 to 7.5.)

Each point in the lipid mixing time course was normalized by subtracting the fluorescence of a comparable assay lacking unlabelled vesicles (F_0) and dividing by the fluorescence achieved by infinite probe dilution determined by the addition of 25 µl of 100 mM Triton X-100 (F_{max}). The percent change in fluorescence was calculated as

$$\% \frac{\Delta F}{\Delta F_{max}} = 100 \times \left(\frac{F - F_0}{F_{max} - F_0} \right)$$

for each point. Complete lipid mixing, as determined by a liposomes prepared with a total lipid composition corresponding to a 1:3 ratio of labelled to unlabelled POPC vesicles, gives a value of $\Delta F/\Delta F_{max}$ of approximately 80% under these conditions, and reported results have not been corrected by this factor.

Exchange of Lipo-AcE4K Between Membranes.

POPC MLVs were prepared in HMA buffer at pH 7.5 as described above and pelleted at 12,000 rpm on a benchtop centrifuge at 5°C. The pellet was resuspended in HMA buffer and repelleted. This procedure was repeated for three washings to ensure removal of any small lipid vesicles prior to determination of lipid concentration by phosphate assay. Thirty microlitres of POPC LUVs (10 mM lipid) was diluted in 1.09 ml of HMA buffer, pH 7.5, and 7.5 µl of 2 mM Lipo-AcE4K was added from DMSO stock. This preparation results in the incorporation of 10 mol% of the lipopeptide into the outer monolayer of the

LUVs. After a 5 minute pre-incubation at 25°C, 375 µl of 12.5 mM POPC MLVs were added as a sink for lipopeptide exchange. This 60-fold lipid excess represents approximately a 6-fold excess of lipid available for lipopeptide exchange, assuming 10 % of the MLV lipid is exposed on the outermost monolayer (Fenske, 1993). Following a five minute incubation at 25°C , the MLVs were pelleted as above and the peptide and lipid content (phosphate assay) of the supernatant was determined. We used a micro-BCA assay kit as provided by Pierce (Rockford, IL) with the provided procedure to analyze for peptide. The results were compared to controls without MLVs or without Lipo-AcE4K.

Contents Mixing and Leakage.

Liposomes of a desired composition were prepared containing either 25 mM ANTS in HMA buffer, 100 mM DPX in HMA buffer, or 6 mM ANTS plus 75 mM DPX (ANTS–DPX), at pH 7.5 as described above. External buffer was exchanged with HMA buffer on Sephadex G-25 columns prior to diluting to 10 mM lipid. To assay for contents mixing, 15 µl of the ANTS preparation on 45 µl of DPX liposomes were combined in 3 ml of HMA buffer. ANTS fluorescence was monitored over 5 minutes with the addition of 15 µl of 1 M HCl at 30 seconds to decrease the pH to 5.0. Excitation and emission wavelengths were 360 nm and 530 nm, respectively, and a 490 nm cut-off filter was used. Maximum quenching and zero leakage was determined by the fluorescence of the preparation containing ANTS–DPX, and zero quenching was measured using only ANTS liposomes, both prior to the addition of acid. Leakage was quantified by comparing the

maximum quenching result (0% leakage) with a similar assay to which 25 µl of 100 mM Triton X-100 was added (100% leakage).

Freeze-Fracture Electron Microscopy.

LUVs consisting of 10 mol% Lipo-AcE4K in EPC/Chol (55:45) were prepared in HMA buffer, pH 7.5, at a total lipid concentration of 5 mM. A sample at pH 5.0 was prepared by adding 1.5 µl of 1 M HCl to 100 µl of liposomes. After 5 minute incubations at 25°C, samples at each pH were mixed 1:1 with glycerol and quickly frozen. Platinum–carbon replicas were prepared as described previously (Fisher & Branton, 1974). EPC/Chol (55:45) liposomes at pH 7.5 and 5.0 were used as controls.

Fluorescence Microscopy.

The dual-labelled LUVs containing 10 mol% Lipo-AcE4K in EPC/Chol (55:45) as described above for the lipid mixing assay were used. One hundred microlitres of 2.5 mM LUVs was added to 650 µl of HMA buffer, pH 7.5. After a 5 minute pre-incubation, a 3-fold lipid excess of erythrocyte ghosts (250 µl of 3 mM lipid) was added. A 5 µl aliquot was removed prior to acidification with 15 µl of 1 M HCl, reducing the pH to 5.0. Samples at each pH were inspected by confocal microscopy using both phase-contrast and fluorescence techniques.

RESULTS

Solubilities of AcE4K and Lipo-AcE4K.

The highly hydrophobic nature and low solubility of native viral fusion peptides cause problems in studying their interactions with lipid vesicles. The peptide AcE4K was soluble in aqueous solutions at pH 7.5 at concentrations up to 10 mM and highly soluble in DMSO. The use of the carboxy terminal lysine residue to couple the peptide to the lipid anchor, rather than the more commonly used cysteine–thioether chemistry, overcame earlier difficulties we had in purifying the corresponding C-terminal cysteine peptide. The lipopeptide Lipo-AcE4K was soluble only in DMSO and was added to assays from a 2 mM stock solution such that the amount of organic solvent was less than one percent by volume.

Circular Dichroism and Tryptophan Fluorescence.

Differences in the secondary structure of AcE4K and Lipo-AcE4K as a function of pH were investigated by CD spectropolarimetry. CD spectra of AcE4K and Lipo-AcE4K are given in Figure 4.3. AcE4K has a random coil structure at neutral pH either in the presence or absence of POPC LUVs (Figure 4.3(a)). At pH 5.0, the random coil signal persists in the absence of lipid membranes. However, in the presence of POPC LUVs at pH 5.0, AcE4K adopts a highly α-helical structure, characterized by the signal minima at 208 nm and 222 nm. This result suggests that AcE4K exists mainly as a amphipathic helix, much like the structure given in Figure 4.1, only in the presence of lipid bilayers and

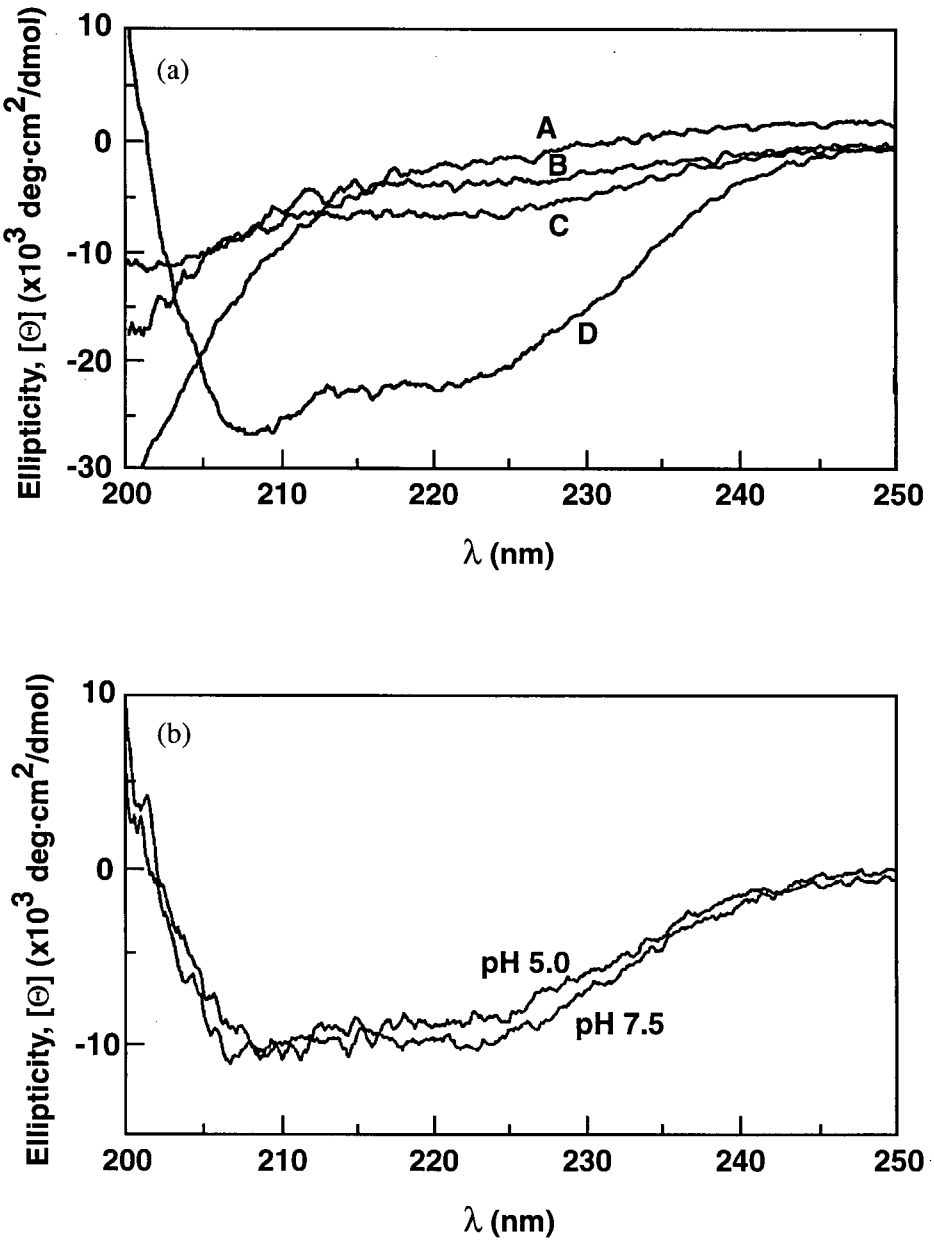

FIGURE 4.3 Effects of pH and the presence of lipid vesicles on the circular dichroism of AcE4K and Lipo-AcE4K. (a) CD spectra of 25 μM AcE4K in 10 mM phosphate buffer at pH 7.5 (**A**, **C**) and pH 5.0 (**B**, **D**) in the absence (**A**, **B**) or presence (**C**, **D**) of POPC LUVs, 2.5 mM lipid. (b) CD spectra of POPC LUVs (2.5 mM lipid) prepared with 1 mol% Lipo-AcE4K in phosphate buffer at pH 7.5 or pH 5.0. All spectra represent the average of 5 scans from which buffer and lipid signal has been subtracted, as appropriate.

upon neutralization of at least some of its acidic residues. The behaviour of the lipopeptide as a function of pH is markedly different from the free peptide. The structure of the peptide in Lipo-AcE4K does not appear to be affected by pH (Figure 4.3(b)). At pH 7.5, the lipopeptide already exists in a α-helical conformation and the CD spectrum is not changed at pH 5.0. This difference in behaviour for the peptide in its free and lipid-coupled form are surprising, but these results do not provide information on the degree of interactions of the peptides with the lipid bilayer or their effects on membrane stability.

The fluorescence of tryptophan is dependent on the polarity of its environment. In an apolar environment, the emission maximum is shifted to lower wavelengths compared to that observed in aqueous media. This effect can be used to study the penetration of peptides bearing tryptophan residues into lipid bilayers (Galla *et al.*, 1985). AcE4K contains a single tryptophan residue at position 14 and has no tyrosine residues. The fluorescence spectrum of tryptophan-14 can therefore be used as a measure of membrane penetration. The spectra of AcE4K at pH 7.5 and 5.0 in the presence and absence of POPC LUVs are given in Figure 4.4(a). No differences are observed, except for the sample at pH 5.0 in the presence of vesicles which exhibits a slight blue shift of λ_{max} and a significant increase in intensity at shorter wavelengths. In contrast to this, the spectra for Lipo-AcE4K in POPC vesicles shown in Figure 4.4(b) indicate that, even at pH 7.5, the tryptophan residue is somewhat protected from the aqueous medium having a λ_{max} of 340 nm compared to 355 nm for the free peptide. At pH 5.0, the λ_{max} is further reduced to 332 nm. This result suggests that, while no structural changes in the peptide were observed in

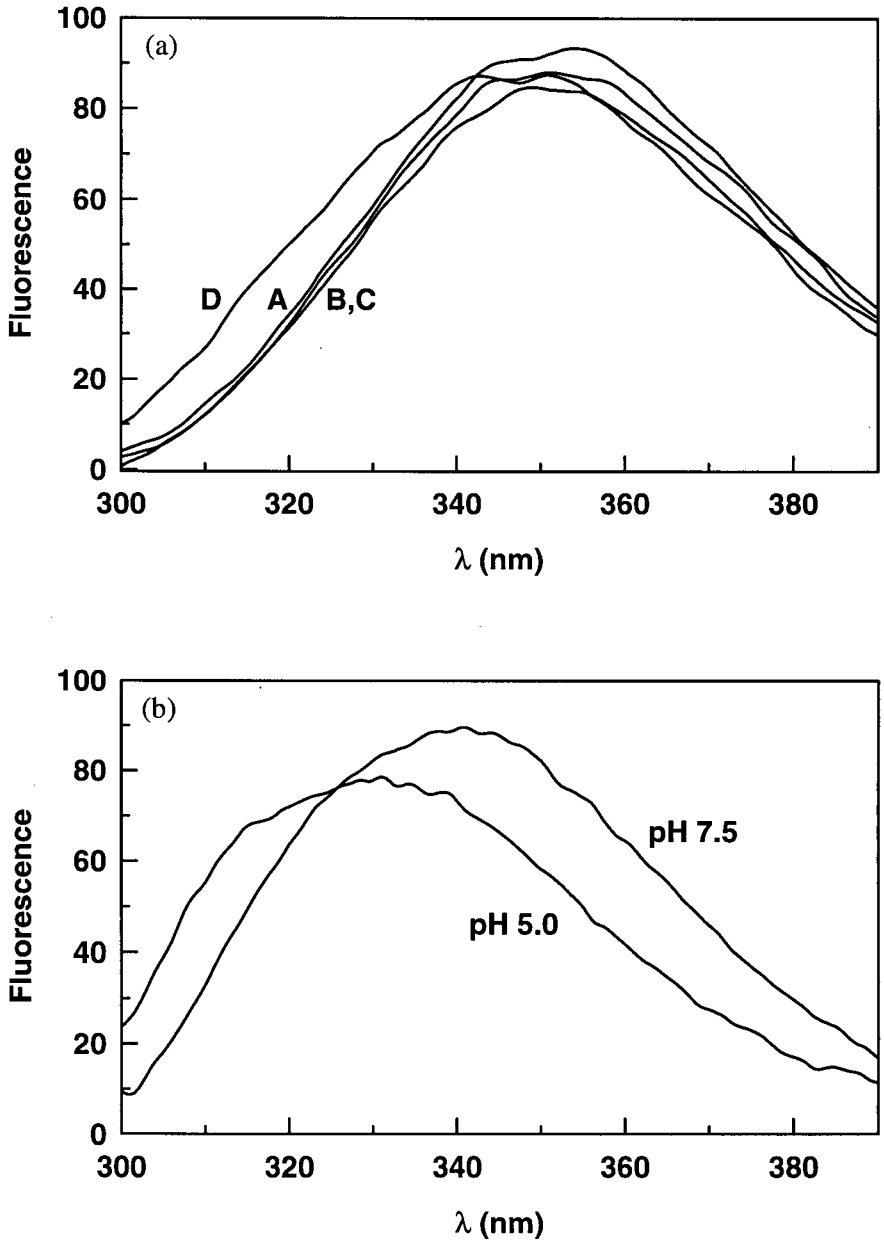

FIGURE 4.4 Tryptophan fluorescence emission spectra of showing the effects of pH and the presence of lipid vesicles: (a) 1 μM AcE4K in 10 mM phosphate buffer at pH 7.5 (**A**, **C**) and pH 5.0 (**B**, **D**) in the absence (**A**, **B**) or presence (**C**, **D**) of POPC LUVs, 0.1 mM lipid; (b) POPC LUVs (0.1 mM lipid) prepared with 1 mol% Lipo-AcE4K in phosphate buffer at pH 7.5 or pH 5.0. Spectra were corrected by subtracting scans of phosphate buffer or LUVs, as appropriate.

the CD spectrum, Lipo-AcE4K penetrates further into the lipid bilayer upon neutralization of the acidic residues. However, the observed changes could also arise from the protection of the tryptophan residue from the aqueous medium through the formation of oligomeric complexes of the lipopeptide within the membrane.

Fusion of POPC LUVs Induced by Lipo-AcE4K.

The destabilization of membranes accompanying the observed changes in peptide structure and membrane penetration was studied by monitoring the fusion of lipid vesicles as measured by lipid mixing, contents mixing and leakage. Membrane fusion was expected to depend on the extent of neutralization of the acidic residues of Lipo-AcE4K and to increase with decreasing pH.

Lipid mixing was monitored by the loss of RET between the fluorescently labelled lipids, NBD-PE and Rh-PE. In this assay, vesicles containing both probes are mixed with unlabelled vesicles, and membrane fusion results in probe dilution and increased NBD-PE fluorescence. Exchange of the labelled lipids does not occur over the duration of these experiments, even in highly aggregated systems (Hoekstra, 1982), and fluorescence increases only upon mixing of membrane lipids.

Initially, we looked at lipid mixing of POPC LUVs with 5 mol% Lipo-AcE4K added to the preformed vesicles from a DMSO stock solution. Lipid mixing fluorescence time courses upon acidification to pH's between 7.0 and 4.0 are shown in Figure 4.5. No lipid mixing was observed above pH 6.0. However, there was a substantial increase in mixing between

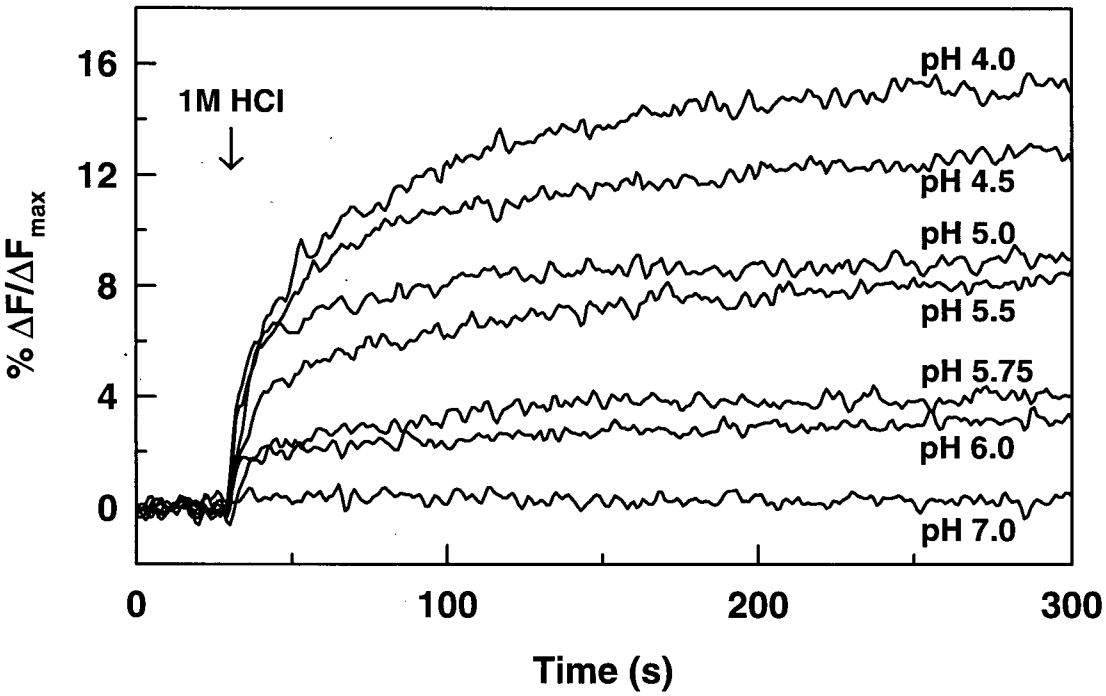

FIGURE 4.5 Effect of pH on lipid mixing for 5 mol% Lipo-AcE4K in POPC LUVs. Lipopeptide was added from a 2 mM DMSO stock solution to a 1:3 mixture of labelled and unlabelled vesicles prior to the addition of 1M HCl to achieve the indicated pH.

pH 5.75 and 5.5. These changes may have physiological importance, in that the pH of the endosomal interior falls in the range of 5 to 6 (Roederer *et al.*, 1987). At pH 5.0 an initial rapid increase in NBD-PE fluorescence levels off over one to two minutes, indicating a transient destabilization of the membrane. Further decreases in pH give even greater lipid mixing, and at pH 4.0 the initial rapid increase in fluorescence is followed by a slower rise over several minutes. Similar experiments in which the free peptide, AcE4K, was added to POPC vesicles also gave lipid mixing, but at levels about half of those observed for the lipopeptide (data not shown).

As described in Chapter 3, the pH experienced by the lipopeptide at the lipid surface is lower than the pH of the bulk solution because of the negative surface potential arising from the membrane bound peptide. The magnitude of this potential decreases with pH. It may be, therefore, that the increases in lipid mixing observed upon lowering the pH arises at least partly as a result of increased vesicle aggegation due to decreased charge repulsion.

The effect of Lipo-AcE4K concentration in the outer monolayer of POPC vesicles on the degree of lipid mixing at pH 5.0 is shown in Figure 4.6(a). Small but significant increases in NBD-PE fluorescence were observed with as little as 1 mol% Lipo-AcE4K, and the level of mixing achieved increased with lipopeptide concentration up to 10 mol%, the maximum level assayed. In all cases, the observed increase in fluorescence is complete within 1 or 2 minutes. The transient nature of the lipid mixing in all of these cases suggests the loss of destabilizing capability of the lipopeptide, perhaps through

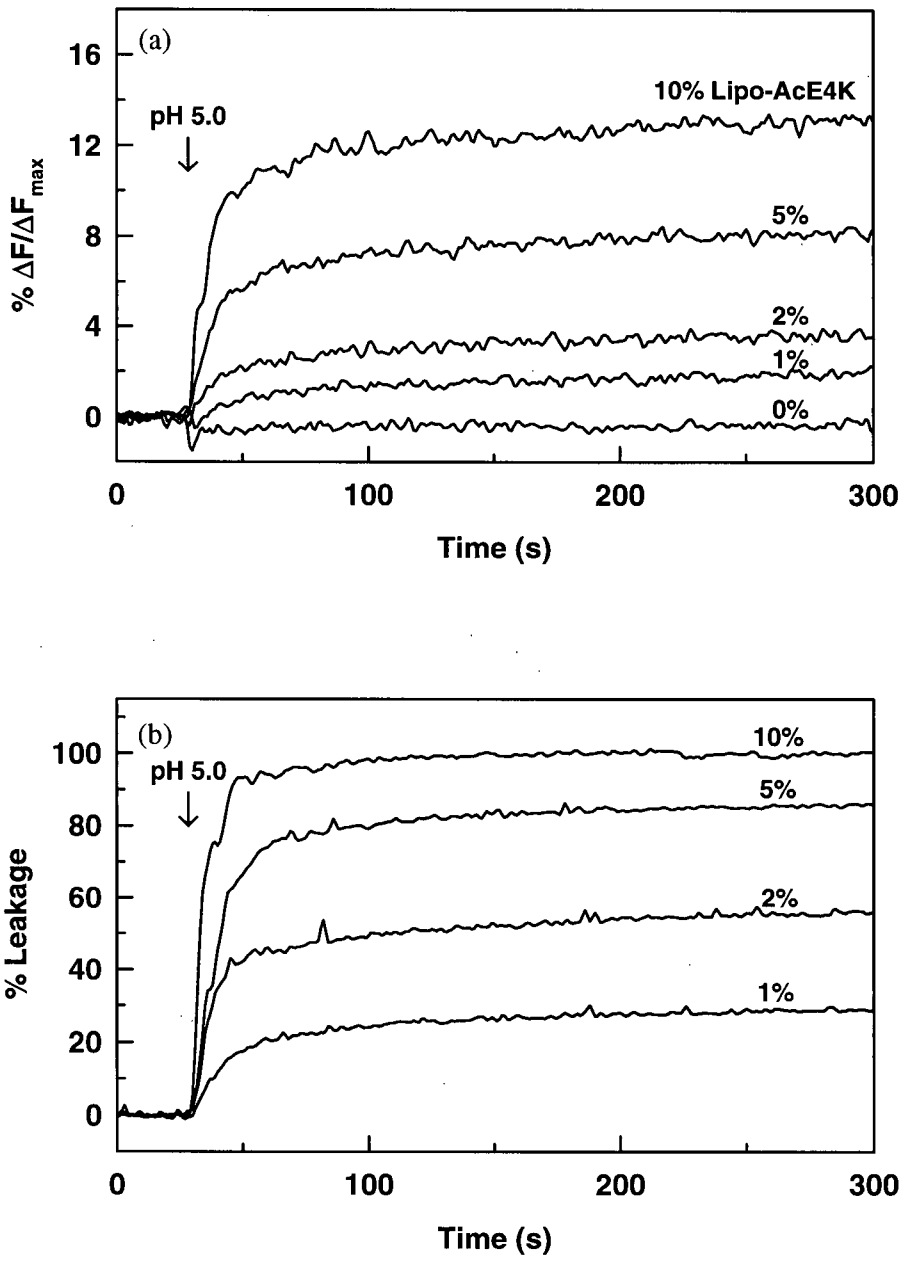

FIGURE 4.6 Effects of Lipo-AcE4K concentration on lipid mixing and leakage in POPC LUVs. (a) Varying amounts of lipopeptide were added to a 1:3 mixture of labelled and unlabelled vesicles (0.2 mM total lipid) from a 2 mM stock solution in DMSO, such that the final DMSO concentration was less than 1% by volume. Lipid mixing assays were as described above, adding 1 M HCl at 30 seconds to achieve a final pH of 5.0. (b) Vesicles containing 6 mM ANTS and 75 mM DPX dissolved in HMA buffer, pH 7.5, were diluted to 0.2 mM lipid prior to addition of varying amounts of lipopeptide from a 2 mM DMSO stock solution. At 30 seconds, 1 M HCl was added to achieve a pH of 5.0.

conformational changes not detectable by CD experiments or through the formation of oligomeric complexes.

To determine whether the pH-induced destabilization of membranes containing Lipo-AcE4K corresponded to fusion events with contents mixing in addition to the observed lipid mixing, we used the ANTS–DPX contents mixing assay (Ellens *et al.*, 1984). In this assay, fusion between a liposome population containing the fluorescent marker ANTS and a second population containing the quencher DPX results in a loss of ANTS fluorescence. The assay is not affected by moderately acidic conditions and can distinguish contents mixing from probe leakage. Leakage was separately determined by monitoring ANTS dequenching for liposomes containing both ANTS and DPX.

For the range of Lipo-AcE4K concentrations used (1 to 10 mol%) in POPC vesicles, no contents mixing was observed. The ANTS–DPX assay revealed only the leakage of vesicle contents upon decreasing the pH to 5.0, and the extent of leakage observed corresponded to the concentration of lipopeptide as shown in Figure 4.6(b). With 10 mol% Lipo-AcE4K in the outer monolayer, all of the probe was released within one minute. At lower lipopeptide concentrations, most of the leakage occurred within the first minute followed by a much slower release of contents. This behaviour corresponds to the transient rapid lipid mixing which was observed, and again suggests a rapid loss of destabilizing capability for the lipopeptide.

The results are consistent with previous studies on the destabilization of lipid vesicles with viral fusion peptides. Contents mixing arising from a non-leaky fusion event induced by a

fusion peptide has not been convincingly demonstrated. However, the ability of the fusion peptides to destabilize lipid bilayers may represent its functional role in destabilizing target cellular membranes, while the entire fusion protein may be required to achieve fusion with contents mixing.

We continued this investigation by looking at the ability of Lipo-AcE4K present in one membrane to destabilize and fuse with synthetic and biological target membranes which are otherwise pH stable. It was first necessary to demonstrate that the lipopeptide does not exchange out of lipid bilayers into potential "target" membranes, which would complicate interpretation of the lipid mixing results. The transfer of Lipo-AcE4K was investigated by incubating POPC LUVs containing 10 mol% Lipo-AcE4K added after vesicle formation with a large excess of POPC MLVs. The MLVs were separated from LUVs by centrifugation. A comparison of the peptide contents of the Lipo-AcE4K-bearing LUVs before and after incubation with MLVs is given in Figure 4.7(a). It is clear that there is no exchange of Lipo-AcE4K out of the LUV population when incubated with MLVs. A small increase in measured peptide content after the incubation can be attributed to interference in the assay caused by phospholipid as shown in the POPC control.

Given this result, we went on to investigate the ability of POPC vesicles containing Lipo-AcE4K to fuse with POPC membranes lacking the lipopeptide. As seen in Figure 4.7(b), very little lipid mixing is observed when only one liposome population contains 5 mol% Lipo-AcE4K compared the level attained when the lipopeptide is present in both membranes. There was only a small difference in this result when the Lipo-AcE4K was

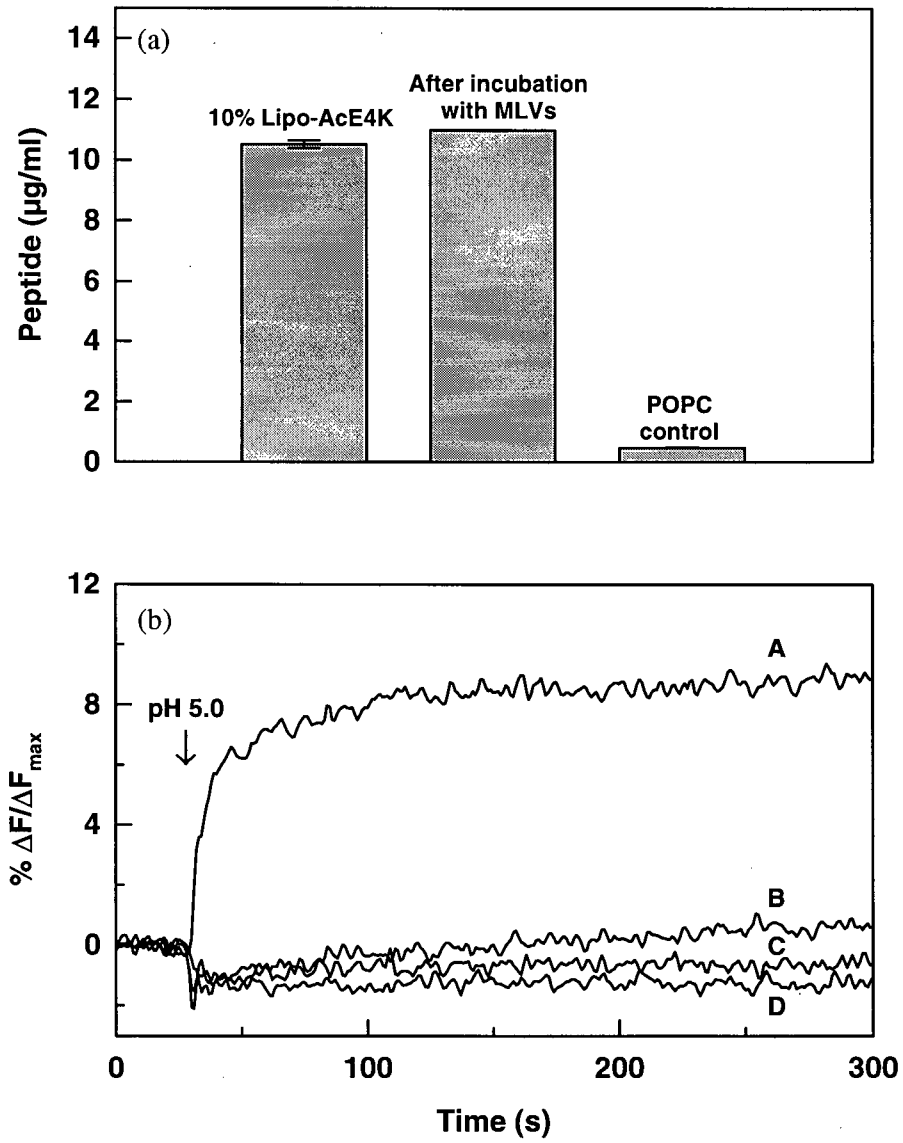

FIGURE 4.7 Exchange of Lipo-AcE4K between vesicle populations and lipid mixing with membranes lacking lipopeptide. (a) 10 mol% Lipo-AcE4K was added to prepared POPC LUVs, and the amount of peptide associated with POPC vesicles was determined by micro-BCA assay before and after incubation with POPC MLVs. A control experiment using LUVs without lipopeptide is also shown. Assays were carried out in duplicate, and deviations from means were negligible except where error bars are shown. (b) Lipid mixing assays were performed after pre-incubation of selected liposome populations with sufficient Lipo-AcE4K to achieve a 5 mol% concentration in liposomal outer monolayers. The lipopeptide was included in both fluorescently labelled and unlabelled populations (**A**), in labelled vesicles only (**B**), in unlabelled vesicles only (**C**), or in neither labelled nor unlabelled liposomes (**D**).

incorporated into the fluorescently labelled population rather the unlabelled population, reflecting the probability differences resulting from the mixing ratio of 1:3 labelled to unlabelled. It appears that, while Lipo-AcE4K can promote lipid mixing in POPC LUVs, it must be present in both vesicle populations to do so.

Fusion and Leakage in EPC/Chol Vesicles.

In order to achieve higher levels of membrane fusion, we have looked at the effect of Lipo-AcE4K on the stability of EPC/Chol (55:45) LUVs which more closely approximate the lipid composition of biological membranes. EPC is a naturally occurring mixture of PC species bearing a variety of fatty acyl chains, and it consists predominantly of POPC. While the addition of cholesterol to phospholipid bilayers decreases membrane permeability by effecting tighter packing of lipids, cholesterol can also enhance the propensity for membrane fusion by promoting the formation of non-bilayer lipid phases (Cullis *et al.*, 1978).

As shown in Figure 4.8(a), Lipo-AcE4K at a concentration of 5 or 10 mol% is more effective at promoting lipid mixing in EPC/Chol (55:45) LUVs than in either EPC or POPC LUVs (cf. Figure 4.6(a)). Again a transient rapid increase in fluorescence is observed; however, higher levels of fluorescence are achieved and lipid mixing continues at a reduced rate for the duration of the assay. Interestingly, the corresponding ANTS–DPX leakage results for EPC/Chol liposomes, given in Figure 4.8(b), indicate lower levels of leakage at all concentrations of Lipo-AcE4K than were observed for POPC (Figure

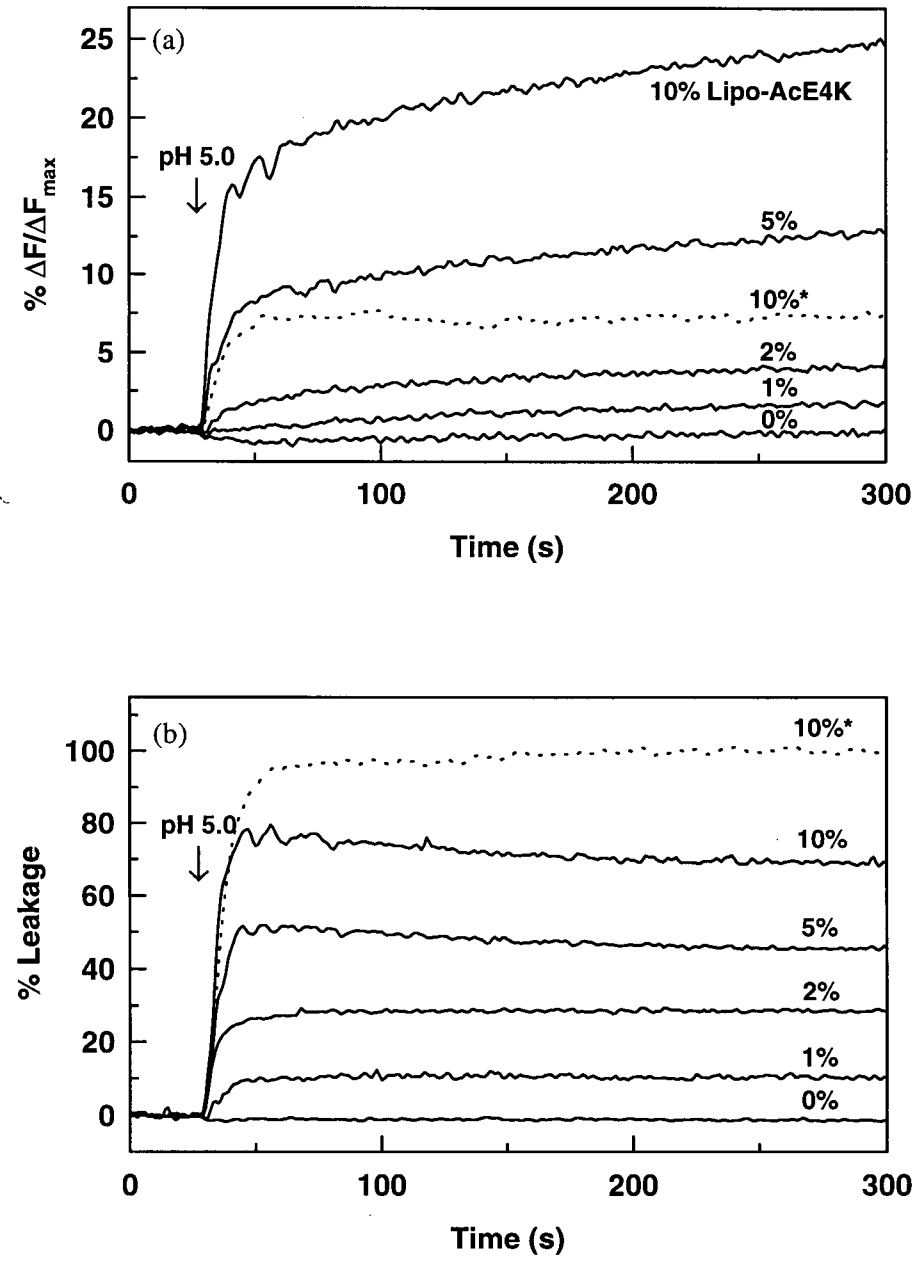

FIGURE 4.8 Lipid mixing and leakage in EPC/Chol (55:45) LUVs. (a) 0 to 10 mol% Lipo-AcE4K was added to a 1:3 mixture of labelled and unlabelled vesicles (0.2 mM total lipid) from a 2 mM stock solution in DMSO. Lipid mixing assays were as described above, adding 1 M HCl at 30 seconds to achieve a final pH of 5.0. (b) Leakage assays for 0 to 10 mol% Lipo-AcE4K added to liposomes containing 6 mM ANTS and 75 mM DPX. *For comparison, corresponding assays for 10 mol% Lipo-AcE4K in EPC LUVs are shown (dotted lines).

4.6(b)) or EPC (only 10 mol% Lipo-AcE4K data shown). It is remarkable that the inclusion of cholesterol appears to increase the destabilization caused by the lipopeptide, perhaps by the promotion of non-bilayer structures, while reducing the permeability of the destabilized membranes to the aqueous medium. However, leakage of vesicle contents remains substantial, and in no case was contents mixing of vesicles observed.

Effects of Transbilayer Distribution of Lipo-AcE4K

Increased levels of lipid mixing were observed in EPC/Chol (55:45) vesicles when Lipo-AcE4K was present on both the inner and outer monolayers of the liposomes. This was achieved by adding the lipopeptide to the lipid preparation prior to freeze-drying, hydration, and extrusion. As shown in Figure 4.9, lipid mixing between LUVs containing 10 mol% Lipo-AcE4K prepared by this method gave values of $\Delta F/\Delta F_{max}$ approaching 60 % at 5 minutes. Furthermore, mixing these LUVs and an EPC/Chol (55:45) preparation lacking lipopeptide also resulted in substantial membrane fusion. In contrast, LUVs prepared as before with 10 mol% Lipo-AcE4K only on the outer monolayer could fuse with themselves, but not with EPC/Chol LUVs.

While, the Lipo-AcE4K on the interior of vesicles is unable to penetrate the target membrane, it can apparently play a role in further destabilizing the membrane in which it is present. Presumably, this is as a result of reduction of the pH in the vesicle interior arising from the leakage induced by initial membrane destabilization.

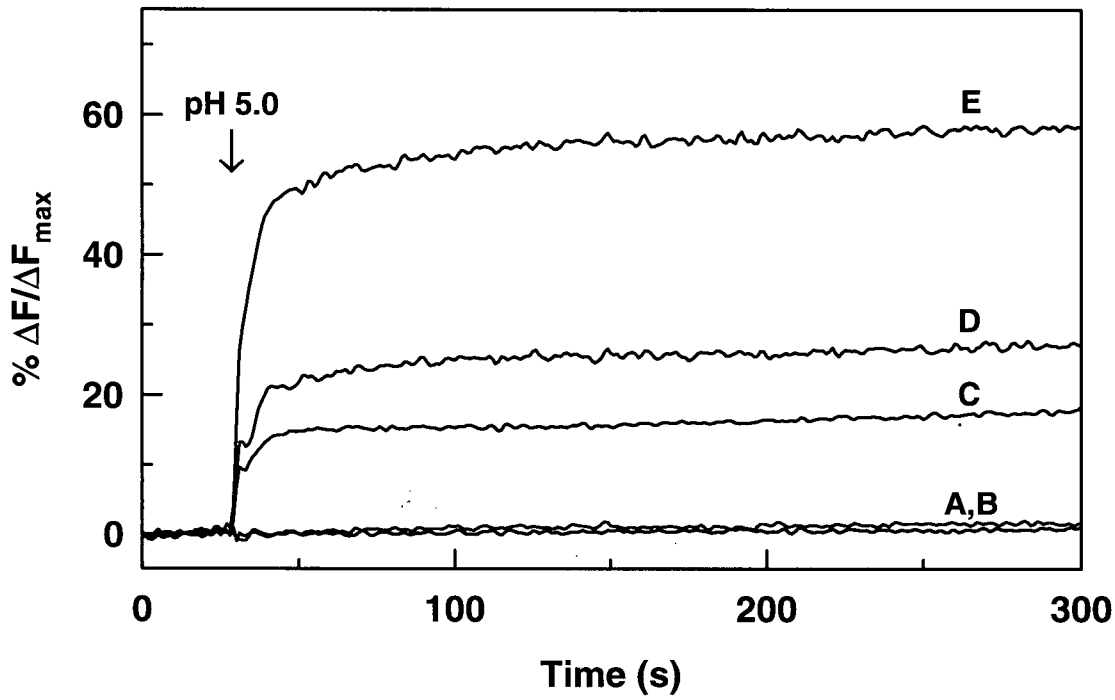

FIGURE 4.9 Effect of transbilayer distribution of Lipo-AcE4K on lipid mixing in EPC/Chol (55:45) LUVs. 10 mol% Lipo-AcE4K was either present in the outer monolayer of liposomes (**B**, **C**) or in both monolayers (**D**, **E**) and was present in only the fluorescently labelled LUV population (**B**, **D**) or in both labelled and unlabelled LUVs (**C**, **E**). A control lipid mixing assay where neither vesicle population contained lipopeptide is also shown (**A**).

Freeze-Fracture Electron Microscopy.

Freeze-fracture micrographs of EPC/Chol (55:45) LUVs bearing 10 mol% Lipo-AcE4K on both inner and outer membranes are shown in Figure 4.10. Samples without Lipo-AcE4K or those containing lipopeptide at pH 7.5 gave smooth fracture surfaces and had size distributions typical of those observed for LUVs extruded through 100 nm filters. Samples with Lipo-AcE4K acidified to pH 5.0, however, exhibited numerous larger lipid structures, indicating fusion of liposomes. In addition, many of these larger structures exhibited rough surfaces which could arise from penetration of the peptide portion of Lipo-AcE4K into the membrane. Furthermore, a large proportion of these vesicles were cross-fractured, suggesting that the preferential cleavage between the inner and outer monolayers of the lipid bilayer is disrupted by the presence of the lipopeptide.

Lipid Mixing with Erythrocyte Ghosts.

Ultimately, we are interested in the destabilizing properties of Lipo-AcE4K directed toward biological membranes. As a model for such systems we examined lipid mixing between EPC/Chol (55:45) liposomes containing Lipo-AcE4K with erythrocyte ghosts. The ghost preparation used here included 1 mM $MgSO_4$ in the lysis and washing buffers as described by Steck & Kant (1974). While this procedure results in the retention of a small amount of hemoglobin within the cells, it ensures rapid resealing and membrane integrity. Analysis for glycerol-3-phosphate dehydrogenase activity confirmed the

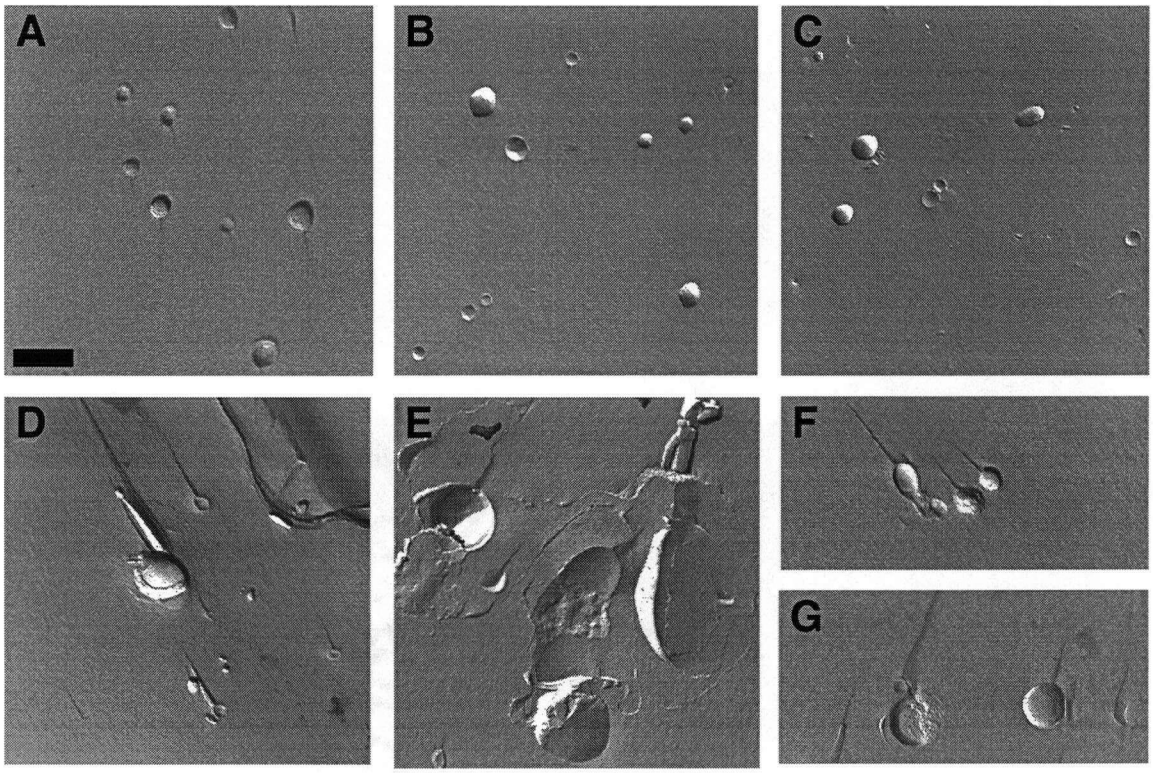

FIGURE 4.10 Freeze-fracture electron micrographs of EPC/Chol liposomes: effect of Lipo-AcE4K and pH. EPC/Chol (55:45) LUVs were prepared with (**C**, **D-G**) and without (**A**, **B**) 10 mol% Lipo-AcE4K at a total lipid concentration of 5 mM in HMA buffer. Platinum-carbon replicas were prepared at pH 7.5 (**A**, **C**) or 5 minutes following acidification to pH 5.0 by the addition of 1 M HCl (**B**, **D-G**). Original magnification was 20,000x, and the bar represents 200 nm.

formation of sealed, right-side-out ghosts which was not the case for a preparation without 1 mM $MgSO_4$ (data not shown).

Fluorescence lipid mixing assays with EPC/Chol and erythrocyte ghosts were performed using two different liposome preparations. First, Lipo-AcE4K was added to EPC/Chol (55:45) LUVs from a DMSO stock solution leading to incorporation of the lipopeptide into the outer monolayers of the LUVs at a concentration of 10 mol% relative to surface-exposed lipid. Addition of erythrocyte ghosts to this preparation gave limited lipid mixing ($\Delta F/\Delta F_{max}$ ~ 2%) when the pH was decreased to 5.0 (Figure 4.11). This result is in agreement with that shown in Figures 7 and 9 in which incorporation of Lipo-AcE4K into the outer monolayer of one population of vesicles was insufficient to give substantial lipid mixing with a second population of membranes. A second liposome preparation with 10 mol% Lipo-AcE4K in EPC/Chol (55:45), incorporating lipopeptide into both inner and outer monolayers, gave much higher levels of lipid mixing with erythrocyte ghosts at pH 5.0, $\Delta F/\Delta F_{max}$ values approaching 40% at 5 minutes.

Further evidence for lipid mixing with erythrocyte ghosts was demonstrated by confocal fluorescence microscopy. The fluorescently labelled liposome preparations from the lipid-mixing assays were also used for this procedure. Rh-PE is present in these preparations at a concentration which is greater than 80% self-quenching (Arbuzova *et al.*, 1994). The NBD-PE fluorescence is masked by a red transmission filter and is also readily photo-bleached under the conditions used here. This permits the detection of lipid mixing between labelled liposomes and erythrocyte ghosts as an increase in Rh-PE fluorescence

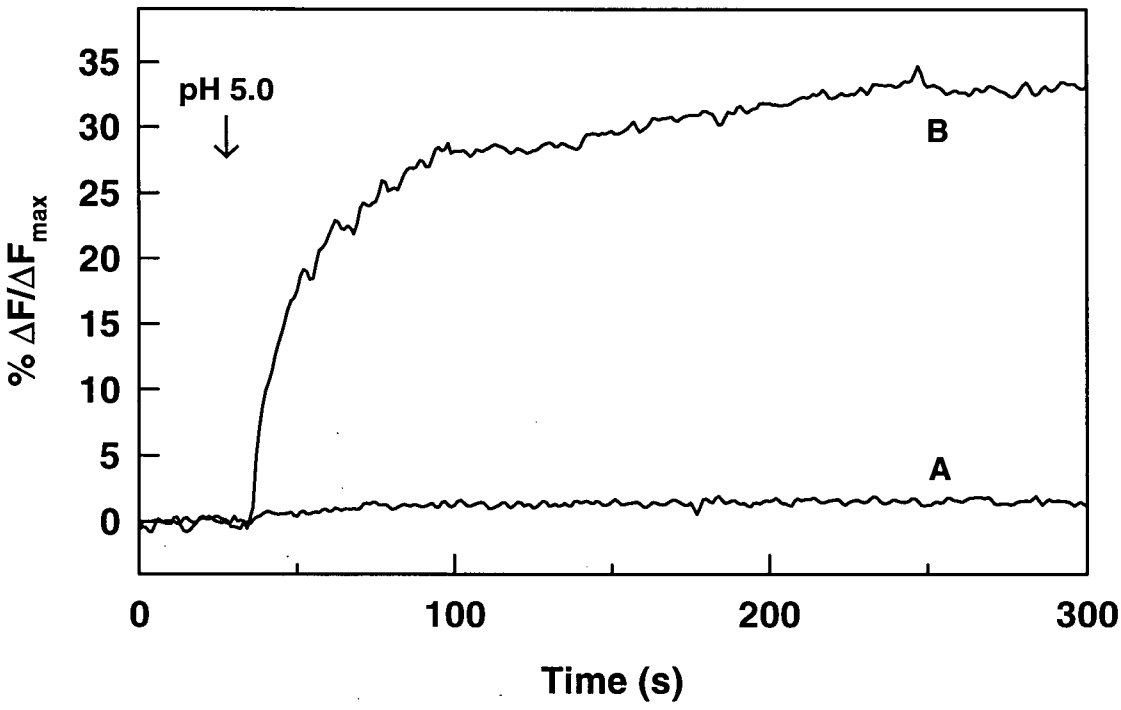

FIGURE 4.11 Effect of method of lipopeptide incorporation into EPC/Chol (55:45) LUVs on lipid mixing with erythrocyte membranes. (**A**) 10 mol% Lipo-AcE4K was added from DMSO stock solution to fluorescently labelled liposomes and pre-incubated at 25°C for 5 minutes prior to addition of erythrocyte membranes. The lipopeptide is present only in the outer monolayer of vesicles. (**B**) Lipid-mixing assay of co-lyophilized 10 mol% Lipo-AcE4K in EPC/Chol (55:45) with erythrocyte ghosts. The lipopeptide is present in inner and outer monolayers of the fluorescently labelled vesicles.

(reduced self-quenching) upon dilution into the target. Figure 4.12 illustrates the effect of decreasing the pH for a mixture of LUVs prepared from EPC/Chol (55:45) co-lyophilized with 10 mol% Lipo-AcE4K and erythrocyte ghosts. Phase contrast micrographs are shown with corresponding fluorescence images at pH 7.5 and 5.0. While the appearance of Rh-PE fluorescence in the erythrocyte membranes is the most striking effect of lowering the pH, aggregation of the erythrocyte ghosts is also apparent. Interestingly, substantial levels of Rh-PE fluorescence and aggregation were also observed for EPC/Chol (55:45) LUVs pre-incubated with 10 mol% Lipo-AcE4K (i.e. outer monolayer only), although a much smaller increase in NBD-PE fluorescence was observed in the quantitative assay. Labelled EPC/Chol (55:45) LUVs without lipopeptide gave no lipid mixing or aggregation with erythrocyte ghosts at pH 5.0 (not shown). These micrographs were obtained using very small sample volumes (~ 5 μl) spread thinly using large coverslips in order to arrest the erythrocyte ghosts without using high lipid concentrations or mounting solutions that can quench fluorescence. As a result, the majority of the membranes appear flattened, and lysis of some membranes was observed.

DISCUSSION

The free peptide AcE4K only adopts an α-helical structure at low pH and only in the presence of lipid vesicles. This behaviour is very similar to the wild-type (X31) and E4 peptides as studied by Rafalski *et al.* (1991). However, they observed a low level of helical structure for E4 even at neutral pH. In that study, SUVs were used in the CD experiments where we have used LUVs, and the higher curvature of small vesicles could

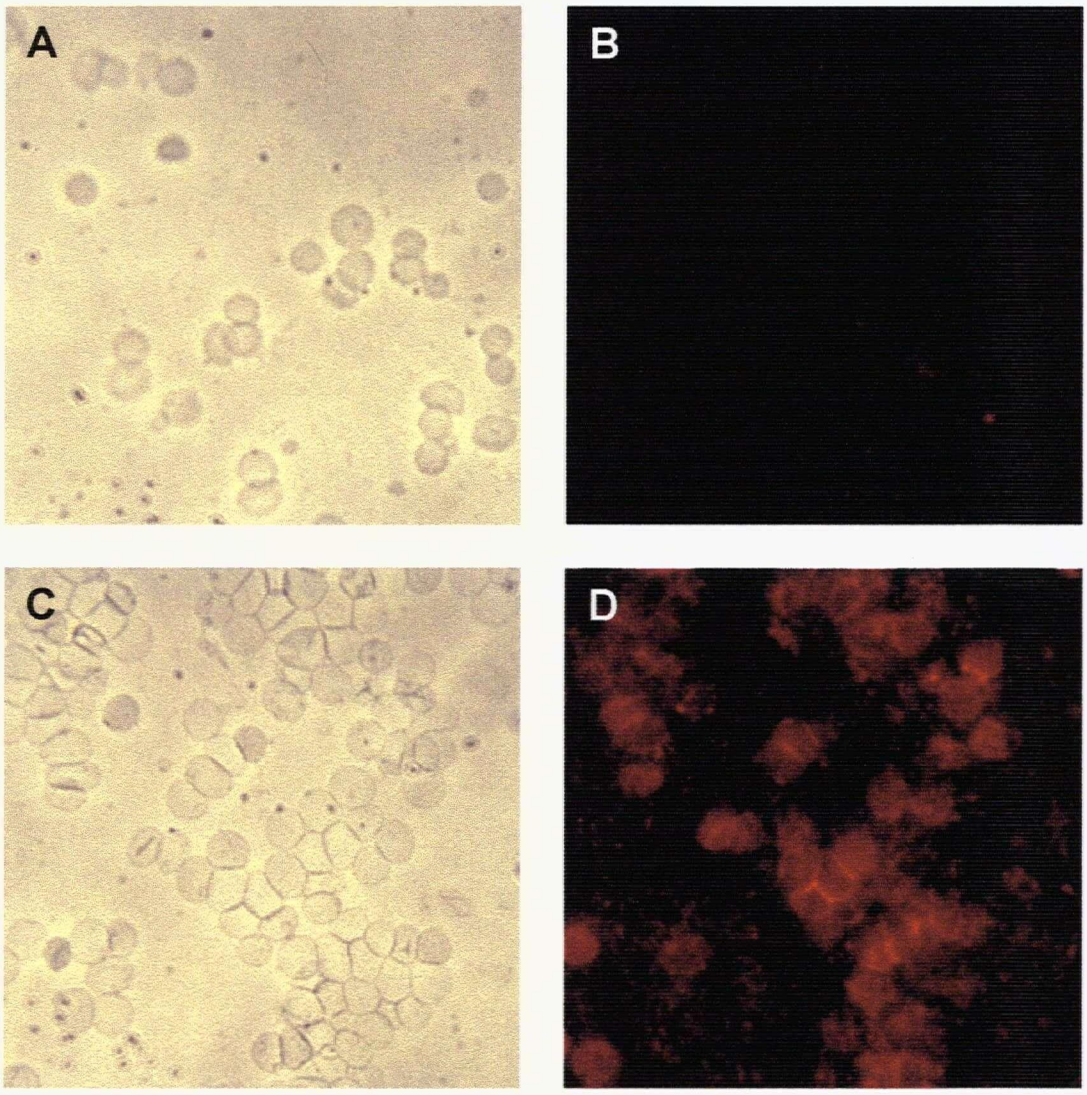

FIGURE 4.12 Fluorescence micrographs showing the appearance of Rh-PE in erythrocyte membranes upon lipid mixing with 10 mol% Lipo-AcE4K in EPC/Chol (55:45). Liposomes were prepared from a co-lyophilized preparation of 10 mol% Lipo-AcE4K in EPC/Chol containing 0.5 mol% each of NBD-PE and Rh-PE. Liposome and erythrocyte membranes were mixed in a 1:3 lipid ratio (1 mM total lipid): (**A**) phase contrast and (**B**) Rh-PE fluorescence at pH 7.5; (**C**) phase contrast and (**D**) Rh-PE fluorescence after reducing pH to 5.0.

conceivably promote hydrophobic interactions at pH 7.5 that are not observed in LUV membranes. It is clear from the CD and tryptophan fluorescence results presented here that AcE4K requires neutralization of at least some of its acidic residues before it will interact with a lipid bilayer.

Coupling the peptide to a lipid anchor and incorporation into liposomes affects both the structure adopted by the peptide portion and the extent of its interactions with the lipid bilayer as a function of pH. The CD spectra of Lipo-AcE4K indicate that the anchored peptide adopts an α-helical structure at both neutral and acidic pH in contrast to the free peptide which is only α-helical at low pH in the presence of liposomes. This suggests that constraints imposed by the lipid anchor induce some peptide structure at neutral pH but prevent any further structural changes upon neutralization of acidic residues. However, the tryptophan fluorescence maxima indicate that the anchored peptide clearly experiences a more hydrophobic environment upon acidification of the medium compared to its uncoupled counterpart. Based on the lipid-mixing and electron microscopy results presented here, we believe that this hydrophobic environment results from increased penetration of Lipo-AcE4K into the lipid bilayer and not simply from a loss of charge on neighbouring residues or the formation of lipopeptide complexes.

Lipo-AcE4K destabilizes POPC and EPC/Chol lipid vesicles at mildly acidic pH, but not at pH 7.5. The extent of destabilization depends not only on pH and lipopeptide concentration, but also on membrane composition and on the transbilayer distribution of peptide. Our results are very different from those previously reported for related peptides

lacking membrane anchors. Düzgüneş & Shavnin (1992) used a 17 amino acid peptide from the N-terminus of HA2 X31 wild-type sequence and found that it gave extensive leakage for EPC LUVs at both neutral and low pH and no lipid mixing under any conditions. Rafalski *et al.* (1991) reported pH-dependent leakage for the 20 amino acid wt and for E4, but no lipid mixing in either POPC or POPC/Chol vesicles. It is clear that features such as peptide length, acidity, and membrane-anchoring all influence the membrane-destabilizing ability of these peptides.

The lipid mixing and leakage results presented here indicate extensive but short-lived membrane destabilization by 1 to 10 mol% Lipo-AcE4K in both POPC and EPC/Chol vesicles. The rapid loss in destabilizing capacity may be due to the formation of a membrane-stable conformation, a re-orientation of the lipopeptide, or the formation of stabilizing oligomeric complexes upon interaction with the lipid bilayer. The event appears to be accompanied by membrane penetration of the anchored peptide.

In addition to lipopeptide concentration, the extent of lipid mixing and leakage depend upon the lipid composition of the membranes involved. Lipo-AcE4K gave higher levels of lipid mixing in EPC/Chol (55:45) LUVs than in EPC or POPC LUVs. We tentatively attribute this difference to the ability of cholesterol to promote non-bilayer intermediates leading to membrane fusion (Cullis *et al.*, 1978), since, again, it is not possible to distinguish whether the increases in lipid mixing result from increased rates of aggregation without further experiments. Curiously, the increases in lipid mixing were accompanied by decreases in the extent of leakage at all lipopeptide concentrations. While cholesterol

is known to reduce the permeability of phospholipid membranes, it was not expected to exhibit this property while also promoting lipid mixing.

The transbilayer distribution of the lipopeptide also influences the degree of lipid mixing observed. When Lipo-AcE4K was added to preformed vesicles, lipid mixing was only substantial between vesicle populations that each contained the lipopeptide. Very little lipid mixing was observed when only one population contained as much as 10 mol% Lipo-AcE4K. This result suggests that when Lipo-AcE4K is incorporated into the outer membranes of lipid vesicles in this way, it can only penetrate and destabilize the membrane in which it is anchored. Alternatively, if it inserts into the membrane of target vesicles, it does not destabilize the target vesicles sufficiently to promote lipid mixing between the two populations. In caution it should be noted that lipid mixing within the labelled population of lipopeptide-bearing vesicles which cannot be detected by the assay may simply be the predominant process and that lipid mixing with a second population would be promoted under more constrained circumstances, e.g. within an endosome.

Incorporation of Lipo-AcE4K into both inner and outer leaflets of EPC/Chol (55:45) LUVs not only gave higher levels of lipid mixing between populations of vesicles containing the lipopeptide, but also caused these vesicles to fuse with liposomes lacking Lipo-AcE4K and with erythrocyte ghosts at low pH. The increase in lipid mixing provided by the presence of lipopeptide on the inner surface of the vesicle membrane must arise from the capability of Lipo-AcE4K to destabilize the membrane in which it is anchored since in this case it is unable to insert into an external lipid bilayer.

Fusion of EPC/Chol (55:45) LUVs containing 10 mol% Lipo-AcE4K in both leaflets was also demonstrated by freeze-fracture electron microscopy. At pH 5.0 large lipid vesicles with diameters of several hundred nanometers were formed. This limited size increase, compared to the extensive fused structures found in calcium-induced fusion of negatively charged liposomes (Eastman *et al.*, 1992), is consistent with the transient destabilization indicated by the lipid mixing and contents leakage results. The freeze-fracture micrographs show very rough lipid surfaces and extensive cross-fracturing, both of which can be attributed to destabilization of the membrane structure by the lipopeptide. Fluorescence microscopy of erythrocyte ghosts incubated with these liposomes indicated not only pH-dependent lipid mixing with but also aggregation of the ghosts at low pH. No Rh-PE fluorescence was observed in the ghosts at pH 7.5 or for EPC/Chol LUVs without Lipo-AcE4K at either pH 7.5 or pH 5.0.

In summary, the lipopeptide Lipo-AcE4K forms stable bilayers in POPC and EPC/Chol LUVs at concentrations up to 10 mol% at pH 7.5. Destabilization of these lipid vesicles can be induced by decreasing the pH below 6.0 which corresponds to the conditions under which the viral protein, influenza HA, from which it is derived causes membrane fusion. This membrane destabilization not only results in extensive leakage of liposomal contents, as has been demonstrated with a variety of other viral fusion peptides and synthetic amphipathic helices, but also in lipid mixing of LUVs as determined by fluorescent lipid probe dilution, and coalescence of lipid membranes shown by freeze-fracture electron microscopy. The extent of lipid mixing depends on pH, membrane composition, and the concentration of the lipopeptide as well as on its distribution between the membrane

leaflets. Addition of 10 mol% Lipo-AcE4K to EPC/Chol (55:45) LUVs gave lipid mixing with erythrocyte ghosts, the first example of fusion induced by a membrane-anchored fusion peptide with a biological membrane.

CHAPTER 5 - SUMMARY

The fusogenic properties of three synthetic lipid derivatives have been studied in model membranes. While the conditions under which each of the three lipids promotes membrane fusion are different, charge neutralization of the fusogenic species and a dependence on the total lipid composition of the fusing membranes are common to all three. In each case, we present evidence that fusion follows membrane destabilization caused by either the promotion of non-bilayer lipid phases or disruption of the lipid bilayer upon penetration of the fusogenic species.

In Chapter 2, experiments on the fusion properties of liposomes containing the cationic lipid DODAC were described. DOPE/DODAC (1:1) LUVs fused with negatively charged target liposomes simply upon mixing the two vesicle populations at neutral pH. It is proposed that fusion in these systems follows a sequence of events: close apposition the two membrane surfaces promoted by attraction of opposite charges; mutual surface-charge neutralization resulting in reduced surface hydration; and formation of non-bilayer structures resulting from diminution of the surface charge and promoted by the presence of DOPE.

Fusion of DOPE/DODAC LUVs with target vesicles was promoted by increased negative surface charge, by the presence of PE in target vesicles, and, for liquid-crystalline lipids, by increased acyl chain unsaturation in target liposomes. Disaturated phospholipids promoted fusion below the gel-to-liquid-crystalline transition temperature, an effect which

was eliminated by the addition of cholesterol. These results indicate that fusion can be promoted by hydrophobic lipid arrangements arising either from the presence of H_{II} phase-promoting lipids or from the presence of lipids in the gel state. We also observed fusion of DOPE/DODAC (1:1) LUVs with erythrocyte membranes; however, fusion does not occur in the presence of serum.

An alternative method to induce membrane fusion by neutralization of a charged lipid species was described in Chapter 3. Fusion of LUVs containing synthetic aminolipids and regulation of this fusion by inducing transbilayer asymmetry of these aminolipids via imposed pH gradients were demonstrated. Liposomes of various compositions containing the aminolipid AL1 were stable at pH 4.0. Increasing the external pH of these vesicles to 7.5 resulted in rapid transport of AL1 to the inner monolayer. Dissipation of the imposed pH gradient led to redistribution of AL1 to the outer monolayer at pH 7.5 and caused liposomal fusion.

Again fusion was promoted by the presence of increasing levels of DOPE. This result along with the observation of H_{II} signals in the NMR data, implicate non-bilayer intermediates in the fusion of these membranes. This was further supported by the effects of varying the hydrocarbon structure of the aminolipid using the synthetic analogues, AL2-AL6. Compounds with longer, unsaturated hydrocarbon chains which would be expected to promote non-bilayer phases gave higher rates of fusion.

In Chapter 4, Lipo-AcE4K, a synthetic lipopeptide based on the amino acid sequence of the fusion peptide of influenza hemagglutinin, was used to demonstrate an alternative

method of inducing membrane fusion using changes in pH. In contrast to the aminolipids described above, LUVs containing Lipo-AcE4K were stable at pH 7.5 and only fused when the pH was reduced below 6.0.

The decrease in pH resulted in penetration of the peptide into the lipid bilayer as indicated by tryptophan fluorescence and freeze-fracture electron microscopy, presumably by neutralization of the acidic amino acid sidechains. Penetration of the membrane resulted in a rapid, transient destabilization of the lipid bilayer leading to extensive lipid mixing and leakage. The extent of fusion increased with increasing lipopeptide concentration and decreasing pH. The addition of cholesterol resulted in increased fusion and decreased leakage of liposomal contents.

While fusion between LUVs bearing Lipo-AcE4K only on the outer monolayer were able to fuse with each other, substantial fusion with liposomes lacking the lipopeptide and with erythrocyte membranes was only achieved when Lipo-AcE4K was present on both monolayers of the fusogenic liposomes.

In the future, the ability to induce fusion of lipid vesicles in a controlled fashion may be useful in elucidating the molecular mechanisms of membrane fusion in the absence of fusion proteins. This could eventually lead to better understanding of the mechanisms by which fusion occurs in biological membranes and of the possible roles for fusion proteins in catalyzing fusion processes. For now, the transient nature of the intermediate structures involved in membrane fusion and the inability to detect the dynamic processes involved make such determinations difficult to achieve. Combining the work described here with

chemical cross-linking in lipid systems with longer-lived fusion intermediates holds some promise for future experiments.

In the meantime, liposomes containing fusogenic lipid components are gaining widespread use as cellular transfection agents and are of ever-increasing interest in the fields of *in vivo* drug delivery and gene therapy. The development of lipid vesicles that can be efficiently targeted to specific sites of disease, and that can then fuse with the membranes of diseased cells to deliver therapeutic agents contained within the vesicles, is the current focus of a very large research effort. An understanding of membrane fusion and the ability to control fusion of lipid vesicles with biological membranes are essential components of this effort.

BIBLIOGRAPHY

Arbuzova, A., Korte, T., Muller, P., Herrmann, A. (1994) *Biochim. Biophys. Acta 1190*, 360-366.

Bartlett, G. R. (1959) *J. Biol. Chem 234*, 466-468.

Behr, J.-P. (1994) *Bioconjugate Chem. 5*, 382-389.

Bennett, M. J., Nantz, M. H., Balasubramaniam, R. P., Gruenert, D. C., & Malone, R. W. (1995) *Biosci. Rep. 15*, 47-53.

Bental, M., Wilschut, J., Scholma, J., Nir S. (1987) *Biochim. et Biophys. Acta 898*, 239-47.

Bloom, M., Evans, E., & Mouritsen, O. G. (1991) *Quarterly Rev. Biophys. 24*, 293-397.

Bosch, M. L., Earl, P. L., Fargnoli, K., Picciafuoco, S., Giombini, F., Wong-Staal F., & Franchini, G. (1989) *Science 244*, 694-697.

Brasseur, R., Vandenbranden, M., Cornet, B., Burny, A., & Ruysschaert, J.-M. (1990) *Biochim. Biophys. Acta 1029*, 267-273.

Bullough, P. A., Hughson, F. M., Skehel, J. J., & Wiley, D. C. (1994) *Nature 371*, 37-43.

Burger, K. N. J., Wharton, S. A., Demel, R. A., & Verkleij, A. J. (1991) *Biochim. Biophys. Acta 1065*, 121-129.

Chemomordik, L. V., Kozlov, M. M., Milikyan, G. B., Abidor, I. G., Markin, V. S., & Chizmadzhev, Y. A. (1985) *Biochim. Biophys. Acta 812*, 643-655.

Chonn, A., & Cullis, P. R. (1995) *Current Opinion in Biotechnology 6*, 698-708.

Clague, M. J., Knutson, J. R., Blumenthal, R., & Hermann, A. (1991) *Biochemistry 30*, 5491-5497.

Cullis, P. R., & de Kruiff, B. (1979) *Biochim. Biophys. Acta 559*, 399-420.

Cullis, P. R., & Hope, M. J. (1978) *Nature 271*, 672-674.

Cullis, P. R., & Hope, M. J. (1985) *Physical Properties and Functional Roles of Lipids in Membranes* in **Biochemistry of Lipids and Membranes** (Vance, D. E., & Vance, J. E., eds.), 25-72, Benjamin/Cummings, Menlo Park, CA.

Cullis, P. R., Farren, S. B., & Hope, M. J. (1981) Can. J. Spec. 26, 89-94.

Cullis, P. R., Hope, M. J., & Tilcock, C. P. S. (1986a) *Chem. Phys. Lipids 40*, 127-144.

Cullis, P. R., Tilcock, C. P. S., & Hope, M. J. (1986b) *Lipid Polymorphism* in **Membrane Fusion** (Wilschut, J., & Hoekstra, D., eds.), 35-64, Marcel Dekker, New York.

Cullis, P. R., van Dijck, P. W. M., de Kruiff, B., & de Gier, J. (1978) *Biochim. Biophys. Acta 513*, 21-30.

Das, S., & Rand, R. P. (1986) *Biochemistry 25*, 2882-2889.

Düzgüneş, N., & Shavnin, S. A. (1992) *J. Membrane Biol. 128*, 71-80.

Düzgüneş, N., & Wilschut, J., (1993) *Methods in Enzymology 220*, 3-14.

Düzgüneş, N., Allen, T. M., Fedor, J., & Papahadjopoulos, D., (1987) *Biochemistry 26*, 8435-8442.

Düzgüneş, N., Goldstein, J. A., Friend, D. S., & Felgner, P. L. (1989) *Biochemistry 28*, 9179-9184.

Eastman, S. J., Hope, M. J., Wong, K.F., & Cullis P. R. (1992) *Biochemistry 31*, 4262-4268.

Eastman, S. J., Hope, M. J., & Cullis, P. R. (1991) *Biochemistry 30*, 1740-1745.

Ellens, H., Bentz, J., & Szoka, F. C. (1984) *Biochemistry 23*, 1532-1538.

Farhood, H., Bottega, R., Epand, R. M., & Huang, L. (1992) *Biochim. Biophys. Acta 1111*, 239-246.

Farhood, H., Serbina, N., & Huang, L. (1995) *Biochim. Biophys. Acta 1235*, 289-295.

Felgner, P. L., Gadek, T. R., Holm, M., Roman, R., Chan, H. W., Wenz, M., Northrop, J. P., Ringold, G. M., & Danielsen, M., (1987) *Proc. Natl. Acad. Sci. U.S.A. 84*, 7413-7417.

Fisher, K., & Branton, D. (1974) *Methods in Enzymol. 32*, 35.

Galla, H. J., Warncke, M., & Scheit, K. H. (1985) *Eur. Biophys. J. 12*, 211-216.

Gao, X., & Huang, L. (1991) *Biochem. Biophys. Res. Comm. 179*, 280-285.

Gething, M. J., Doms, R. W., York, D., & White, J. (1986) *J. Cell Biol. 102*, 11-23.

Gruner, S. M., Cullis, P. R., Hope, M. J., & Tilcock, C. P. S. (1985) *Ann. Rev. Biophys. & Biophys. Chem. 14*, 211-238.

Gunther-Ausborn, S., Praetor, A., & Stegmann, T. (1995) *J. Biol. Chem. 270*, 29279-29285.

Hoekstra, D. (1982) *Biochemistry 21*, 2833-2840.

Hoekstra, D., & Düzgüneş, N. (1993) *Methods in Enzymology 220*, 15-32.

Hoekstra, D., & Martin, O. C. (1982) *Biochemistry 21*, 6097-6103.

Hope, M. J., & Cullis, P. R. (1981) *Biochim. Biophys. Acta 640*, 82-90.

Hope, M. J., & Cullis, P. R. (1987) *J. Biol. Chem. 262*, 4262-4268.

Hope, M. J., Walker D. C., & Cullis, P. R. (1983) *Biochem. Biophys. Res. Commun. 110*, 15-22.

Houslay M. D., and Stanley, K. K. (1982) **Dynamics of biological membranes: influence on synthesis, structure, and function**. New York: Wiley.

Hughson F. M. (1995) *Current Biology 5,* 265-74.

Ishiguro, R., Kimura, N., & Takhashi, S. (1993) *Biochemistry 32*, 9792-9797.

Israelachvilli, J. N., Marcelja, S., & Horn, R. J. (1980) *Q. Rev. Biophys. 13*, 121-148.

Ito, A., Miyazoe, R., Mitoma, J., Akao, T., Osaki, T., & Kunitake, T. (1990) *Biochem. Inter. 22*, 235-241.

Kato, T., Lee, S., Ono, S., Agawa, Y., Aoyagi, H., Ohno, M., & Nishino, N. (1991) *Biochim. Biophys. Acta 1063*, 191-196.

Kemble, G. W., Danieli, T., White, J. M. (1994) *Biochemistry 76*, 383-91,

Klappe, K., Wilschut, J., Nir, S., & Hoekstra, D. (1986) *Biochemistry 25*, 8252-8260.

Lakowicz, J., (1983) *Principles of Fluorescence Spectroscopy*, Plenum, New York.

Leventis, R., & Silvius, R.J. (1990) *Biochim. Biophys. Acta 1023*, 124-132.

Leventis, R., Gagne, J., Fuller, N., Rand, R.P., & Silvius, J.R. (1986) *Biochemistry 25*, 6978-6987.

Lindblom, G., & Rilfors, L. (1989) *Biochim. Biophys. Acta 988*, 221-256.

Madden, T. D., & Cullis, P. R. (1982) *Biochim. Biophys. Acta 684*, 149-153.

Malone, R. W., Felgner, P. L., & Verma, I. M. (1989) *Proc. Natl. Acad. Sci. U.S.A. 86*, 6077-6081.

Markin, V. S., Kozlov, M. M., & Borovjagin, V. L. (1884) *Gen. Physiol. Biophys. 5*, 361-377.

Marquardt, M. T., Phalen, T., & Kielian, M. (1993) *J. Cell Biol. 123*, 57-65.

Marsh, D. (1990) **CRC Handbook of Lipid Bilayers**. CRC Press: Boca Raton, FL.

Mayer, L. D., Hope, M. J., & Cullis, P. R. (1986) *Biochim. Biophys. Acta 858*, 161-168.

McLughlin, S. (1977) *Current Topics in Membranes and Transport 9*, 71-144.

Mimms, L.T., Zampighi, G., Nozaki, Y., Tanford, C. & Reynolds, J. A. (1981) *Biochemistry 21*, 833-840.

Murata, M., Takahashi, S., Shirai, Y., Kagiwada, S., Hishida, R., & Ohnishi, S. (1993) *Biophys. J. 64*, 724-734.

Nayar, R., Hope, M. J., & Cullis, P. R. (1989) *Biochim. Biophys. Acta 986*, 200-206.

Nieva, J.L., Nir,S., Muga, A., Goñi, F.M., & Wilscut, J. (1994) *Biochemistry 33*, 3201-3209.

Puyal, C., Maurin, L., Miquel, G., Bienvenüe, A., & Philippot, J. (1994) *Biochim. Biophys. Acta 1195*, 259-266.

Rafalski, M., Ortiz, A., Rockwell, A., van Ginkel, L.C., Lear, J.D., DeGrado, W.F., & Wilschut, J. (1991) *Biochemistry 30*, 10211-10220.

Rand, R. P., Pangborn, W. A., Purdon, A. D., & Tinker, D. O. (1975) *Can. J. Biochem. 53*, 189-195.

Roederer, M., Bowser, R., & Murphy, R. F. (1987) *J Cell. Physiol. 131*, 200-9.

Seddon, J. M. (1990) *Biochim. Biophys. Acta 1031*, 1-69.

Senior, J. H., Trimble, K. R., & Maskiewicz, R. (1991) *Biochim. Biophys. Acta 1070*, 173-179.

Sessions, A., & Horowitz, A. F. (1983) *Biochim. Biophys. Acta 728*, 103-111.

Siegel, D. P. (1993) *Biophys. J. 65*, 2124-2140.

Siegel, D. P., Banschbach, J., Alfred, D., Ellens, H., Lis, L. J., Quinn, P. J., Yeagle, P. L. & Bentz, J., (1989) *Biochemistry 28*, 3703-3709.

Stamatatos, L., Leventis, R., Zuckermann, M. J., & Silvius, J. R. (1988) *Biochemistry 27*, 3917-3925.

Steck, T. L., & Kant, J. A. (1974) *Methods in Enzymology 31*, 172-180.

Stegmmann, T., Doms, R.W., & Helenius, A. (1989) *Annu. Rev. Biophys. Biophys. Chem. 18*, 187-211.

Struck, D. K., Hoekstra, D., & Pagano, R. E. (1981) *Biochemistry 20*, 4093-4099.

Szoka, F., & Papahadjopoulos, D. (1978) *Proc. Natl. Acad. Sci. USA 79*, 4194-4198.

Szoka, F., & Papahadjopoulos, D. (1980) *Ann. Rev. Biophys. Bioeng. 9*, 467-508.

Tilcock, C. P. S., & Cullis, P. R. (1982b) *Biochim. Biophys. Acta 684*, 212-218.

Tilcock, C. P. S., & Cullis, P. R. (1987) *Ann. New York Acad. Sci. 492*, 88-102.

Tilcock, C. P. S., Bally, M. B., Farren, S. B., & Cullis, P. R. (1982a) *Biochemistry 21*, 4596-4601.

Tilcock, C. P. S., Cullis, P. R., & Gruner, S. M. (1988) *Biochemistry 27*, 1415-1420.

Tullius, E. K., Williamson, P., & Schlegel, R. A. (1989) *Biosci. Rep. 9*, 623-633.

Verkleij, A. J. (1984) *Biochim. Biophys. Acta 779*, 43-63.

Verkleij, A. J., Van Echteld, C. J. A., Gerritsen, J., Cullis, P. R., and de Kruiff, B. (1980) *Biochim. Biophys. Acta* 600, 620-624.

Walter, A., & Siegel, D. P. (1993) *Biochemistry 32*, 3271-3281.

White, J.M. (1991) *Science 258*, 917-924.

Wilschut, J., Scholma, J., Bental, M., Hoekstra, D., & Nir, S. (1985) *Biochim. Biophys. Acta 821*, 45-55.

Wilschut, J., & Hoekstra, D., eds. (1991) **Membrane Fusion**. New York : Dekker.

Wrobel, I., & Collins, D. (1995) *Biochim. Biophys. Acta 1235*, 296-304.

Zabner, J., Fasbender, A. J., Moninger, T., Poellinger, K. A., & Welsh, M. J. (1995), *J. Biol. Chem. 270*, 18997-19007.

Zschörnig, O., Arnold, K., Richter, W., & Ohki, S. (1992) *Chem. Phys. Lipids 63*, 15-22.